A COGNITIVE PHASED ARRAY USING SMART PHONE CONTROL

A Thesis

by

JEFFREY SCOTT JENSEN

Submitted to the Office of Graduate Studies of
Texas A&M University
in partial fulfillment of the requirements for the degree of

MASTER OF SCIENCE

May 2012

Major Subject: Electrical Engineering

A Cognitive Phased Array Using Smart Phone Control

A COGNITIVE PHASED ARRAY USING SMART PHONE CONTROL

A Thesis

by

JEFFREY SCOTT JENSEN

Submitted to the Office of Graduate Studies of
Texas A&M University
in partial fulfillment of the requirements for the degree of

MASTER OF SCIENCE

May 2012

Major Subject: Electrical Engineering

ABSTRACT

A Cognitive Phased Array Using Smart Phone Control. (May 2012)

Jeffrey Scott Jensen, B.S., Texas A&M University

Chair of Advisory Committee: Dr. Gregory H. Huff

Cognitive radio networks require the use of computational resources to reconfigure transmit/receive parameters to improve communication quality of service or efficiency. Recent emergence of smart phones has made these resources more accessible and mobile, combining sensors, geolocation, memory and processing power into a single device. Thus, this work examines an integration of a smart phone into a complex radio network that controls the beam direction of a phased array using a conventional method, but utilizes the phone's internal sensors as an enhancement to generate beam direction information, Bluetooth channel to relay information to control circuitry, and Global Position System (GPS) to track an object in motion.

The research and experiments clearly demonstrate smart phone's ability to utilize internal sensors to generate information used to control beam direction from a phased array. Computational algorithms in a network of microcontrollers map this information into a DC bias voltage which is applied to individual phase shifters connected to individual array elements.

To test algorithms and control theory, a 4 by 4 microstrip patch array is designed and fabricated to operate at a frequency of 2.4 GHz. Simulations and tests of the array provide successful antenna design results with satisfactory design parameters. Smart phone control circuitry is designed and tested with the array. Anechoic test results yield successful beam steering capability scanning 90 degrees at 15 degree intervals with 98% accuracy in all cases. In addition, the system achieves successful beam steering operable over a bandwidth of 100 MHz around resonance. Furthermore, these results demonstarate the capability of the smart phone controlled system to be used in testing further array formations to achieve beam steering in 3-Dimensional space. It is further noted that the system extends capabilities of integrating other control methods which use the smart phone to process information.

DEDICATION

This thesis is dedicated to my wife and parents.

ACKNOWLEDGEMENTS

I would like to thank my committee chair, Dr. Huff, for his help and experience throughout this project. I would also like to thank my committee members, Dr. Chamberland, Dr. Pfister, Dr. Hogan, for their guidance and support throughout the course of this research.

In addition, I would like to thank my wife whose support and love has helped me through hard work and difficult times. My success thrived with each day of her support. In conjunction, I would also like to thank my parents who taught me that you always need to love what you do and hard work always pays off. Thank you.

NOMENCLATURE

GPS	Global Positioning System
ROM	Read Only Memory
RAM	Random Access Memory
OS	Operating System
PHY	Physical Layer
MAC	Media Access Control
QOS	Quality of Service
TCP	Transport Control Protocol
UDP	User Datagram Protocol
SSH	Secure Shell
SMTP	Simple Mail Transfer Protocol
SDA	Serial Data Line
SCL	Serial Clock Line
SPI	Serial Peripheral Interface
I2C/I^2C	Inter-Integrated Circuit
ISM	Industrial, Scientific, and Medical Radio Bands
VSWR	Voltage Standing Wave Ratio

TABLE OF CONTENTS

LIST OF FIGURES

Page

Page

LIST OF TABLES

CHAPTER I

INTRODUCTION

As an integral part of many complex communications systems, phased arrays provide a technical enhancement in beam steering that single antenna arrays cannot provide. In lieu of mechanically steering an antenna by physically moving its radiating surface in a desired direction, the same objective may be achieved through electrical control without mechanical intervention. Through various control methods [1-3] the progressive phase shift of individual array elements is controlled to achieve directional beam steering that is found in many applications such as satellite, military, and commercial applications. PAVE PAWS, a U.S. military defense system, uses phased array radar to detect missiles and other objects in space by steering a beam from single locations [4]. In another example, the MESSENGER spacecraft is currently performs deep space missions which utilize a linearly polarized phased array for communications from Mercury to Earth [5]. While the concept of phased arrays or directional antenna transmission was originally developed more than 100 years ago [6], progressive research of array fabrication, development of control circuitry and algorithms, and design of electromagnetic components have allowed phased arrays to evolve to what they are today. Without continued research, phased arrays would not possess necessary technical enhancements such as multi-beam steering or cost-effective implementation of radio control networks [7].

This thesis follows the style of *IEEE Transactions on Antennas and Propagation*.

As new technology becomes available, it is important to continue to develop and integrate these new technologies into phased array systems to further enhance their efficiency and operability, further introducing phased arrays into new communication domains.

Smart phones, although widely viewed as mobile entertainment devices, carry many useful electrical tools that are often found in complex networks. Sensors, memory, processors, and wireless communications hardware are fundamental components of information networks today. Naturally, smart phones have the capability to be integrated into the future of cognitive radio networks, as their presence has been seen into the integration of energy management, automation and control, and other fields as tools that gather information or implement signal controls. Many Android applications such as in literature [8] allow a user to control and monitor vital functions of their home such as air conditioning, humidity, lighting, and other electrical systems with their phone. As pervasive use of smart phones and tablets continues in society, there should exist to some extent, an integration of these devices into academia and in particular, engineering research of many types. As a new technology, smart phones offer new possibilities of integration into complex communications systems as the primary computing resource, allowing conventional systems to become more mobile and new systems to emerge as communication networks of the future. These thoughts were conceived more than 40 years ago best said by F. J. Langley, “Low cost commercial microcomputers, (currently used in many diverse applications, e.g. point-of-sale terminals, desk top computers, check processors, etc.), … provide the opportunity for computing beam steering and shaping phase shifts for large phased-array antennas …" [9].

This research promotes the future of phased array development by integrating a smart phone into a conventional phased array control method. As aforementioned, smart phones have become integral in society in the last decade and their mobile computing prowess provides a natural assimilation into a conventional phased array control method. Some immediate advantages provided by this research are the capability to bring conventional phased array control methods into a new domain by providing a powerful mobile computing resource and to introduce smart phones as a pivotal research tool in future electromagnetics research. Furthermore, the ability to program the smart phone allows for multiple modes of operation of the control network, by either allowing a human operator to directly control the beam direction in the palm of their hand or setting the phone into an autonomous control mode with little to no human interaction. With this knowledge and capability, this research provides new insight and understanding to controlling phased arrays and serves as an innovative implementation of a fundamental technology.

CHAPTER II

SURVEY

Tracking an object using antennas was, for a long time, mechanically instrumented by physical rotation. To this end, radar and other antenna tracking systems could be optimized by machinery to track an object through space whether static or in motion. Coinciding with these efforts were groups of engineers that performed math and calculated an object's projected path through space to steer antenna beams in the appropriate direction. However, upon realization of electronic beam steering using phased arrays coupling advancements in development with computing technology, tracking algorithms for phased arrays have exceedingly progressed far beyond the mechanical predecessors [10]. Algorithms for phased array on different surfaces such as ground, water and air have been developed to track objects in space to avoid collision, detect intrusion or track an object. Heavily found in military applications, object tracking algorithms primarily serve to detect missiles or flying objects; whereas, other applications extend to tracking an object such as a satellite, to maintain a line of sight communication channel as it passes through space. For all applications, it is necessary to survey relevant literature that tracks an object to help further explain the advantages of a system integrated smartphone leading to exciting future work of this project.

Fundamentally, tracking any object, whether static or moving, requires information to be analyzed by a control system. Many authors attempt object tracking methods using more complex schemes with filters that analyze object history, while some adapt basic control theory concepts to estimate the state of an object as it moves through space. Questions of uncertainty such as location of the object, future movement of the object, future movement of the tracker, system sampling rate and so on, have provided researchers an extensive task of developing an accurate control methodology. In order to develop a control method, arbitrary or unknown system variables need to be estimated or ignored. One method of doing this is to apply a basic Kalman filter [10-13]. Kalman filters analyze a history of data to predict the future state of the system [10-13]. In one such algorithm using an alpha-beta filter, the refresh rate time is set constant to determine the system update rate while assuming that the input measurement, or target state, is known for every measurement [10, 12]. This simplifies the Kalman filter equations and provides an estimation of state upon choosing appropriate linear values of alpha and beta. The Kalman filter approach also assumes that there is a single measurement input and that this input is a linear function of the target state. In the case of tracking an object, this filtered approach would allow the system to estimate the target's new position based on its current path and would therefore reconfigure the phased array to track this target.

In another approach, it can be assumed that the system has some distribution of Gaussian noise which could be sourced from many references such as measurement interference or unknown state of the measurement. It is necessary to then choose a measurement of the target that is based on practical data association [10, 11, 14]. The Nearest Neighbor

(NN) algorithm provides a probability association of measurement data to a set of predicted measurements, where the measurement received is compared to the next closest predicted measurement and is validated [14]. This model reflects a practical application of tracking an object from a system that is in the presence of noise such as a changing non-linear position as given during an object's acceleration. The NN algorithm can be coupled with a Kalman filter to provide a multiple layered algorithm that reflects a validation of the measurement in addition to tracking the object's position based on its previous position or state.

In other related studies, many filters have been combined to aggregate noise cancellation and reduce unknown variables for tracking objects in the Interacting Multiple Model (IMM) algorithm [15]. The IMM algorithm performs exceptionally well in tracking objects at high speeds and when performing arbitrary maneuvers. Comprised on a basis of Markov chain models, the IMM algorithm determines the object's state by comparing multiple filter outputs and determining the objects state by combining the outputs coupled with data association [15]. Each model has advantages and disadvantages tracking an object. This survey of works demonstrates the active participation of research in this field and incorporates the phased array control model into computations and algorithms.

CHAPTER III

BACKGROUND

3.1 Array Theory

In order to control the beam direction of a microstrip antenna phased array, it is necessary to grasp fundamental concepts both in array theory and microstrip antenna design to understand the electromagnetic behavior of the system. To develop this knowledge, basic linear array theory is presented as a precursor to planar arrays where planar arrays add another dimension of complexity to linear array equations. Design characteristics of microstrip patches are also presented. Power splitters and dividers are explained in their pertinence to this research, followed by the selection of phase shifters used for the array elements.

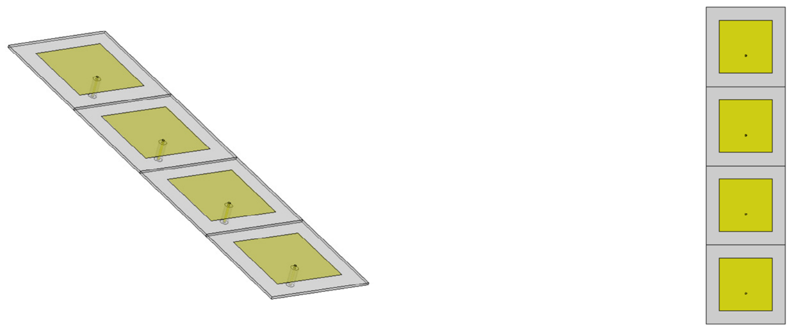

Figure 1. Linear Microstrip Patch Array

Linear arrays, as shown in Figure 1, provide the fundamental equations needed to analyze phased arrays. To adequately address the operation of linear arrays, the formulation of an array factor may be found by the superposition of electric fields from periodic spaced antenna elements. If each element has equal amplitude and has a progressive phase shift *β*, the array is said to be a uniform array [16]. If the elements are considered to be point sources, the array factor for an *N* element linear array is shown by

$$AF = \left[\frac{\sin(\frac{N}{2}\psi)}{\sin(\frac{1}{2}\psi)} \right] \tag{0.1}$$

where the character ψ is represented by

$$\psi = kd\cos(\theta) + \beta \tag{0.2}$$

The realization of (0.1) is the compact form of the array factor for an *N* element array. To normalize the array factor among the number of elements, (0.1) is divided by the total number of elements *N* shown by

$$AF = \left(\frac{1}{N}\right)\left[\frac{\sin(\frac{N}{2}\psi)}{\sin(\frac{1}{2}\psi)} \right] \tag{0.3}$$

The calculation of the array factor is necessary as it is used in calculating the total array pattern by multiplying it with a single element pattern. From this formulation, the theory is used to help determine phase shifts to steer the beam in Euclidean space. In this research, the beam is always configured to radiate at a maximum along an axis that is normal to the surface of the antenna array, which is referred to as broadside [16]. To achieve a broadside radiation, the array factor's progressive phase shift β must be equal to zero as shown by

$$\psi = kd\cos(\theta) + 0 \tag{0.4}$$

The introduction of (0.3) and (0.4) allows a linear array to steer a beam within a two dimensional plane; however, the goal of this research is to achieve beam steering in three dimensions. To further analyze other directions in addition to the broadside and two dimensional planar directions, analysis of the planar array, as shown in Figure 2, reflects the array used in research.

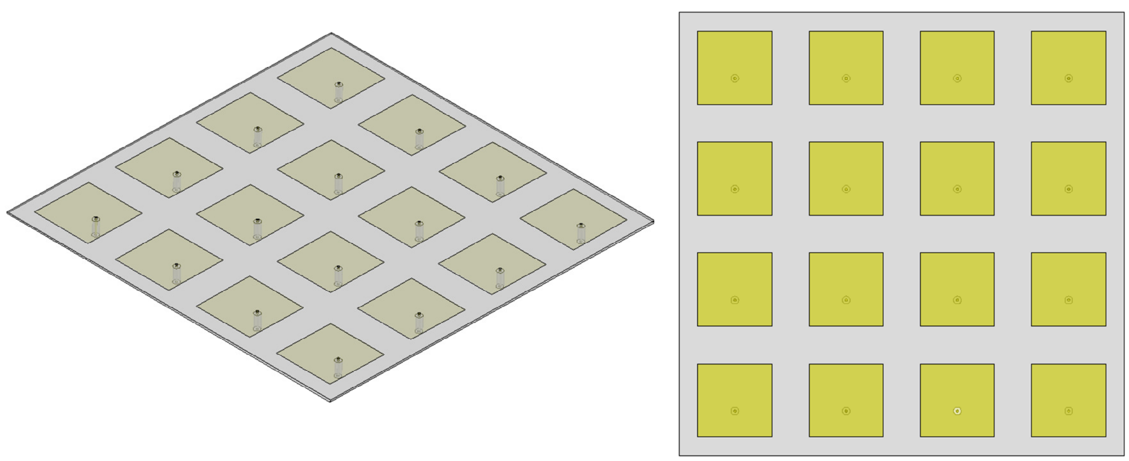

Figure 2. Planar 4x4 Microstrip Patch Array

Planar array theory is similar to linear theory; however, it has an added dimension of complexity as the methods to solving planar array structure problems may be analyzed as linear arrays in two dimensions. The array factor for an *N* element array along the x axis of (0.5), is the summation of the current distribution for each linear element, where elements have an equal spacing of d_x and a progressive phase shift β_x.

$$AF_x = \sum_{n=1}^{N} I_0 e^{j(m-1)(kd_x \sin\theta\cos\phi + \beta_x)} \tag{0.5}$$

The directional cosine *sinθcosφ* accounts for the phase separation of linear elements along the x axis in Cartesian coordinates that observe a point in spherical coordinates. Now, consider a similar array that is parallel along the y axis represented by

$$AF_y = \sum_{m=1}^{M} I_0 e^{j(n-1)(kd_y \sin\theta\sin\phi + \beta_y)} \tag{0.6}$$

where d_y is the spacing between elements, β_y is the progressive phase shift and *sinθsinφ* is the directional cosine along the y axis. To find the total array factor for an *M* by *N* element array, a dot product of (0.5) and (0.6) yields

$$AF = \sum_{n=1}^{N} I_{0x} \left[\sum_{m=1}^{M} I_{0y} e^{j(m-1)(kd_y \sin\theta\sin\phi + \beta_y)} \right] e^{j(n-1)(kd_x \sin\theta\cos\phi + \beta_x)} \tag{0.7}$$

The directional cosines were derived using the relationship

$$\begin{aligned} \hat{x}\cdot\hat{r} &= \sin\theta\cos\phi \\ \hat{y}\cdot\hat{r} &= \sin\theta\sin\phi \end{aligned} \tag{0.8}$$

The compact normalized form of the total array factor is

$$AF_n(\theta,\phi) = \left[\left(\frac{1}{M}\right) \frac{\sin(M\frac{\psi_x}{2})}{\sin(\frac{\psi_x}{2})} \right] \cdot \left[\left(\frac{1}{N}\right) \frac{\sin(N\frac{\psi_y}{2})}{\sin(\frac{\psi_y}{2})} \right] \tag{0.9}$$

where ψ_x,ψ_y are represented in equation (0.2). The formulation of (0.9) realizes that the maximum location is dependent from *θ* and *φ*. The primary concern of this research is to point the primary beam in the direction of an object using a primary θ and φ. If these are known, the progressive phase shift for individual array elements can be calculated by

$$\begin{aligned}\psi_x &= kd_x \sin\theta\cos\varphi + \beta_x \\ \psi_y &= kd_y \sin\theta\sin\varphi + \beta_y\end{aligned} \tag{0.10}$$

The fundamental calculations in all algorithms use (0.10) provided further assumptions. Beam width, side lobes and other array characteristics are not factored into equations and calculations as they are not concerned with the primary goal of this research. Using (0.10), the individual phase shifts may be calculated by realizing that maximums of (0.10) occur under the conditions shown in (0.11).

$$\begin{aligned}\psi_x &= \pm 2m\pi \\ \psi_y &= \pm 2n\pi\end{aligned} \tag{0.11}$$

From (0.11), it is clear that the maximums occur when both *m* and *n* are equal to 0. From before, (0.10) now becomes (0.12).

$$\begin{aligned}\beta_x &= -kd_x \sin\theta_0 \cos\varphi_0 \\ \beta_y &= -kd_y \sin\theta_0 \sin\varphi_0\end{aligned} \tag{0.12}$$

With this analysis, individual phase shifts are calculated by using (0.12) directly in the smart phone's code. This fundamental theory and analysis provides the essentials to understanding linear and planar arrays. Although the arrays shown in Figure 1 and Figure 2 are comprised of patch antennas, arrays utilize many other types of antennas such as wire dipoles and other microstrip dimensional forms. However, this research utilizes microstrip rectangular patch antennas which require analysis to understand the single element operation.

In order to fabricate a planar array, it is necessary to consider the individual antenna element type. A simple structure used in many applications is the microstrip patch antenna [16]. Microstrip patch antennas, as shown in Figure 3, are notably directional antennas as the primary concentration of their radiation pattern exists along an axis normal to the radiating boundary. Their existence and function has been explained through much research and they are commonly used today [16-18]. The composition of this antenna is typically a copper strip in a geometric shape such as a rectangle or circle that sits upon a dielectric slab and ground plane [16]. Typical current feeds for patch antennas are through microstrip lines or probes. This research considers only a rectangular microstrip patch that is probe fed.

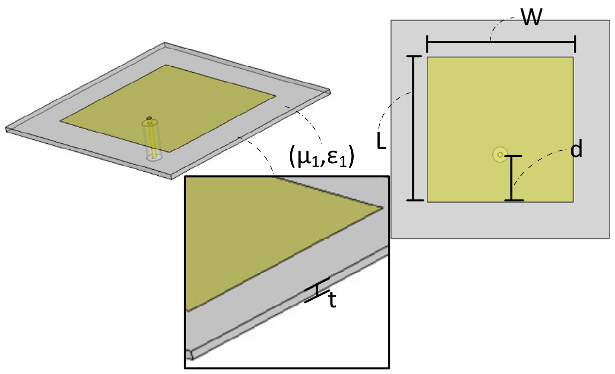

Figure 3. Microstip Patch with Design Parameters

The design parameters for microstrip patch antennas focus on dimensional characteristics of the copper upon the dielectric. Initial design characteristics are concerned primarily with these factors: width, length, dielectric constant, probe position and operating frequency [16]. The width *W,* length *L*, probe spacing *d*, and dielectric thickness *t*, are shown in Figure 3. Probe spacing calculations require additional complex mathematics that will not be discussed in this work. Simulation optimization techniques are used to determine the final probe placement values. The thickness or height of the substrate is dependent on manufacturer design. It can be shown that the width required for an operating frequency is given by

$$W = \frac{c}{2f_r}\sqrt{\frac{2}{\varepsilon_r + 1}} \tag{0.13}$$

where c is the speed of light in air, f_r is the desired resonance frequency and ε_r is the dielectric constant. The length can be calculated using

$$L = \frac{1}{2f_r\sqrt{\varepsilon_{reff}}\sqrt{\mu_0\varepsilon_0}} \tag{0.14}$$

where f_r is the desired resonant frequency, ε_{reff} is the effective dielectric constant represented by (0.15)

$$\varepsilon_{reff} = \frac{\varepsilon_r + 1}{2} + \frac{\varepsilon_r - 1}{2}\left[1 + 12\frac{h}{W}\right]^{-1/2} \tag{0.15}$$

The basic design requirements are sufficient for this research to produce a fabricated antenna that produces necessary results. With this basic analysis, the fundamentals for array design and fabrication are supported. Other realizations of network components are now examined to complete the system. With this in mind, array theory required that patches be fed with equal amplitude and phase from a signal so that the progressive phase shifts achieve accurate beam steering. The following analysis presents adequate theory to perform this action.

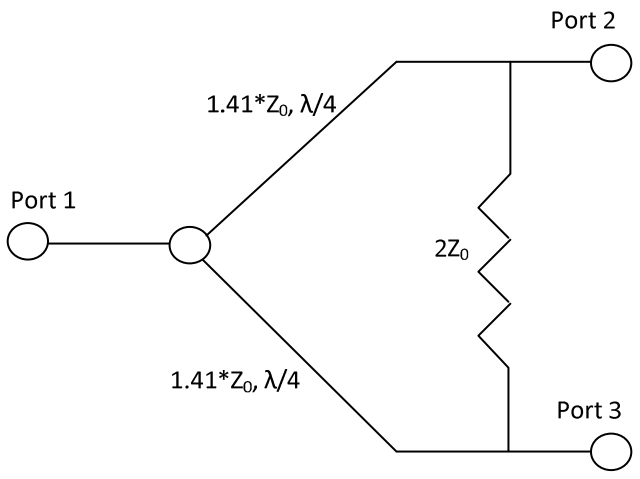

Figure 4. Wilkonson Power Divider Schematic

Although the array can be designed and fabricated, the interface between the array and the feed signal is essential to the operation of the array. Because this research incorporates a 4x4 array, all elements should be fed with a signal whose amplitude should be equal to satisfy the design requirement of the array factor of (0.9). This can be achieved by using a power divider. There are many RF power divider circuits that exist in industry and academia. A common structure is the Wilkonson Power Divider as shown in Figure 4. A unique feature of the power divider is that it allows a signal to be distributed equally among all elements for transmission, and it allows for equal power superposition upon receiving a signal [19]. This feature allows this research to be used both for transmission and reception purposes. Instead of designing a 16 split trace Wilkonson power divider, a divider was purchased from Instock Wireless Components with the following specifications [36].

Table 1. Instock Wireless Components Power Divider Specifications

Frequency	Impedance	Insertion Loss	Amplitude Balance	Phase Balance
.7-2.7 GHz	50 Ohms	1.8 dB (max)	.6 dB (max)	10 Degrees (max)

These specifications suffice the basic need of the system. Before the signal can be sent to the individual radiating elements, the proper phase shift must be applied to achieve correct beam steering. Analysis of phase shifter operation is necessary to understand the implications in network operation. Physical analysis of a phase shifter is not discussed in this research.

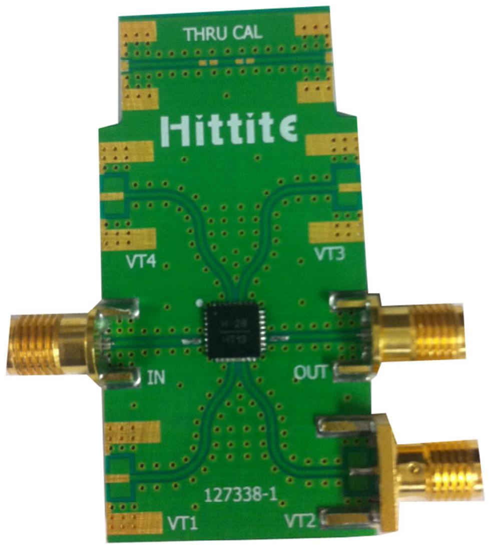

Figure 5. Hittite Analog Phase Shifter (2-4 GHz) with Evaluation Board

After the signal has been distributed through the power divider, it must pass through a phase shifter before arriving at the radiating patch. The phase shifters chosen for this project are from Hittite Corporation. As analog phase shifters, they require a control voltage ranging from 0-12 Volts which thereby produces a respective phase shift from 0 to 450 degrees as shown in Figure 6 .

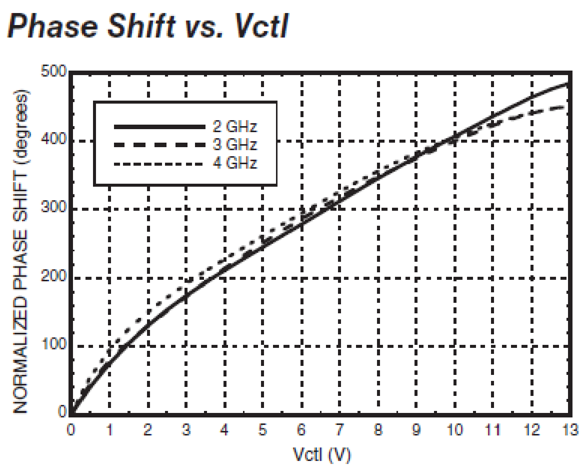

Figure 6. Hittite Phase Shifter Voltage Control of Phase Shift

The system requires that a phase shift be related to a voltage. To do this accurately, it is necessary to approximate the graph in a linear manner to design simple algorithms at the control level. An equation relating the desired phase shift to an expected voltage is required at the control level to achieve beam steering.

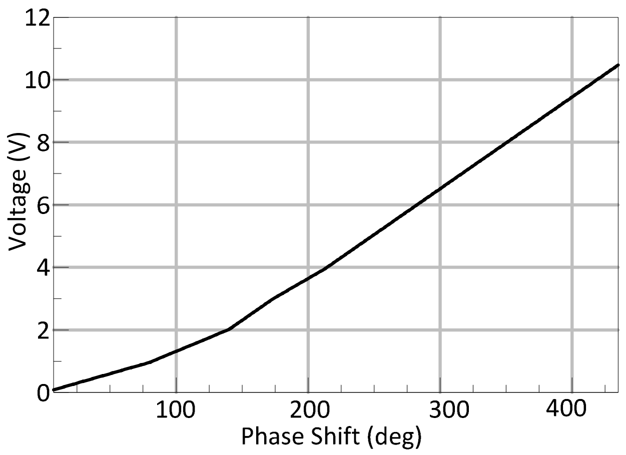

Figure 7. Hittite Phase Shifter Approximation with Equation

From Figure 7, an approximation for an input phase related to the voltage is provided in the equation which is also listed below.

$$Voltage = -8E-08*\deg^{3}+8E-05*\deg^{2}+0.005*\deg+0.1039 \qquad (0.16)$$

(0.16) is tested in the algorithm as a first pass to determine whether this approximation will provide sufficient control. The variable *deg* is the input degree value that is converted to a voltage output. Electromagnetic hardware design and analysis has been presented. Given a proper beam shift capability of the system, the algorithms require and object or direction to reference in Euclidean space. Discussion of basic mathematic point determination and rotation is discussed.

Provided the relevant background of antenna arrays, microstrip patch design, power dividers and phase shifters, it is important to highlight brief mathematic calculations to determine essential information for the system. Because this system needs to track objects and steer the main beam in three dimensional space, there exists a need to relate a position to angles θ_0 and φ_0 to be used in (0.12). This can be done in a number of ways such as Pythagorean's Theorem, change of coordinates, or directional cosines. In this case, the Pythagorean Theorem presents a straightforward approach to calculating position and direction for the system. To begin, it is assumed that a point in space has a known position of (x ,y ,z) with respect to the origin as shown in Figure 8.

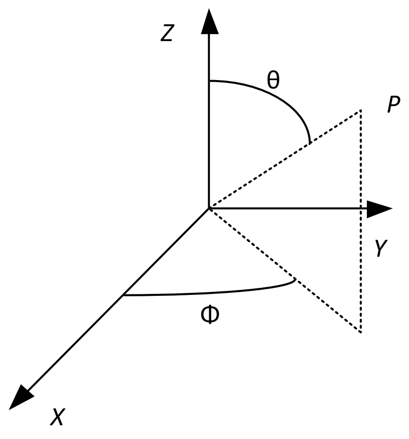

Figure 8. Point in Cartesian Coordinates

The point can also be given as a vector shown in (0.17)

$$P = [x, y, z]^T \tag{0.17}$$

In order to calculate *θ* and *φ*, some fundamental relationships are drawn given the point's known position. The angle *φ* can be calculated using

$$\phi = \cos^{-1}\left(\frac{x}{\sqrt{x^2 + y^2}}\right) \tag{0.18}$$

while from Figure 8, *θ* can be calculated using

$$\theta = \cos^{-1}\left(\frac{z}{\sqrt{x^2 + y^2 + z^2}}\right) \tag{0.19}$$

Now that angles can be calculated using geometric relationships, it is necessary to also consider an object moving in three dimensional space, as the system must be able to track an object under three different scenarios: the object is moving and the system is stationary, the system is moving and the object is stationary or the system and the object are both moving. Under any circumstance, it is simple to always consider that the system is static so as to maintain a constant coordinate system. Thus, whether the system or the object is moving, it can be modeled as the object moving in space using a rotation technique. Widely used in computer graphics and animation, a three dimensional rotation matrix can provide the rotation of a point *(x ,y ,z)* to a new coordinate of *(x',y',z')* given rotation angles φ, θ ,ψ which are directional cosines from the *x*, *y*, and *z* axes respectively as shown in Figure 9.

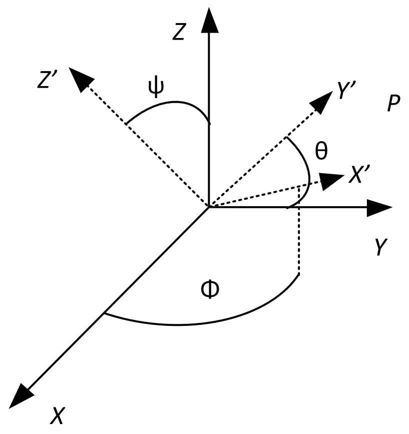

Figure 9. Euler Angles to Construct Rotation Matrix

In particular, there exists a combination of rotation matrices depending on the order of rotation. For instance, similar matrices can be derived to model a *Y-X-Z* transformation or a *Z-X-Y* transformation. This research utilizes *X-Y-Z* as it is a straightforward approach to coordinate transformation. To implement this in software, the original point (*x, y, z*) can be modeled as a vector while the corresponding rotation angles can be substituted into the *X-Y-Z* rotation matrix given by

$$\begin{pmatrix} \cos\theta\cos\psi & -\cos\phi\sin\psi+\sin\varphi\sin\theta\cos\psi & \sin\phi\sin\psi+\cos\phi\sin\theta\cos\psi \\ \cos\theta\sin\psi & \cos\phi\cos\psi+\sin\phi\sin\theta\sin\psi & -\sin\phi\cos\psi+\cos\phi\sin\theta\sin\psi \\ -\sin\theta & \sin\phi\cos\theta & \cos\phi\cos\theta \end{pmatrix}$$

(0.20)

The matrix shown in (0.20) is valid for φ, θ ,ψ *X-Y-Z* convention.

Thus, the new point can be determined by multiplying (0.17) and (0.20) to achieve

$$P' = [x, y, z]^T \cdot \begin{pmatrix} \cos\theta\cos\psi & -\cos\phi\sin\psi+\sin\varphi\sin\theta\cos\psi & \sin\phi\sin\psi+\cos\phi\sin\theta\cos\psi \\ \cos\theta\sin\psi & \cos\phi\cos\psi+\sin\phi\sin\theta\sin\psi & -\sin\phi\cos\psi+\cos\phi\sin\theta\sin\psi \\ -\sin\theta & \sin\phi\cos\theta & \cos\phi\cos\theta \end{pmatrix}$$

(0.21)

Once the transformation is performed, (0.12) can be used to calculate a θ and φ for the new point given by (0.21). These systems of equations are the fundamental equations used in the control algorithm and will be further discussed in the design section.

3.2 Control theory

Complex networks require control that governs behavior on multiple levels to achieve optimum system efficiency and performance. Accordingly, to solve complex network control problems, it is necessary to use a "Divide and Conquer" method to project a large objective into subsequent smaller objectives. By doing this, a control schema for individual subcomponents develops that accurately fit the operation of that component. Accordingly, the control schema of individual components should also follow a general control schema for the entire system so that subcomponents mesh efficiently as a whole during operation. These fundamental concepts provide significant advantages for the system designer in that the project may be built in a modular fashion, thereby setting achievable milestones that provide functional network components. Furthermore, the control concepts and design of each module or subcomponent becomes formidably easier as the complex problem divides into simpler problems.

Divide and conquer is a methodology or practice that is commonly found in many aspects of problem solving. For the purpose of this research, divide and conquer will be associated in definition most closely with that found in the field of computer science, particularly algorithm development [21]. Because this project implements software algorithms to implement control theory, it is fitting to use this association. Divide and conquer has two specific approaches that will be referenced in this research.

The first method derives from an approach to recursively divide a problem into subcomponents using a specific method continuously until the problem becomes directly solvable. This assumes that while the original problem could possibly be solved from induction or a complex algorithm, repeating a process at subsequent stages reduces the problem to a simplified basic solution which applies to all other subdivisions. This method of divide and conquer assumes that each subsequent stage contains similar problems to the stage before. An example of this type of divide and conquer is in a binary search algorithm. Take the following list of random numbers that have been sorted from smallest to largest shown in Figure 10.

1,2,4,5,8,13,15,17,18,19,23,45,46,48,51,53,55,60,67,71,77

Figure 10. Random Ordered List of Numbers

The goal of this divide and conquer approach is to find the position of a given number by randomly picking a position in the list of numbers and asking a yes or no question "Is number greater than this random position?". Here, the method of divide and conquer is the yes or no question and is performed at subsequent stages until the exact number is found. Thus, the number *46* is to be found in the list. A number *60* is chosen from the list and is compared with *46*. Because *46* is less than *60*, all numbers greater than *60* are eliminated from the search. Now, a new number *51* is selected from the remaining numbers and is compared to *46*. Thus, *46* is still less than *51* so all numbers greater than *51* are again eliminated. This process is recursive until the number selected equals *46*. In the same way, problems in this research are divided recursively until directly solved.

The second method takes a complex problem and divides it into subcomponents that are different from each other but are more directly solvable than the original problem. Fundamentally, this method uses a more theoretical sense to solve a problem, rather than being specifically implemented in software; however, this methodology allows a complex problem to become modular and as aforementioned, sets achievable goals that are integral to the development of a solution. For example, an engineering team comprised of electrical, mechanical, and chemical engineers works on a project. Because each group is specialized in a particular area of engineering, it is only logical to take the project goal and subdivide it into simpler projects for each team to solve separately. Upon completion of each subcomponent by the respective engineering team, the project compiles together to function as a whole. This method of divide and conquer is most often referenced in this research as a way to develop modular control theories and algorithms. In addition to divide and conquer methodologies, it is necessary to introduce a fundamental concept in control theory itself that is relevant to this project.

In order to control a system, there exists some knowledge or data about the system with which the control algorithm can analyze to determine the respective output. Fundamentally, every system has some type of data flow from input to output; however, the control used to determine the output from the input may be different. Accordingly, it is necessary to present two different control methodologies and correlate the usage of one method into this research.

The first control method is referred to as open loop control, and it is the control methodology that is used in this project. Open loop control requires no previous estimation of the system's operating state [22]. The data arrives at an input *I* and then travels through a control plant *P*, and then flows to the output *O*. Control of the system is handled strictly within the plant *P* by analyzing the incoming data, passing the input through some algorithm that determines the output as seen in Figure 11.

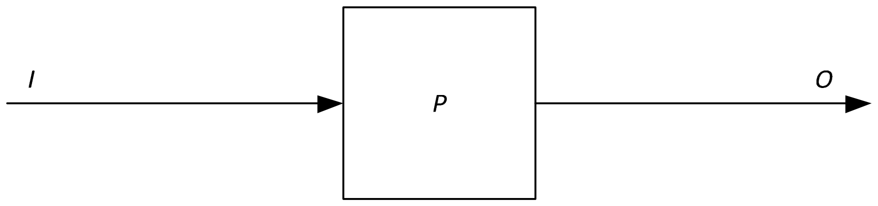

Figure 11. Open Loop Control from Input to Output

There are several advantages in using open loop control. One advantage is that the system requires no knowledge of a previous system state; the design of the plant or algorithm is considerably easier in that the data flow is unidirectional from input to output. Thus, no stability criterion of the plant needs to be assessed. Another advantage of open loop control is that it is often cheaper to implement in hardware. Because no feedback of data or signals is required, it eliminates the need to provide the circuitry to implement a feedback loop. Open loop control comes with disadvantages as well. Although an equivalent advantage, no knowledge of the system's state can be detrimental to the system's operation. Without previous knowledge, a system may be operating in an undesired state, thereby not producing the proper outputs. This leads to another disadvantage in that errors are difficult to correct without feedback. Errors must be corrected at the plant; whereas, a feedback may be able to provide error correction as will be presented in closed loop control.

Closed loop control, as its name states, differs from open loop control in that there is some type of feedback from the output to the input. This provides the entire system knowledge of the system's current state of operation [22]. Similar to open loop control, the system is fed data at the input; however, the input data is in some way compared to the feedback loop data to determine a proper input to the operating plant. The combination of input and feedback data is sent through the plant and arrives at the output. Data at the output is then sent to the input to be re-analyzed against the input as shown in Figure 12.

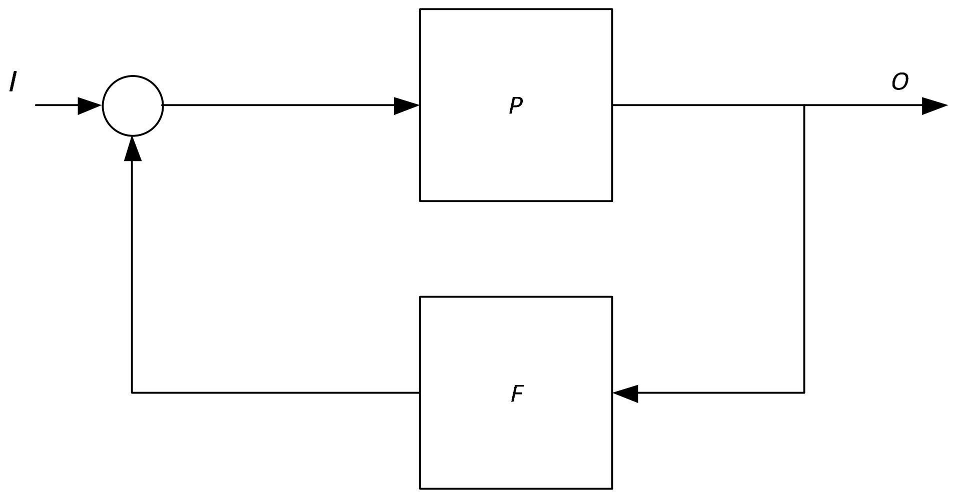

Figure 12. Closed Loop Control from Input to Output

Clearly, closed loop control has some immediate advantages compared to open loop control. Data feedback from output to input allows the overall system to be more autonomous, as it is able to correct errors, change system state, and reconfigure based on operating state information. Consequently, inherent disadvantages also come from closed loop control. The plant is more difficult to design as it must meet a different set of stability criterion as it analyzes both input and feedback data. Comparable to open loop control, there may be a need for additional circuitry in the feedback loop, depending on what type of feedback is needed.

Although open and closed loop control has their respective advantages and disadvantages, open loop control will be primarily used in this research for a couple of reasons. First, this project primarily serves to explore a proof of concept. As such, a design of system feedback as found in closed loop control would amplify the difficulty of the original project goal and may hinder the success of showing proof of concept. In addition, open loop control is implementable into available circuitry that is used in this project.

3.3 Control circuitry

Hardware is an implementation for network theory and concepts, complementing intangible equations and processes by bringing these elements into a physical, measurable environment. In this research, hardware implementation has many different components with variable functionality. This section serves to provide the reader with a background of individual circuit elements in order to understand the physical role that each individual piece of hardware plays; as well as, introduce potential platforms and capabilities of hardware components that the system uses as a whole.

As the title of this research suggests, a smart phone plays a fundamental role in the overall operation of the system. As aforementioned, the system requires dense computing resources in alignment with various wireless capabilities, dynamic programming ability, and the integration of various sensors. Accordingly, an appropriate smart phone was chosen to satisfy these requirements and was generously donated by Google. The HTC Evo, as shown in Figure 13, comes equipped with a broad array of sensors: accelerometer, gyroscope, magnetometer and many others. In addition, it has enabled Bluetooth, Wi-Fi and 3G/4G wireless capability, and it also comes with a 1 GHz processor, 1 Gigabyte of ROM and 512 Megabytes of RAM [23]. These specifications adequately supply the computing resources and networking tools needed in this project.

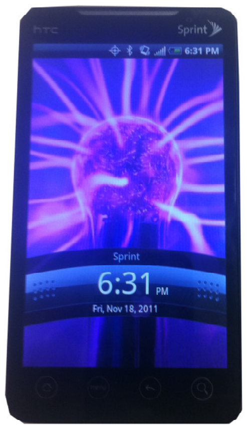

Figure 13. Picture of HTC Evo Smart Phone

Most notably, the accelerometer and gyroscope sensor will the most common referenced and utilized sensors in the system. The tilt or yaw, pitch and roll information as shown in Figure 14, is used to generate necessary information for the system's algorithms to use. The Evo also provides a 4.3 inch LCD display that provides a user with real-time network information and system control, through a developed application running on Android OS [23].

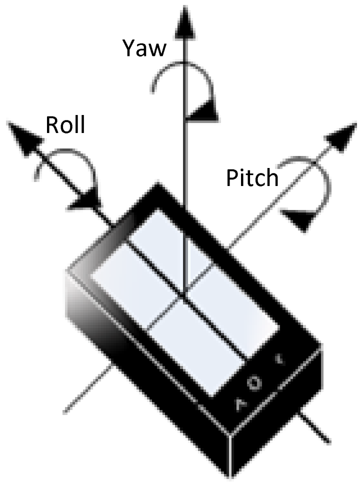

Figure 14. Smartphone and Respective Yaw, Pitch, and Roll

In order to bridge the phone with control circuitry, necessary microcontrollers interact with the system to provide wireless communications, a platform to run algorithms and electrical control ability over circuit components. Arduino microcontrollers are increasingly common devices that are relatively easy to program and provide adequate functionality to serve this project. Specifically, this project incorporates two separate models of Arduino: Arduino BT and Arduino Uno. The Arduino BT as shown in Figure

15, is a model of the standard Arduino microcontroller with an embedded Bluetooth receiver. Playing a vital role in establishing a Bluetooth connection with the smart phone, the Arduino BT also comes with I^2C networking capability which will be explained later in further detail.

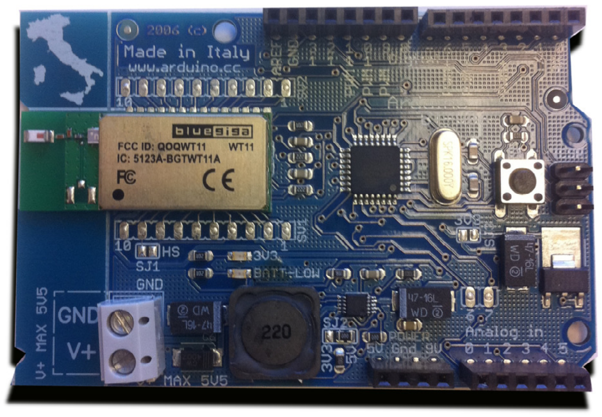

Figure 15. Arduino BT (Bluetooth Enabled)

While the Arduino BT interacts with the phone via Bluetooth, it also interacts with Arduino Uno via I^2C. The Arduino Uno as shown in Figure 16, is a standard microcontroller from the Arduino family that has multiple capabilities including Analog and Digital inputs and outputs, PWM, SPI and I^2C [24]. It is primarily used in this project to interact with control circuitry.

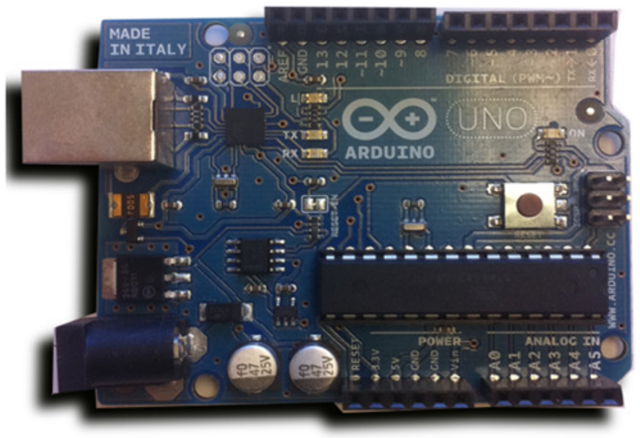

Figure 16. Arduino Uno Microcontroller

The circuitry that generates voltages for phase shifters is controlled by an Arduino Uno. While the functionality of the circuitry will be explained in full detail in the design section, a small background on each circuit element will be explained now. A demultiplexor from Texas Instruments [25], has 2 select inputs that follow the truth table in Table 2 to determine the state of four output lines.

Table 2. Truth Table for Demultiplexor

Select	Input A	Input B	OUT 0	OUT 1	OUT 2	OUT 3
L	X	X	X	X	X	X
H	L	L	L	H	H	H
H	H	L	H	L	H	H
H	L	H	H	H	L	H
H	H	H	H	H	H	L

A digital potentiometer from Microchip is used to divide the VCC voltage of 5 Volts to an appropriate voltage between 0 and 5 Volts that is sent to an amplifier stage and the phase shifters thereafter. The digital potentiometers have onboard memory which can be written to using an SPI interface. More information on SPI can be found in the next section. Table 3 shows the digital words that may be written to the digital potentiometer to set the value of the wiper which controls the voltage at the output [26].

Table 3. Digital Words for Microchip 4131

ACTION	DIGITAL WORD
WRITE	0000 00xx xxxx xxxx
READ	0000 11xx xxxx xxxx
INCREMENT	0001 0100
DECREMENT	0001 1000

An amplifier stage is necessary to provide an appropriate gain to the voltage output by the digital potentiometer before arriving at the phase shifter. To achieve this, the project incorporates operational amplifiers (op-amp) in a non-inverting configuration. The gain of the op-amp stage is found by observing the voltage input in relation to the voltage output.

$$V_{out} = (1+\frac{R2}{R1})V_{in} \tag{0.22}$$

Assuming that the operational amplifier is ideal, (0.22) can be derived as V_{in} is present on the negative pin and is therefore, the output of voltage division of V_{out} as shown in Figure 17.

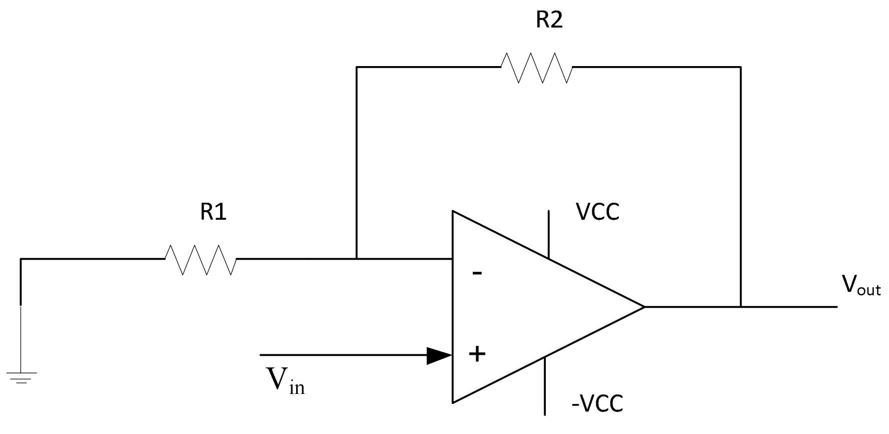

Figure 17. Non-inverting Operational Amplifier Configuration

Because the op-amps, digital potentiometers, and other circuit elements function at different voltage levels, it is necessary to regulate the voltage to each of these elements respectively. Voltage regulators from Texas Instruments are selected based on their voltage and power ratings to supply and regulate voltages of 5 and 12 Volts to the entire system.

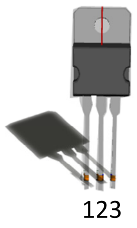

Figure 18. Linear Regulator with Pinout (Pin1 - Voltage Input, Pin2 - Ground, Pin3 - Voltage Output)

3.4 Communications

The ability of hardware to communicate with other hardware is paramount to the development and success of a control network. More specifically, devices are created by an array of vendors who often don't design a product to be used for one purpose; therefore, there exists a necessary layered communications model in any communications system that all devices adhere to so that data exchange is possible.

Common practices or implementations of layered communications models are ubiquitous and many of these implementations interact with one another. A common referenced model to provide a necessary background is the Open Systems Interconnection model or commonly referred to as the OSI model. The model was initially created by International Organization for Standardization in order to implement a fundamental structure for communications [27, 28]. The OSI model is broken up into seven separate layers as shown in Figure 19, with each layer providing two main functions (1) Each layer is responsible for handling data in a specific way so as to minimize communications between respective layers (2) Provides a virtual set of rules for data handling at each level when necessary [28, 29]. To provide an important overview of the communications used in this research, each layer of the OSI model will be briefly explained, followed by a parallel model of communications used specifically in this research at their equivalent layers.

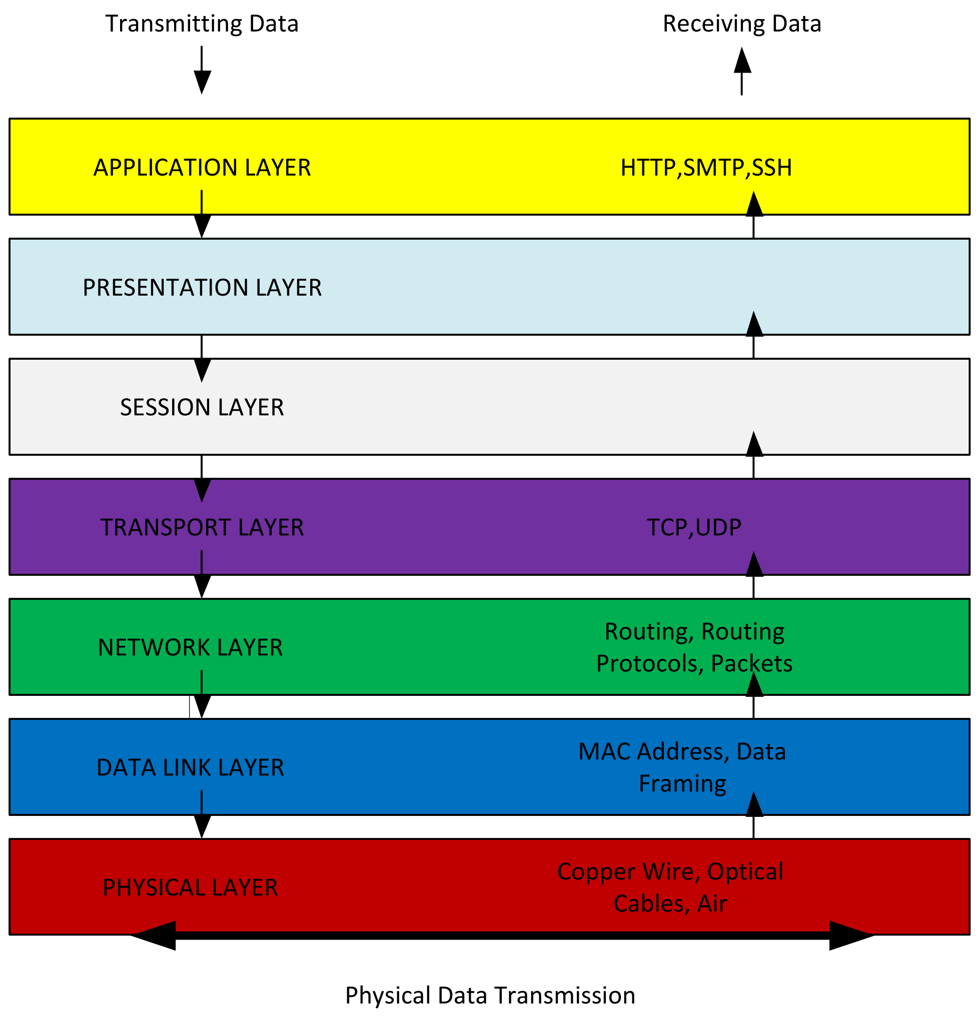

Figure 19. OSI Model and Data Flow

The first layer of the OSI model is the Physical Layer or often referred to as PHY. It serves primarily to establish a physical connection in between two communicating endpoints and physically send data across this medium. In addition to connecting an interface to a transmission medium, the PHY layer is also responsible for termination of a physical connection, flow control and physical modulation of signals when necessary [28]. Examples of the PHY layer include and are not limited to copper cables, optical cables, dielectric materials, wireless communications mediums and many more [29].

The second layer is called the Data Link Layer. Many responsibilities of this layer include framing of data, detection of physical error connections, flow control and relative functional communication with a communicating layer two endpoint [28]. This layer also has a sub-layer within it called Media Access Control or MAC protocol. MAC addresses are assigned to communicating layer two endpoints to achieve some of layer two's responsibilities such as flow control and functional sending of frame data. These addresses essentially serve as a street address. When sender *A* in Washington desires to send mail to receiver *B* in California, sender *A* needs an address to send the mail. MAC addresses provide the same functionality at layer two.

The Network Layer is the third and has the primary responsibilities of routing packets to communicating layer three devices. This ability and responsibility is important for routing information in between different sub-networks. Layer three packets differ from layer two frames in that packets have additional header information that is attached to data that contains routing and other important layer three information [28]. In addition, routing protocols and algorithms are implemented at this level to achieve congestion control, least cost routing and QOS policies. Common examples of network layer devices include routers and switches [29].

The fourth layer is the Transport Layer. The primary responsibilities of this layer include the routing error process handling, connection and termination channels of routing endpoints and network congestion control [28]. Many protocols exist at this level that handle data flow and error correction in order to improve network efficiency or maintain data integrity. Common examples of these protocols are found in TCP and UDP [29]. Whereas TCP has the functionality of handshaking between two endpoints to ensure data integrity at a slower communication cost, UDP delivers data from one communicating endpoint to the other as quick as possible at the expense of data integrity [28].

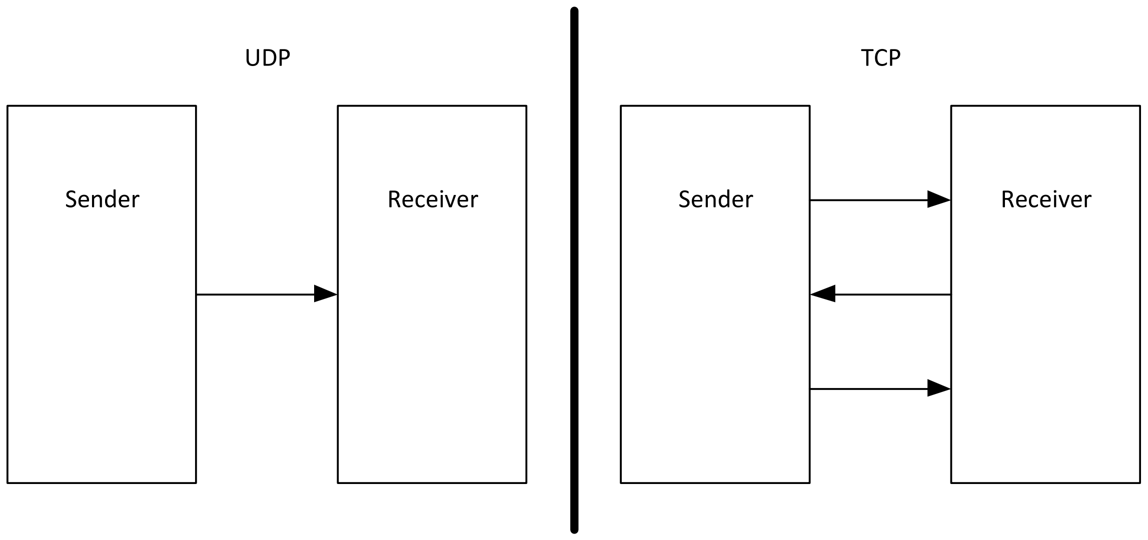

Figure 20. TCP Versus UDP

The final fifth through seventh layers are often bundled together as their pertinence into communication networks is highly dependent on the setup and operability of the network. The fifth layer is called the Session Layer and is responsible for establishing, maintaining and terminating remote procedures between computing endpoints [28]. The sixth layer is called the Presentation Layer and functions as a translator between network communication layers and the Application Layer which is the seventh layer. The Application Layer is responsible for implementing many known protocols such as SSH, Telnet, SMTP and many others [28].

For this research, it is necessary to analyze several different transmission mediums, protocols, and network communication objects, in order to gain practical perspective into how each networking component operates within a layered model. To begin, there are clearly two important transmission mediums that exist at the PHY layer: copper wires for circuitry communication and air for wireless communications. At the second layer, two important addressing and communication protocols exist to allow microcontrollers and circuit components to communicate with one another. Inter-Integrated Circuit protocol or I^2C is a two-wire, multi-master and slave interface developed originally by Phillips to allow low-speed peripheral devices to communicate with larger devices such as computers, microcontrollers and other high speed operating devices [30]. The protocol encapsulates data into a specific framing type and uses an address placed in the frame header to communicate with a specific device. All I^2C devices connect to the system bus using two wires at the connection interface, where both bus wires SDA and

SCL are connected to VCC via a pull-up resistor. SCL is used as a clock line which is generated by a master device connected to the I^{2}C bus and SDA is the data line through which all data is communicated. As aforementioned, there exist two types of devices that may connect to the I^{2}C busses. A master device is responsible for setting a system clock on the SCL line and providing unique 7-bit addresses to all other slave devices on the network, although this may be alternatively statically configured with each slave. A slave device connects to the I^{2}C busses sharing the same SCL and SDA as a master device, and may have a dynamically assigned 7-bit network address or one that is statically configured. Operation of I^{2}C can be seen from Figure 21.

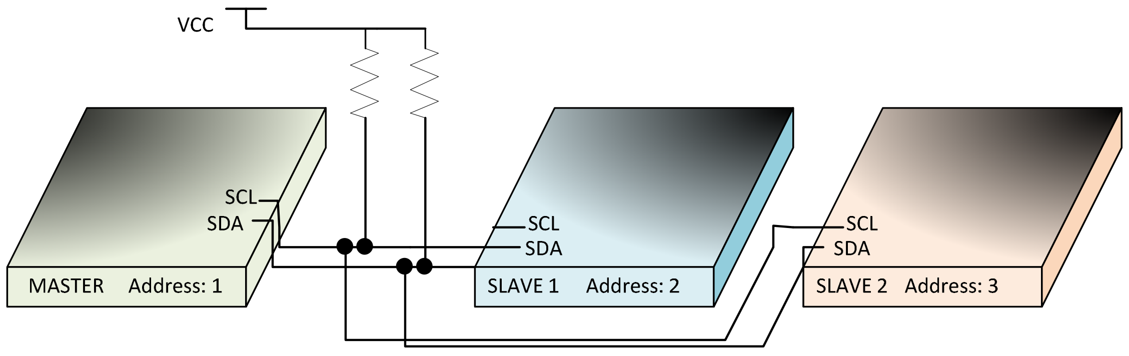

Figure 21. I^{2}C Network with Master and Two Slaves

Timing is especially important on the I^{2}C bus. Because I^{2}C is a synchronous protocol, as all devices transfer data at the rate of the clock speed on SCL, a specific protocol must be followed. A graphical representation of I^{2}C timing is shown in Figure 22.

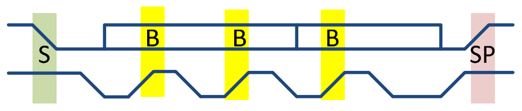

Figure 22. I^{2}C Timing Diagram

The communication process begins with a start condition, labeled *S* in Figure 22, when the SDA line goes low and the SCL line maintains high. Next, the data is set on the SDA line while the SCL line is low and then is sent or read by devices when the SCL line proceeds high. This continues for the entire data stream and then is stopped by a condition *SP*, where SCL maintains high and SDA rises from low to high as shown in Figure 22. Although I^{2}C is useful for data communications of devices it also comes with limitations. The 7-bit network address clearly restricts the amount of devices that may be connected to a single bus. In a larger system with thousands of devices, this may pose a problem; however, this research doesn't incorporate this many devices. Another limitation is the ability to use I^{2}C over large distances, as it is restricted primarily to a few meters [30]. This too is not a problem in this research, as all the devices are within half a meter of one another.

Like I^{2}C, another layer two protocol is used to provide communications between the microcontrollers and voltage circuitry. SPI is a three sometimes four wire interface that operates in a master-slave relationship, capable of half-duplex and full-duplex communications [31]. Shown in Figure 23, SPI utilizes synchronous communication between a master device and slave devices using a clock line called SCLK.

Communicating endpoints are selected using the SS or slave select line, which can be active high or low. The two remaining lines labeled MISO and MOSI stand for “Master In Slave Out” and “Master Out Slave In” respectively, are used for data communication between the devices.

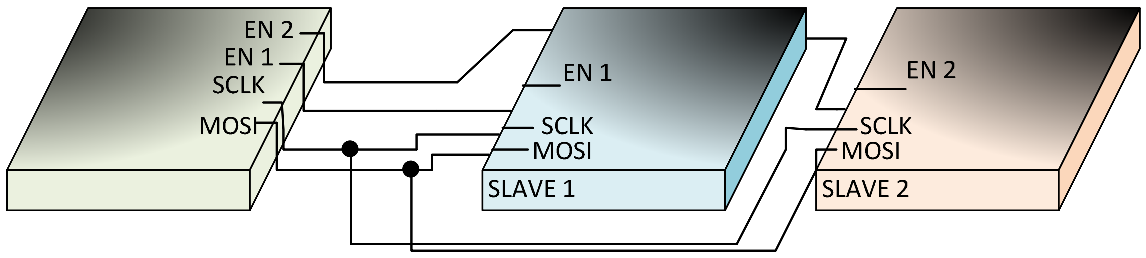

Figure 23. SPI Network with Master and Two Slaves

SPI has some distinct advantages over I^2C in that it is a full duplex communication protocol, meaning that both the slave and master may be talking at the same time. In addition, because SPI uses SS lines instead of an addressing protocol, more devices may be connected to the bus network depending on how many SS control lines are available. SPI also has inherent disadvantages in that it requires more lines for connections than I^2C, which in turn require chips and devices that use SPI to require more connecting pins. Furthermore, SPI can only support one master device on the network. The inability to provide network addresses may be a disadvantage depending on the network needs.

Because a smart phone is the primary control unit for the network in this research, it is necessary to include wireless communications protocols at are utilized in research. Although these protocols are multi-layered protocols in that they have functions that operate at several levels of the communications model, it is important to provide a brief overview of how they work. Bluetooth is a common wireless communications protocol developed by Ericsson in 1994 as a way to wirelessly interface communication devices in a serial-communication style [32]. The network operates at a frequency of 2.4 GHz over short distances depending on the output power of the antenna [33]. Furthermore, similar to SPI and I^2C, Bluetooth devices form a master-slave network with all slaves sharing the clock provided by the master device. Up to seven devices may be connected in a piconet, which is an ad-hoc network that is proprietary to developed Bluetooth technology [33]. Bluetooth devices are split into separate categories depending on their output power, which determines their transmission distance and versions, which determine the maximum data transmission rate they support. Bluetooth also is attractive from a security standpoint in that it provides encryption of data from endpoint to endpoint.

Wi-Fi is a wireless communications mechanism to connect devices that have an enabled wireless network card, to access the internet through a wireless access point or AP. In order to achieve a connection, wireless network cards are created to meet IEEE 802.11*x* standard, where *x* stands for a version of the standard protocol. Available standards and their frequencies are shown in Table 4 [34].

Table 4. 802.11 Protocols and Relevant Communications Information

Protocol	Frequency (GHz)	Bandwidth (MHz)	Data Rate (Mbit/s)
a	3.7, 5	20	6,9,12,18,24,36,48,54
b	2.4	20	5.5, 11
g	2.4	20	6,9,12,18,24,36,48,54
n	2.4, 5	40	7.2, 14.4, 21.7

Wi-Fi is maintained by the Wi-Fi Alliance [34]. In addition, Wi-Fi enabled devices support a TCP/IP protocol stack to support internet communication protocols in order for the device to communicate with other devices on the network.

A protocol is a virtual known set of rules that two communicating parties adhere to when exchanging data [29]. For instance, languages such as French, English and German are protocols, as there are specific known rules that make words and sentences understandable. In the same way, computer and control networks utilize many protocols to normalize and unify communications between devices. Specifically, this research refers to protocols that are implemented in software and have therefore been programmed to interpret transmitted and received data in a certain way. Software protocols allow data processing, transmission and reception to be easier from device to device, by providing a unique set of rules that both parties understand. Customized protocols developed specifically for this research are discussed in the design portion.

To allow computing devices to communicate with one another across a network, a physical connection medium exists to allow data transfer coupled to a virtual connection medium called a socket. Creating a socket is necessary for communicating endpoints in this research that use both Bluetooth and Wi-Fi connection mechanisms because once data is physically transmitted and received by two endpoints, the devices must buffer the data, and determine to which application the data belongs. Creation of a socket is handled by the operating system and is implemented through an Application Programming Interface or API. To successfully create a socket, there must be both a server and a client active in a communications medium. The server decides to open a socket to listen for information while also creating a receiving buffer to store data packets as they are sent from the client, and a transmitting buffer, in case data packets need to be sent back to the client. Internet sockets on computers are then assigned or complete a “bind” action to a virtual port or connection, to listen for incoming data [28]. Port values range from hexadecimal numbers 0x0000 to 0xFFFF. If the port has not been occupied by another program, the server application is ready to receive data from the client and is deemed to be “listening”. Table 5 lists some reserved ports for internet protocols [28].

Table 5. Common Protocols and Respective Ports

Protocol	Port
FTP (File Transfer Protocol)	20,21
SSH (Secure Shell)	22
Telnet	23
SMTP (Simple Mail Transfer Protocol)	25
HTTP/HTTPS (Web Browsers)	80/443

On the client side, the computing device goes through a similar process of creating buffers and then creating a socket. The client will then specify the network address of the server and listening port in the software. Once these tasks have been completed, the client makes a request to the server, and when the server accepts, a communications channel has been established. The server and client will now abide by a communications protocol written in the API to pass information back and forth.

From the description of sockets, a clarification of the word server is discussed and will be further presented, as it is an integral part of the research. Server is a name for a computer that is capable of storing information and enabling endpoints to view this information via the internet. Typical servers such as Microsoft IIS and Apache listen on ports 80 and 443 or corresponding protocols HTTP and HTTPS respectively for requests made from computing endpoints. The server interprets these requests and delivers information back to a client which can be viewed in an internet browser as shown in

Figure 24. In this research, a server is used to display real time information about the control network and allow users with an internet connection to observe critical values in the system.

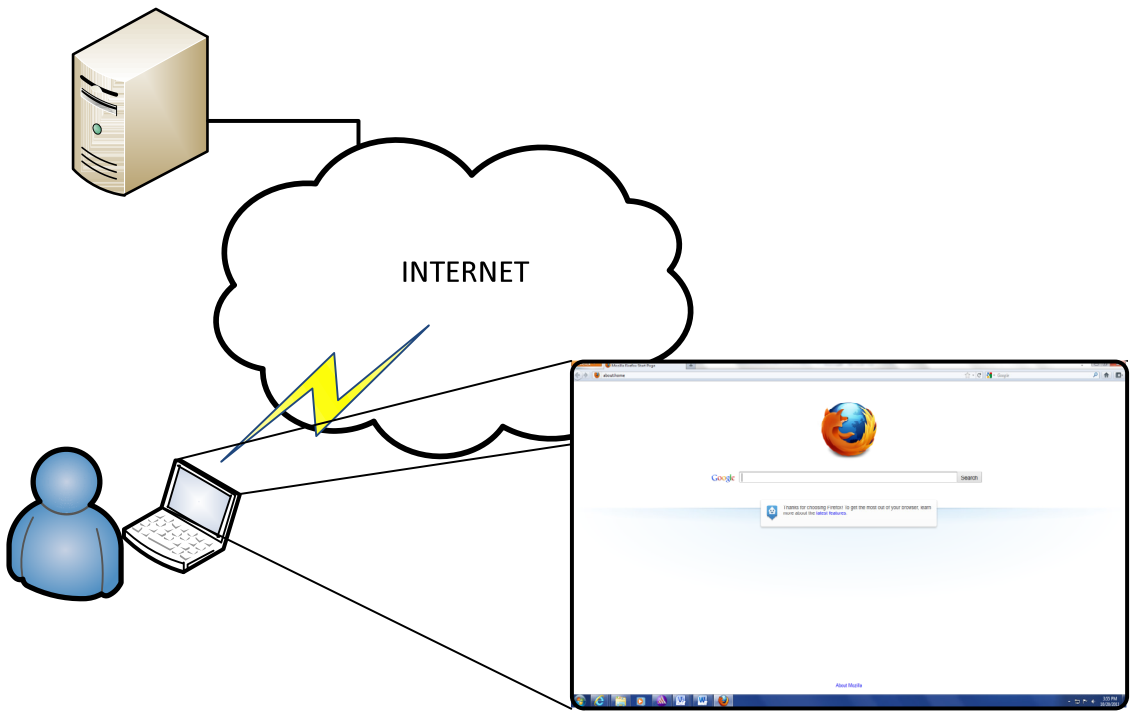

Figure 24. User with Internet Connection to Server

CHAPTER IV

SYSTEM DESIGN

4.1 Array design

This project utilizes the background aforementioned to design and fabricate a four by four microstrip patch antenna array. The process includes designing a single microstrip patch. A sufficient single model of a microstrip patch will have similar characteristics when placed in an array. Next, simulate the single patch in an infinite array association to observe how the patch will respond when surrounded by other similar patches. Last, design a four by four finite array model that includes cross coupling among the patches and other losses. It is from the final design that the physical array is constructed. Throughout this process, the analytical use of the simulation tool will help to improve the design as observations of VSWR, input impedance and resonant frequency can be tweaked to improve the overall design.

To begin, the design of a microstrip patch is straightforward. From (0.13) and (0.14) we can determine the dimensions of the microstrip patch. For this design, the microstrip patch is going to use Rogers 5880. The characteristics are shown from Table 6 [35].

Table 6. Design Characteristics for Antenna Dielectric

Duroid	ε_r	Thickness
Rogers 5880	2.2	.787 mm

The project desires a resonant frequency of $f_r = 2.44$ GHz. Using the values from Table 6, the width and length are determined to be

$$W_{initial} = 48mm, L_{initial} = 40mm, d = 7mm \tag{0.23}$$

Numerical analysis for probe placement can be done using the cavity model [18]; however, for this project, the probe placement relies on analytical analysis from the results of software. After simulating these dimensions, the results were not satisfactory. Using knowledge of probe placement effect on input impedance and an adjustment of width and length to a near unity ratio, a satisfactory simulation is achieved. The final dimensions of the microstrip patch are represented from (0.24).

$$W_{final} = 39.75mm, L_{final} = 40mm, d_{final} = 5.75mm \tag{0.24}$$

From these dimensions we achieve the following VSWR and input impedance results.

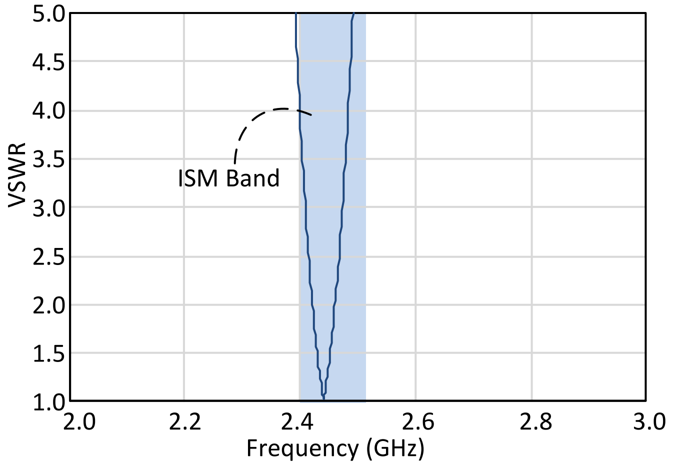

Figure 25. VSWR for Single Patch Antenna

From Figure 25, it is clear that the VSWR is below 1.10 for a frequency of f_r=*2.45 GHz*. This is satisfactory for design standards as we note that a perfect VSWR would be exactly 1.0. The VSWR provides an indication for the standing wave ratio between the incident and reflected voltages. In addition, the input impedance at our resonant frequency is near 50 Ohms shown in Figure 26.

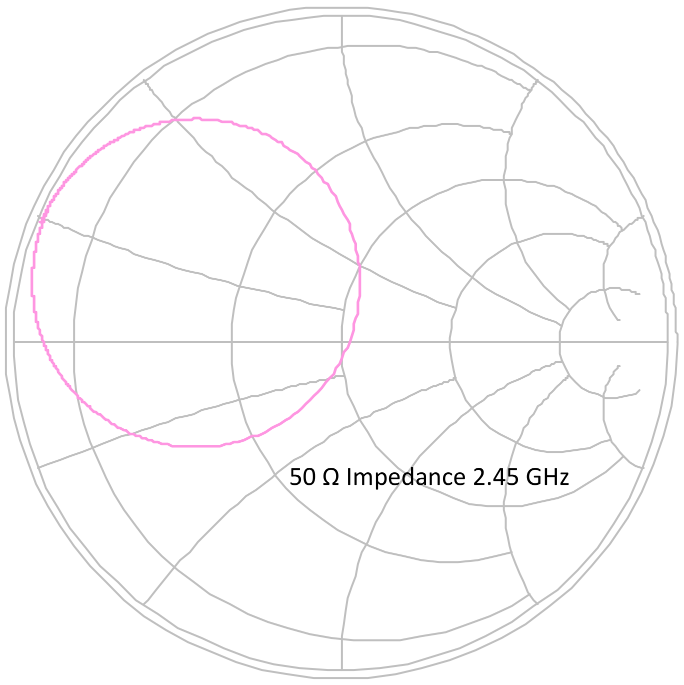

Figure 26. Input Impedance Single Patch Antenna

It is necessary to look at the single element beam pattern to determine possible beam patterns for the entire array. In addition, from the theory discussed in Chapter III, the single element beam pattern multiplied by the array factor will provide the array pattern. The beam pattern will also provide information of estimated maximum scan angles and any radiation anomalies that may occur.

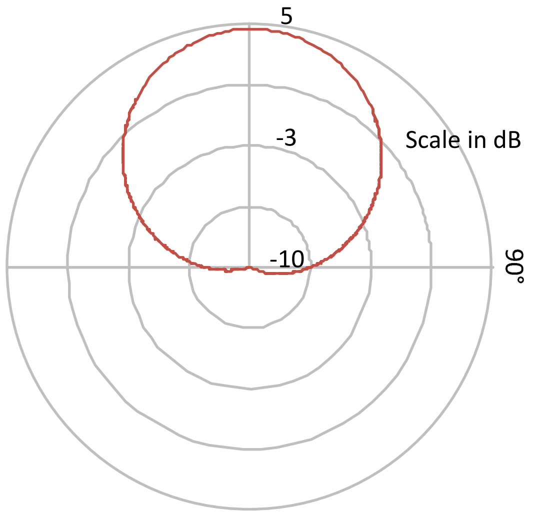

Figure 27. Single Element Radiation Pattern

The result shown in Figure 27 is the vertical cut plane and is indicative of common microstrip patch designs. From these successful results, this design of the microstrip patch is now used in further simulations to build an array that emulates these characteristics.

After completing a single microstrip patch, it is necessary to see how the patch reacts in an infinite array. In order to construct a finite array, knowledge of an infinite array is pertinent to changing design parameters if needed. The microstrip patch is inserted into the infinite array simulation with λ/2 spacing and gives with satisfactory results. The VSWR in Figure 28 shows that the patch has similar characteristics in an infinite array.

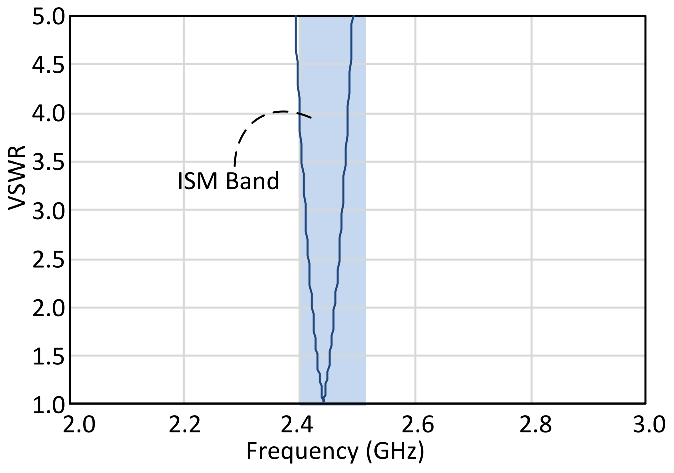

Figure 28. VSWR Infinite Array Simulation

In addition, the input impedance represented in Figure 29 nearly emulates that of the single patch. Provided these results, a finite, four by four microstrip patch array is now designed. The new array takes on the same dimensions of the individual microstrip patch cell. It is placed consecutively along an axis to resemble the final image shown in Chapter III. The array requires a matching of all elements equally spaced by a distance of half a wavelength. This standard spacing allows the unit cell to operate cohesively when placed in the array.

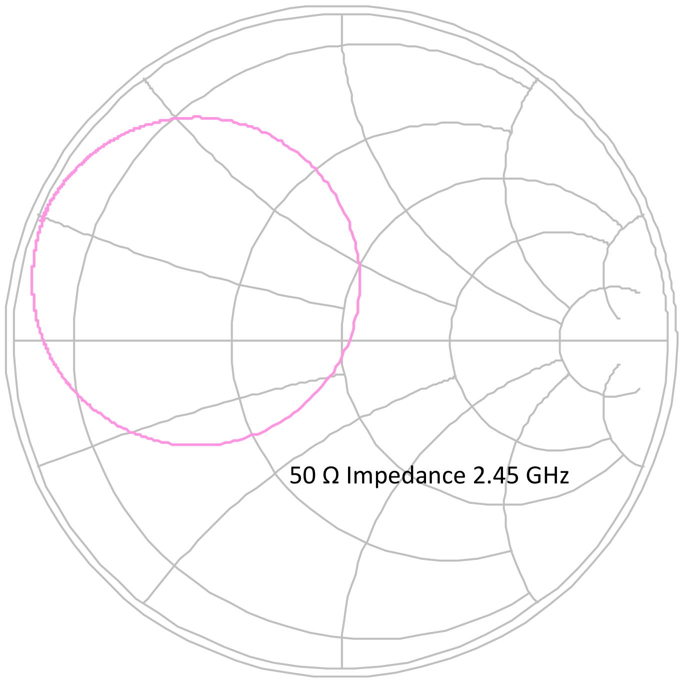

Figure 29. Input Impedance Infinite Array

From previous results, the finite array is constructed as shown in Chapter III, by copying the original patch design into a four by four array pattern. The simulation is set up so that each patch receives the same amplitude and phase; however, each has an individual wave port so that separate VSWR and input impedance may be observer. Results from the simulation yield satisfactory outcomes. The VSWR for all 16 elements is shown in Figure 30.

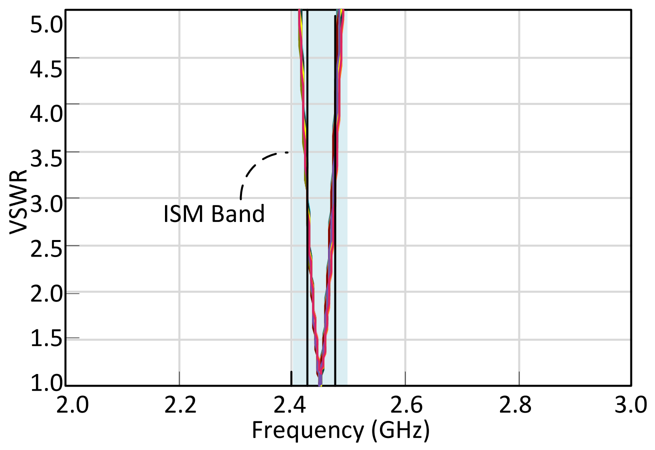

Figure 30. VSWR Finite 16 Element Microstrip Patch Array

Notably, the VSWR for all elements nearly overlaps one another and is contained within the ISM frequency band having a resonant frequency of f_r*=2.45* GHz. We note that the many elements share a similar VSWR which indicates a similar response among the connected unit cells. In addition, observation of the smith chart in Figure 31 yields that while some variance of input impedance exists between the elements; the general input impedance is near the 50 Ohms design criterion. Some variation exists due the proximity of the elements to one another, however; we have considered to neglect these effects in this research.

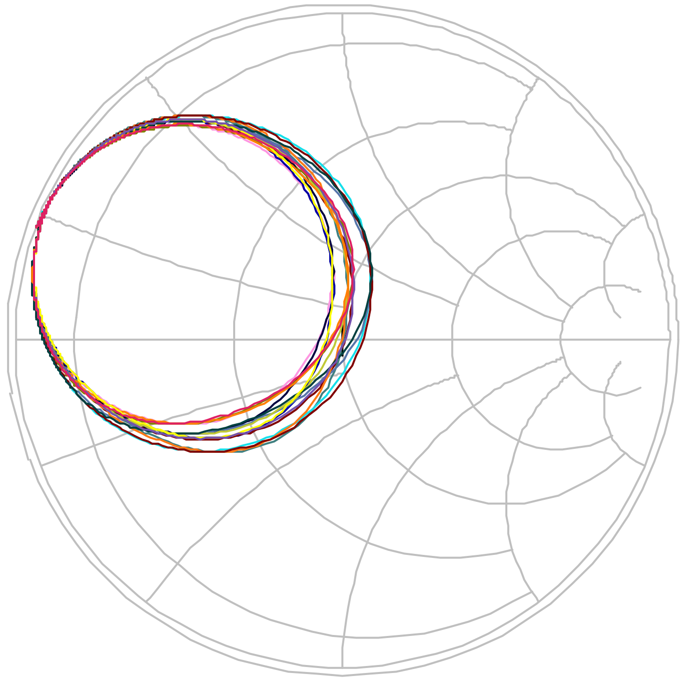

Figure 31. Input Impedance Finite 16 Element Microstrip Patch Array

Provided these results, it is sufficient that a formidable array model for this project is complete. This model will be used in fabrication and final testing presented in the experiments and results section.

4.2 Control design

This research incorporates many aspects of electrical engineering, coupling systems and control with electromagnetics and antennas. Programming and mathematical algorithms comprise network control theory while a system of digital logic and analog circuitry provide the necessary hardware implementation to generate control voltages for phase shifters. Bringing together different components requires an astute understanding of how data flows from one point of the system to another while interfacing many inputs such as phone control or GPS. Therefore, this section of design covers general network operation followed by a detailed account of data algorithms at a system level.

Functionally, the network has many states of operation that are possible through dynamic programming in the phone. This centers the phone as the primary tool of operation for both control and data generation. With this functionality, it is imperative that the phone establish connections with two other components that will implement physical control of the system and analyze data for system operability and observation. One connection exists using Wi-Fi where the phone connects to a remote server using a TCP/IP implementation of data exchange. This is under the assumption that the smart phone is within range of either an access point or a 3G-4G connection and the server is at an accessible IP address. Data exchanged between the phone and server consists of the current yaw, pitch and roll information of the smart phone, the progressive phase shifts for all antenna elements, system power usage information and object position, if the phone is in tracking mode. This exchange of information allows information of the system to be remotely gathered in near real time. In addition to the server connection, the phone connects to an Arduino BT via Bluetooth, which allows for full-duplex communication between the phone and phase shifter control circuitry. Through this connection, the phone passes only the progressive phase shift information for antenna elements, as this information is used by algorithms on the microcontrollers to control phase shifters. In the opposite direction, data from the Arduino BT consists of system power usage information, and when necessary, system operating state information that will be discussed shortly. These two connections sustain the entire system and allow both the control and operation of the system to succeed; whereas, without these connections and exchange of data, the system would not be able to operate.

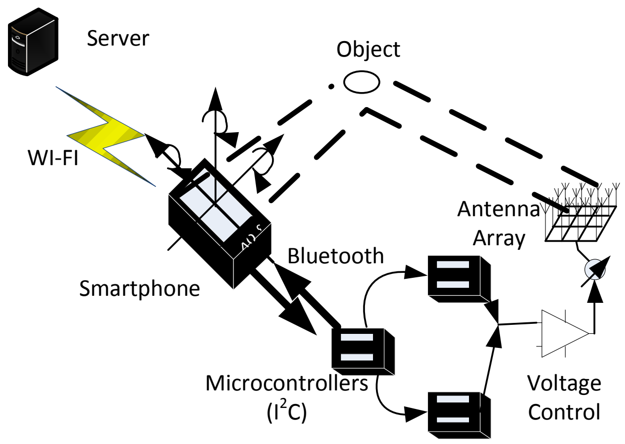

Figure 32. General Network Overview

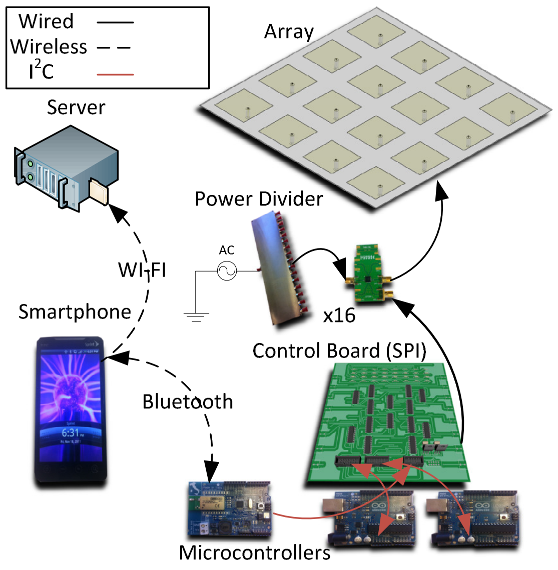

Figure 33. Network Overview with Physical Implementation

Figure 32 provides a graphical overview of individual network components from a high level, whereas; Figure 33 shows the physical depiction of each individual network element including microcontrollers, power divider, PCB control board and antenna array. As aforementioned, because of many system components it is necessary to use a divide and conquer approach to designing all components, especially data flow and algorithms.

The system operates in three different states which conduct what algorithms should be run at the system and sub-system levels. The first mode of operation is defined as "Manual User Control". In this mode, the phone's face, when calibrated coplanar with the face of the antenna array, will determine the direction of the main beam of the phased antenna array as shown in Figure 34.

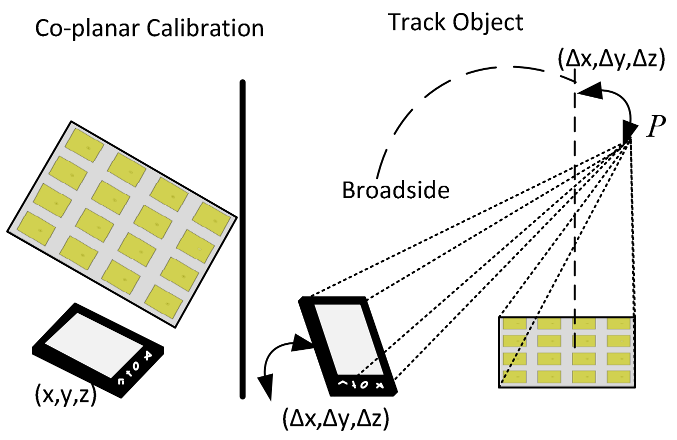

Figure 34. Manual Tracking Mode of Operation

The system algorithm differs from the other states primarily within the smart phone's algorithm itself. The algorithm pseudo code is shown in Figure 35 and the explanation is as follows. The user accesses the smart phone and establishes two connections: one with the server via Wi-Fi and one with the Arduino BT via Bluetooth. Once connected, the user calibrates the phone coplanar with the radiating face of the phased array, and establishes the appropriate broadside radiating direction. Next, the user generates yaw, pitch and roll information from the phone by interacting with the program's interface. However, from the broadside direction, the phone generates phase shifts according to the movement of yaw, pitch and roll information, not based on an object's position in space as this feature is included in other operating states. Upon generating progressive phase shifts, the information is dispersed to the server and Arduino BT whereby the microcontrollers interact with the control circuitry to produce a control voltage and respective phase shift among all antenna elements. Gathering state information such as power usage is optional in this operating state.

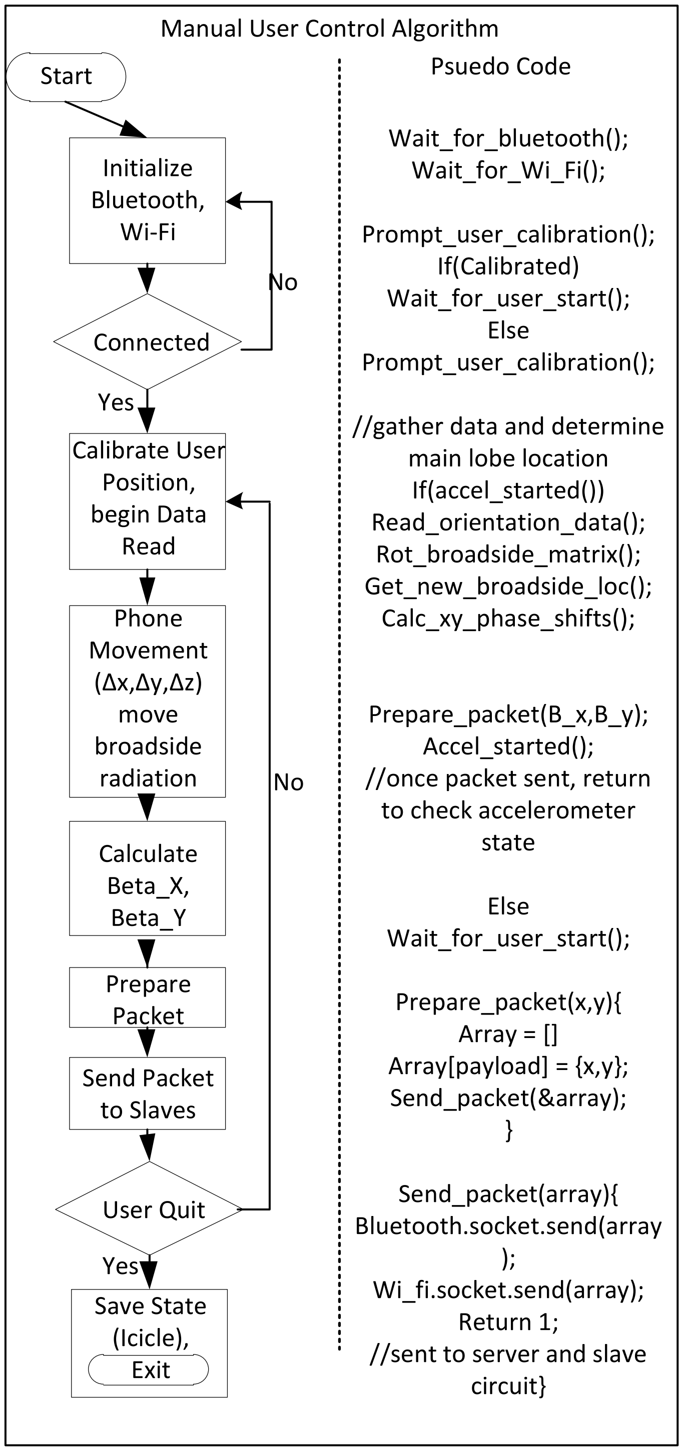
Manual User Control Algorithm
Start
Initialize Bluetooth, Wi-Fi
Connected
No
Yes
Calibrate User Position, begin Data Read
Phone Movement (Δx,Δy,Δz) move broadside radiation
Calculate Beta_X, Beta_Y
Prepare Packet
Send Packet to Slaves
User Quit
No
Yes
Save State (Icicle),
Exit

```
Psuedo Code

Wait_for_bluetooth();
Wait_for_Wi_Fi();

Prompt_user_calibration();
If(Calibrated)
Wait_for_user_start();
Else
Prompt_user_calibration();

//gather data and determine
main lobe location
If(accel_started())
Read_orientation_data();
Rot_broadside_matrix();
Get_new_broadside_loc();
Calc_xy_phase_shifts();


Prepare_packet(B_x,B_y);
Accel_started();
//once packet sent, return
to check accelerometer
state

Else
Wait_for_user_start();

Prepare_packet(x,y){
Array = []
Array[payload] = {x,y};
Send_packet(&array);
}

Send_packet(array){
Bluetooth.socket.send(array
);
Wi_fi.socket.send(array);
Return 1;
//sent to server and slave
circuit}
```

Figure 35. Manual User Control Algorithm System Level

The second mode of operation is defined as “Manual Object Tracking”. As the name implies, the phone’s algorithm focuses the main beam of the array at a particular point in space, rather than allowing a user to manually control the direction of the beam. The term ‘manual’ in this case refers to the system using the smart phone’s tilt information to generate progressive phase shifts that track the object instead of the tilt information from the accelerometer and gyroscope that are physically mounted to the array. This mode of operation may be used in a case where a soldier desires to calibrate their phone with an antenna array to track an object in space, but as they move the antenna tilts and does not stay focused on the object. Thus, the movement of the smart phone would resemble the movement of the array itself and therefore, the tilt information can be used to generate phase shifts to allow the beam to track the object.

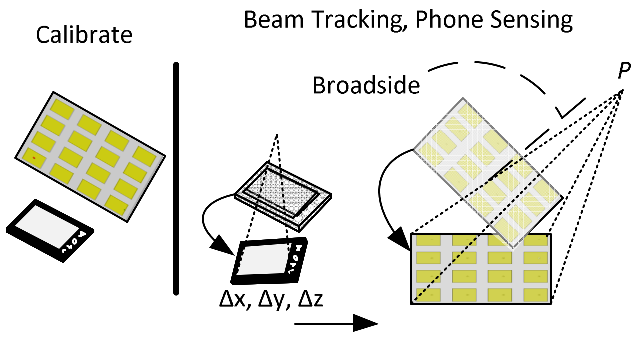

Figure 36. Manual Object Tracking Physical Representation

The system algorithm as shown in Figure 37, differs slightly from 'Manual User Control' in that the phone's tilt information is now used to shift a point in space using (0.21). Corresponding phase shifts are generated from the transformed Phi and Theta and are then used in microcontroller and voltage control circuits similarly to "Manual User Control". Here, the internal sensors of the phone are used to the greatest extent to over compensate for the physical systems movement. The overall algorithm doesn't change with its processes, however; it is indicitavely the math that changes so as to produce correct results in the system. Similar correspondences are made between these two algorithms, however; the purpose of the second algorithm is used in an object tracking sense, whereas, the manual user control more demonstrates a proof of concept. It is noted that the method of object tracking in this algorithm is very simple in design. It uses the coordinates of two objects in space to determine the distance and angles in a respective coordinate system. It then assumes that the refresh rate of the system is faster than the objects speed; whereas, other algorithms discussed in Chapter II apply historical data to estimate an object's future position.

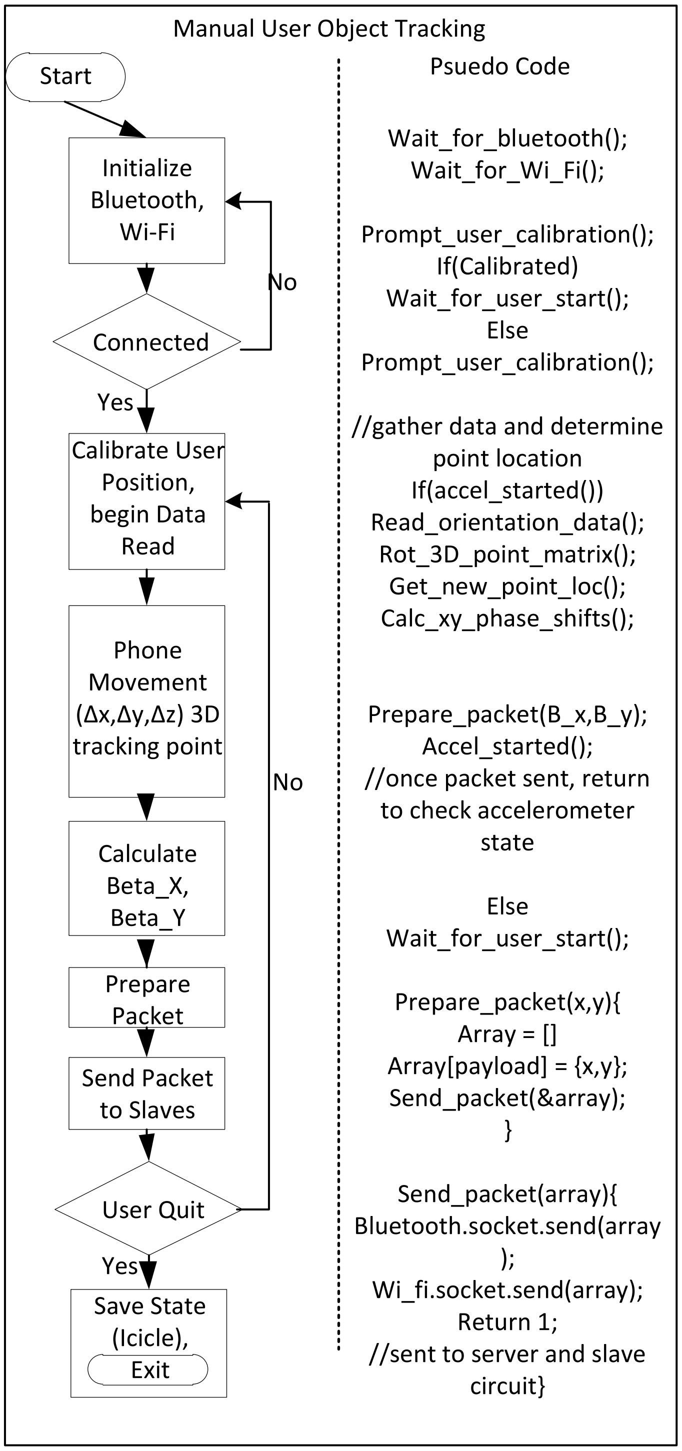
Manual User Object Tracking
Start
Initialize Bluetooth, Wi-Fi
Connected
No
Yes
Calibrate User Position, begin Data Read
Phone Movement (Δx,Δy,Δz) 3D tracking point
Calculate Beta_X, Beta_Y
Prepare Packet
Send Packet to Slaves
User Quit
No
Yes
Save State (Icicle),
Exit
Psuedo Code

```
Wait_for_bluetooth();
Wait_for_Wi_Fi();

Prompt_user_calibration();
If(Calibrated)
Wait_for_user_start();
Else
Prompt_user_calibration();

//gather data and determine
point location
If(accel_started())
Read_orientation_data();
Rot_3D_point_matrix();
Get_new_point_loc();
Calc_xy_phase_shifts();


Prepare_packet(B_x,B_y);
Accel_started();
//once packet sent, return
to check accelerometer
state

Else
Wait_for_user_start();

Prepare_packet(x,y){
Array = []
Array[payload] = {x,y};
Send_packet(&array);
}

Send_packet(array){
Bluetooth.socket.send(array
);
Wi_fi.socket.send(array);
Return 1;
//sent to server and slave
circuit}
```

Figure 37. Manual Object Tracking Algorithm and Pseudo Code

The third mode of operation is defined as “Autonomous Object Tracking”. This system level algorithm is similar to ‘Manual Object Tracking’ with the difference that the tilt information to track an object is generated from an accelerometer and gyroscope on the antenna array; however, the calculation to track an object using tilt information is still performed on the phone. The system algorithm is similar to the first two with the aforementioned difference of generated tilt information. In this case, the smart phone must wait for generated tilt information from the Arduino BT via the Bluetooth connection. Because there is a specific protocol that does this, error checking and delay cause this system algorithm to be slightly slower than the first two. Gathering the tilt information is discussed in the Arduino BT algorithm design. Upon receiving the tilt information from the Arduino BT, the smart phone performs the same algorithm as the ‘Manual Object Tracking’ case, then sends phase shift information back to the Arduino BT and control circuitry.

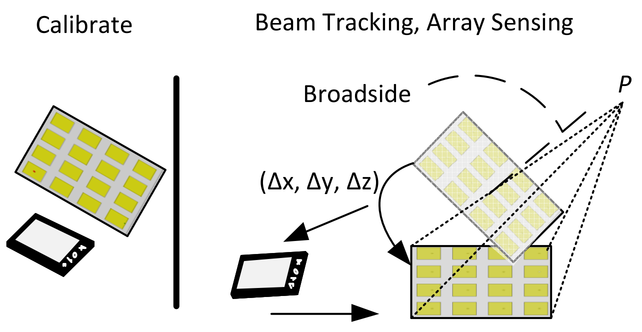

Figure 38. Autonomous Array Object Tracking

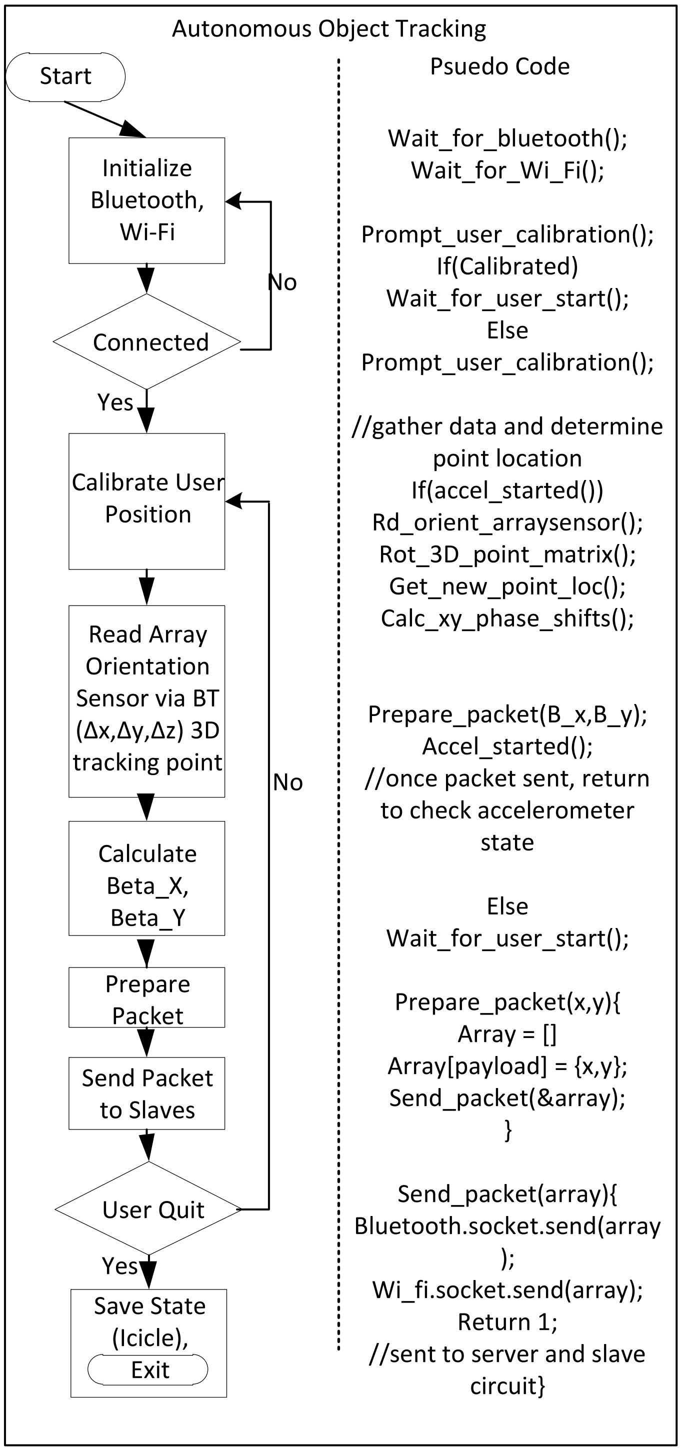

```
Wait_for_bluetooth();
Wait_for_Wi_Fi();

Prompt_user_calibration();
If(Calibrated)
Wait_for_user_start();
Else
Prompt_user_calibration();

//gather data and determine
point location
If(accel_started())
Rd_orient_arraysensor();
Rot_3D_point_matrix();
Get_new_point_loc();
Calc_xy_phase_shifts();


Prepare_packet(B_x,B_y);
Accel_started();
//once packet sent, return
to check accelerometer
state

Else
Wait_for_user_start();

Prepare_packet(x,y){
Array = []
Array[payload] = {x,y};
Send_packet(&array);
}

Send_packet(array){
Bluetooth.socket.send(array
);
Wi_fi.socket.send(array);
Return 1;
//sent to server and slave
circuit}
```

Figure 39. Autonomous Object Tracking Algorithm and Pseudo Code

The simulations and results presented in this research focus on the system level algorithm “Manual User Control” as this demonstrates the broadest proof of concept and satisfies the original requirement of the project. The latter algorithms present the dynamic programming ability of the smart phone and other possible states of operation of the overall system.

4.3 Circuit design

The algorithm on the phone determines system clock synchronization, tilt information for beam control and handles data communication between the control network and server. From the block diagrams in Figure 35, Figure 37, and Figure 39 it is clear that the phone algorithm has multiple threads that execute asynchronously to meet the demands of different system components. Upon opening the application, the phone establishes a Bluetooth connection by default to the Arduino BT microcontroller. This assumes the MAC of the Arduino BT is known. It also begins reading data from the orientation sensor in the phone after calibration. If desired, the user may input the IP address of the server to send network information, assuming that a server’s IP address resides on a reachable subnet and that the server listens on a socket. The user must now calibrate the position of the phone to the desired calibration location of the array. Most often, the user calibrates the phone coplanar with the array to calibrate the default position at broadside. The phone data algorithm begins if the user presses the start button on the screen. Data is read from the orientation sensor to determine the angular shift from the calibrated positions along the *x*, *y*, and z axis. This data is sent to the function which performs the rotation matrix calculation. Analysis of the current system operation algorithm i.e.(Manual User Control, Manual Object Tracking, Autonomous Object Tracking) determines which rotation matrix is used. Note that the user has instantaneous access through the phone's interface to change the system operation mode as discussed in earlier in this section. New primary θ and φ locations are generated and the respective phase shifts are put into an array. The phone creates a packet using the correct protocol and sends the phase shift information to the Arduino BT. This process is illustrated in Figure 40.

```
If(!manual_user_control())
        Point[] =|object_position[]-our_position[]|

Else
        Point[] = [0,0,1] //broadside radiation

(ψ,θ,Φ) = Get_orientation_data();
New_Point[]=Point[]*Rot_matrix(ψ,θ,Φ);
(θO,ΦO) = calc_new_point_angles(New_Point[]);
(βX,βY) = calc_phase_shifts($\theta_O$,$\Phi_O$);

Packet[startbyte,type,length,βX,βY,checksum];
Send_to_control_circuit_via_bluetooth(Packet[]);
```

Figure 40. Pseudo Code Phone Algorithm Calculating Point

Under a separate thread, the phone actively listens for information from the Arduino BT to send to the server. The information received references a different protocol when received in the buffer. Data is stripped from the packet and stored in an array. If the phone is connected to the server, it will read the array and store the data in a packet to be sent to the server.

The algorithm run on the Arduino BT for protocol communications varies dependent on system operation state. The general implementation is as follows. The packet is received at the Arduino BT RFCOMM port and is stored in a buffer. An algorithm runs on the Arduino BT that determines slaves connected to the I^2C bus, send phase shift data to slaves and read network information such as tilt values from the onboard accelerometer. As shown in Figure 41, the Arduino BT reads the RFCOMM buffer and parses the packet based on protocol information. It determines which slaves are listening to the I^2C network and forwards the packet if the checksum of the packet is correct. If the checksum is not correct, the Arduino BT drops the packet and waits for the next packet of data from the phone implementing a UDP style communication. After the packet is sent to the slaves, the Arduino BT reads network information, creates a packet and sends the information to the phone. This process repeats with each packet that is received into the RFCOMM buffer; therefore, it is the rate at which the phone sends information that determines the rate for the Master-Slave I^2C network to process information.

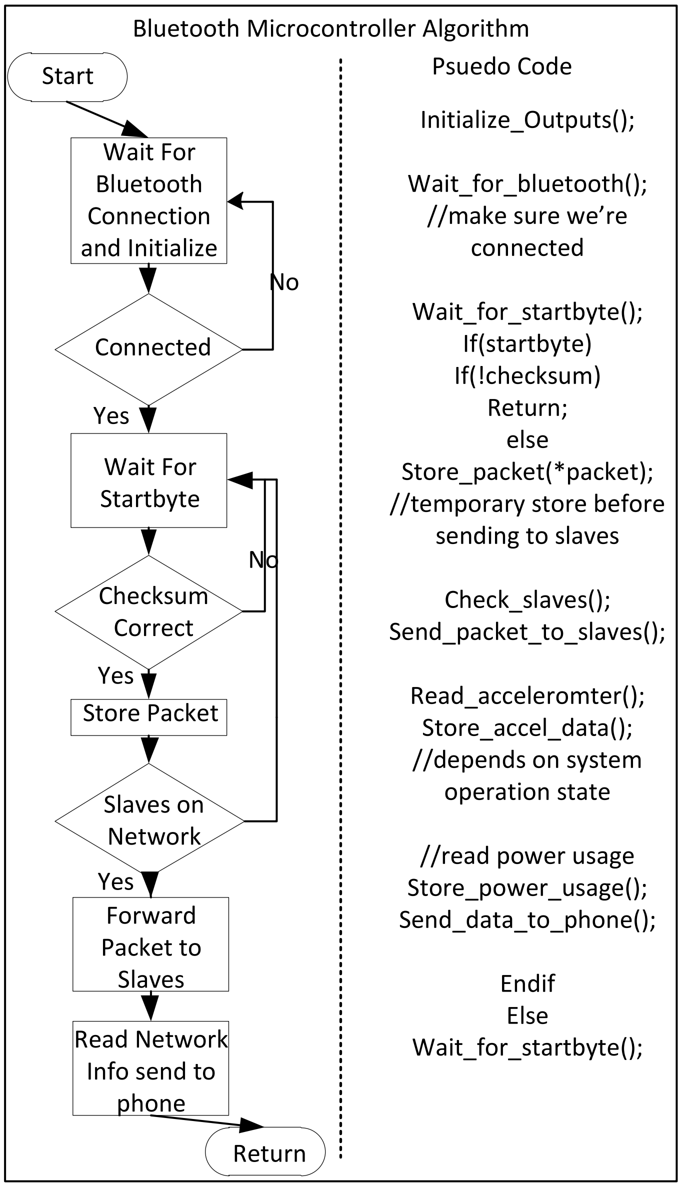

```
Initialize_Outputs();

Wait_for_bluetooth();
//make sure we're
connected

Wait_for_startbyte();
If(startbyte)
If(!checksum)
Return;
else
Store_packet(*packet);
//temporary store before
sending to slaves

Check_slaves();
Send_packet_to_slaves();

Read_acceleromter();
Store_accel_data();
//depends on system
operation state

//read power usage
Store_power_usage();
Send_data_to_phone();

Endif
Else
Wait_for_startbyte();
```

Figure 41. Arduino Bluetooth Master Control Algorithm

The data is received by the slaves as the same packet that was received by the Arduino BT under the checksum condition. The checksum is checked again. If the checksum is valid, the phase shift values are used in the algorithm to generate a phase shift voltage, however; if invalid, the slave waits for the next packet to arrive. This algorithm analyzes the signs of the phase shifts, as different signs on the phase shifts indicate θ and φ in various quadrants as viewed in Table 7.

Table 7. Phase Shift Signs for Quadrants of X-Y Coordinate System

Quadrant	Phase X	Phase Y
I	-	-
II	+	-
III	+	+
IV	-	+

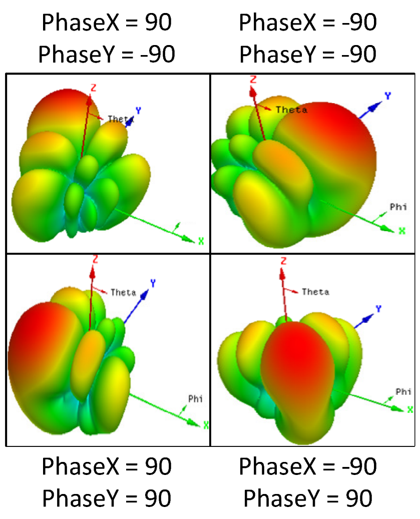

Figure 42. Main Beam Location in Various Cartesian Quadrants

Each slave is responsible for generating voltage values for 8 individual phase shifters. From the analysis of the phase shifters in Chapter III, (0.16) relates an input phase shift to a respective output voltage. The phase shifts are calculated for the respective elements which produce a corresponding voltage. The voltage is related to an 8-bit word that the potentiometer uses to adjust the wiper position between 0 and 5 Volts. The digital word is placed in an array to be delivered to the SPI network control circuitry.

Once the correct 8-bit word is stored in the array, the slave activates the SPI network by addressing the de-multiplexor with an activate signal referenced in Table 2. The de-multiplexor from section 2, is inactive until this signal arrives from the slave. Next, the slave uses two digital outputs, A and B, to address the appropriate digital potentiometer according to Table 2. The de-multiplexor receives signals A and B and activates a digital potentiometer as seen in Figure 43.

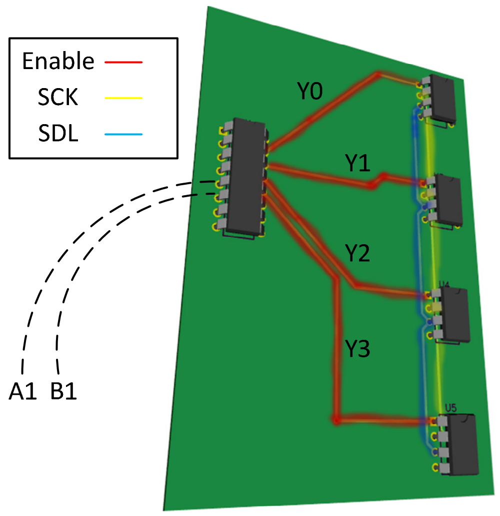

Figure 43. De-Multiplexor with Digital Potentiometer

The slave now uses the SCLK and the MOSI line to communicate the respective 8-bit word to the digital potentiometer. The word is stored in ROM on the digital potentiometer and accordingly produces a voltage on the wiper pin of the digital potentiometer that is sent to a non-inverting operational amplifier configuration. A static gain is configured by adjusting the values of the resistors according to (0.22). Whereas, the voltages produced by the digital potentiometers range from 0 to 5 Volts, the static gain provided by the operational amplifiers provides a range from 0 to 12 Volts, which the phase shifter requires for full 360 degree phase shift capability. The SPI algorithm is highlighted in Figure 44 and the data flow from slave to output voltage is seen in Figure 45.

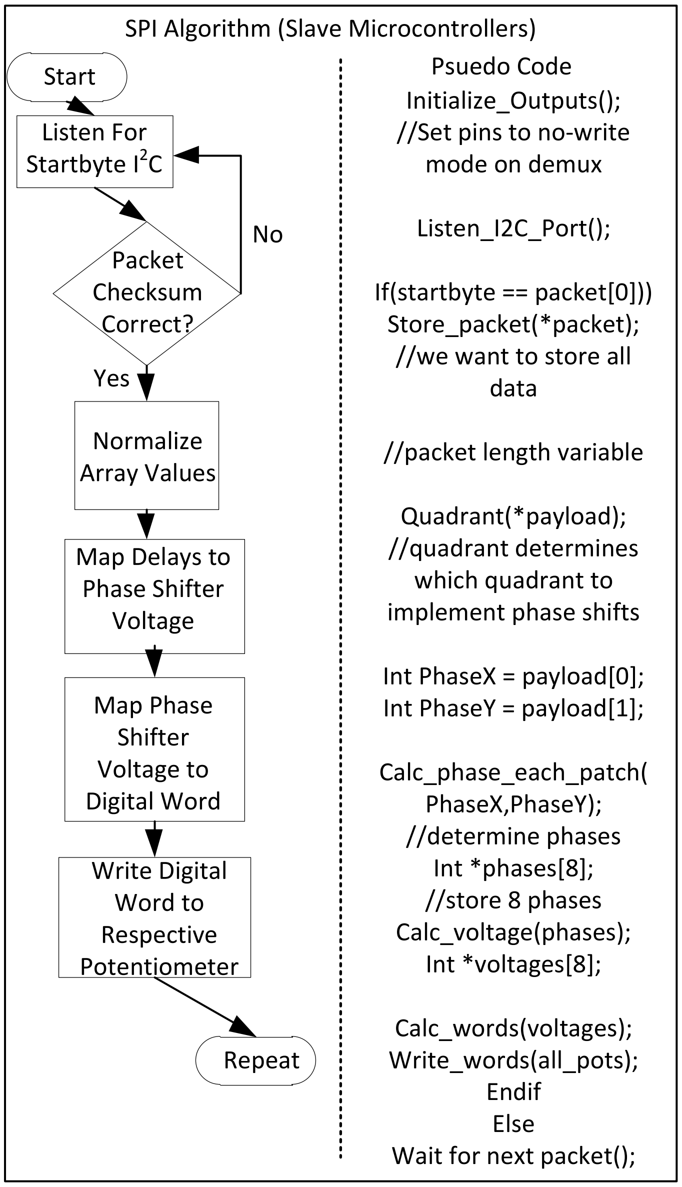
SPI Algorithm (Slave Microcontrollers)
Start
Listen For Startbyte I^{2}C
Packet Checksum Correct?
No
Yes
Normalize Array Values
Map Delays to Phase Shifter Voltage
Map Phase Shifter Voltage to Digital Word
Write Digital Word to Respective Potentiometer
Repeat

```
Psuedo Code
Initialize_Outputs();
//Set pins to no-write
mode on demux

Listen_I2C_Port();

If(startbyte == packet[0]))
Store_packet(*packet);
//we want to store all
data

//packet length variable

Quadrant(*payload);
//quadrant determines
which quadrant to
implement phase shifts

Int PhaseX = payload[0];
Int PhaseY = payload[1];

Calc_phase_each_patch(
PhaseX,PhaseY);
//determine phases
Int *phases[8];
//store 8 phases
Calc_voltage(phases);
Int *voltages[8];

Calc_words(voltages);
Write_words(all_pots);
Endif
Else
Wait for next packet();
```

Figure 44. SPI Algorithm Implemented on Arduino Uno

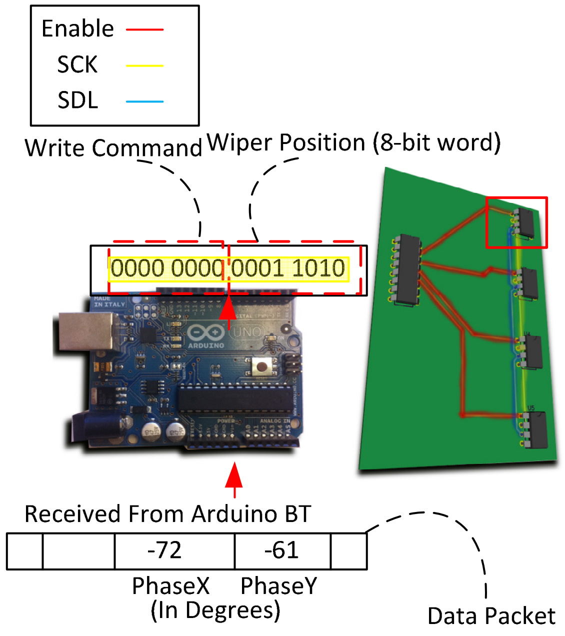

Figure 45. Microcontroller Writing Process to Digital Potentiometer

In addition, the SPI algorithm implements extended mathematical calculations that weren't previously covered in the background section. Because the system is using general phase delay and not true time delay, the phase differences for all elements must be normalized to one another. In other words, the maximum phase difference for any element is 360 degrees while the minimum for any element is 0 degrees. This means that for negative degree phase shifts and phase shifts which exceed 360 degrees require some scaling in reference to other elements. When the algorithm checks the sign of the phase shift, it determines the element which has the greatest positive phase shift and the least negative phase shift. To have all phase shifts negative, the algorithm subtracts the greatest positive phase shift to all element calculations as this normalizes the starting value to 0. Each phase shift is now calculated with respect to the normalized value. Furthermore, the SPI algorithm must find an appropriate digital word to write based on a calculated voltage. In this system, there are 127 possible voltages that may be achieved from 0 to 12 Volts or each digital potentiometer voltage step size is approximately .04 Volts. The algorithm finds the best match with the calculated voltage rounding the number if it is not an integer. This number corresponds to a wiper position which is the number in binary format that is written to the digital potentiometer.

The voltage control circuitry is designed to be modular to the entire system. Its specific function is to react to control signals from the microcontrollers and produce output voltages. In addition, it has the ability to link many separate system sub-components together. With this in mind, it is pertinent to design a printed circuit board (PCB) in order to organize system components, and provide a natural structure for control circuitry elements. In the same way that the voltage control logic was designed, the schematics for the system were designed at sub levels, instantiated with each layer of hierarchy. The first layer is the digital potentiometer and de-multiplexor layer.

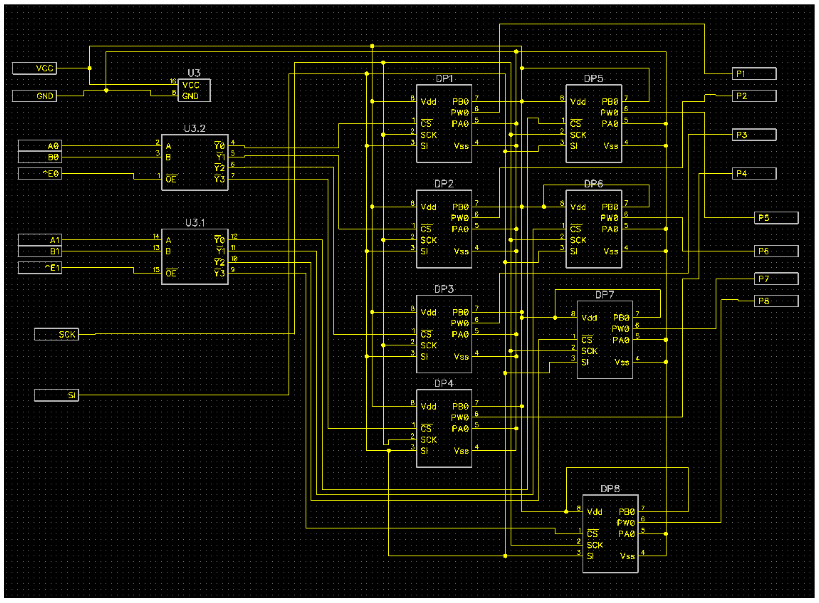

Figure 46. Digital Potentiometers and De-multiplexor Stage

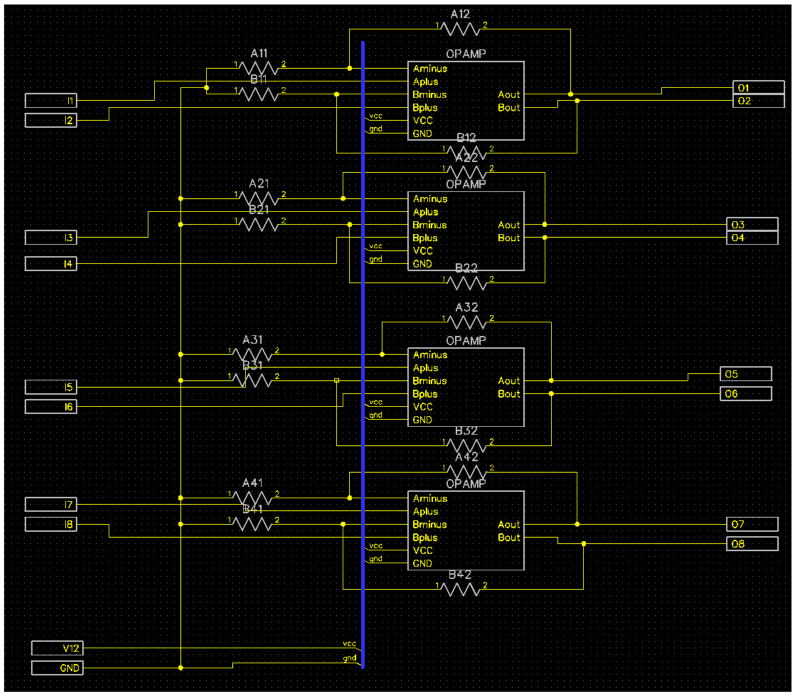

Figure 47. Operational Amplifier Stage, 8 Op-Amps Shown

From Figure 46, one can see the de-multiplexor in the upper left with 16 inputs and 8 digital potentiometers on the right. Next, an op-amp stage is created to take the outputs from the digital potentiometers and amplify the voltage from 0 to 12 Volts.

From Figure 47, one can see the combination of resistors that produce the static gain. At the next level of hierarchy, these are combinational logic blocks. The top layer, as shown in Figure 48, provides access to these blocks; in addition, to the other needed electrical connections at this layer such as external I^2C and power connections. This top level also has copper traces that extend to the edge of the board where SMA connectors will bring the DC voltage to the respective phase shifter. There are 8 SMA connectors on the right and left sides of the board corresponding to phase shifters 1-8 on the right and 9-16 on the left.

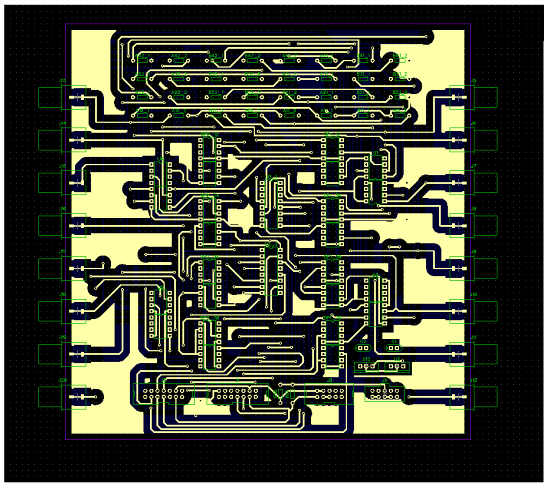

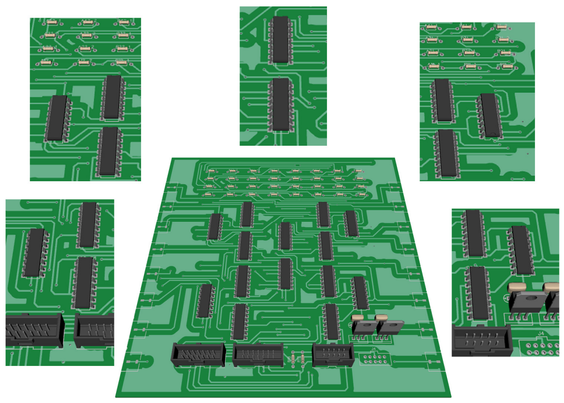

Figure 48. Final PCB Design (Top Layer) Schematic (Left) 3-D Representation (Right)

The external pin connectors allow both Arduino Uno slaves to be connected via a 14 pin connector cable. The I^2C and power connectors are connected with a 10 pin connector. From Figure 48, one can see that in the middle exist two ICs. These are two separate de-multiplexors. On both sides, extending from the middle, exist 4 ICs in a straight line. These 4 ICs comprise 8 total digital potentiometers. Furthermore, 4 additional ICs exist at each corner. These contain 4 op-amps. This final design of the PCB allows the systems sub components to come together in a modular fashion and in addition, provide a convenient way to connect many ICs together.

4.4 Communications design

The algorithms that process the data generated by the phone, network and user ultimately provide the functionality for the control system; however, without communication between device peripherals, control would not be possible. Therefore, it is necessary to provide a unified communications scheme between devices to help simplify the overall network design and to establish a layered approach to inter-device communication as discussed in section 2. Accordingly, custom protocols are designed specifically for this project to achieve the aforementioned objectives; in addition to, providing increased communications efficiency and improving network operability.

Naturally, the most important protocol of the system is that which determines the communications standard between the phone and control circuitry. Each packet sent from the phone carries phase shift information, but it may carry other information under various system operations. The length of the packet is variable because of the payload information, thus; a protocol is designed to fit these needs. The protocol states that the first byte of a packet is classified as a start byte. The start byte is an 8 bit integer that the device recognizes as the beginning of a packet. In this case, packets sent from the phone to the control circuitry start with the number 255. Next, the receiving device needs to allocate memory to store the payload, therefore; a length byte is included which is an 8-bit integer signifying a count of the number of bytes after it. Because the system may have a variable length packet, dynamic memory allocation is very important on the slave devices. Because the system may have various operation modes, all which require different payload data, a frame type byte is included that informs the sender and receiver what type of information is sent. In this case, when phase shift data is sent, the sender inserts a 200 to signify that the payload is phase shift data. In addition, if TCP communication is desired, the packet must have a frame id byte for SYN and ACK to be accurate. This is included after the frame type. The payload, or data being sent, is the remaining bytes inserted into the packet. A checksum byte to ensure data integrity is the last byte in the packet and is calculated by

$$Checksum = (startbyte + lengthbyte + type + payload)\%6 \qquad (0.25)$$

Therefore, the receiver and subsequent receiving stages can compute a checksum using (0.25) and compare to the original checksum to ensure data integrity. The evaluation of checksums in the algorithms is discussed in Chapter 3.4.

Startbyte	Length	Frametype	FrameID	Payload	Checksum

Figure 49. System Wide Protocol Packet Structure

While a protocol exists to send information from the phone to the control circuitry, a similar protocol is instantiated for the control circuitry, mainly the Arduino BT, to communicate information to the phone. The packets utilize a start byte, length byte and frame id; however, a different frame type is used for the payload information. In one case, the Arduino BT sends accelerometer information from an onboard sensor back to the phone. This type of information utilizes a frame type byte of *201*. In another case, the Arduino BT captures power usage of the system by reading a sensor and communicates this usage with a frame type of *202*. It is important that the protocol is similar in both directions as to not use substantial programming overhead.

Communication also exists between the phone and network server, relaying information about system operation, power usage and other peripherals. A similar protocol is established to pass information from the phone to the server which is processed by the server before displaying to a web page. The server resides on an IP address and opens port *4444* to listen for data from the phone. Similarly to the circuitry protocol, the phone to server protocol uses a start byte, length byte and frame id, although UDP is used in the project. The frame type changes with each variation in payload that is sent from the phone to the server. To update users of the system's operational state, the phone communicates phase shift information to the server using frame type *200*. For power readings, the phone inserts frame type *202* into the packet.

The protocol for communication between the server and the phone is implemented in software on a continuously running thread which updates a web page. Using an HTTP browser, a user from the internet may remotely see system information in real time by observing the display of information. This display updates the user of current phase shifts, beam direction, system operational state and power usage. Although not vital to system operation or control, the information gathered by the server provides details that are important for real world implementation. Reading and trending power usage may indicate when system circuitry components are wearing down or observing phase information can inform a user how the system is performing in tracking an object. In addition, a real time display of information pertinent to the system expands ideas on how to better improve the system and design system components for improved efficiency.

4.5 Phone and server display design

Accurately showing data and visually appealing graphics, while not completely necessary to this project, enhance the results and usability of this project as a whole. The partial goal of using a smart phone in this system is to allow a user to integrate easily into an otherwise, complex radio system. With this in mind, the design of the phone interface is somewhat important. The design allows the user to take advantage of the aforementioned dynamic programming capability of the phone. In addition, it is necessary to observe the phase shifts and angular values that the system is using for calculations. This ensures system operation is correct from a user standpoint.

Because the phone has many threads running concurrently, it is difficult to fully display all of them synchronously; however, separate visual designs still offers advantages to the system. In this design, the primary viewing screen of the phone displays important information including: θ and φ values, generated phase shifts from these angles, operation state and operable buttons whose functions control internal flags within the phone's algorithm. These criterions allow the user to fully observe the system state and important information from the screen as this is especially useful if the user is controlling the direction of the beam with "Manual User Control". In addition to the primary screen, the user needs the option to connect to a server for to transfer information; however, this need not be displayed continuously. A separate screen is created to input the IP address and accordingly, display server connection information. The Bluetooth is managed by a separate library called "Amarino", which runs as its own process in the background of the phone. An initial screen design is shown in Figure 50.

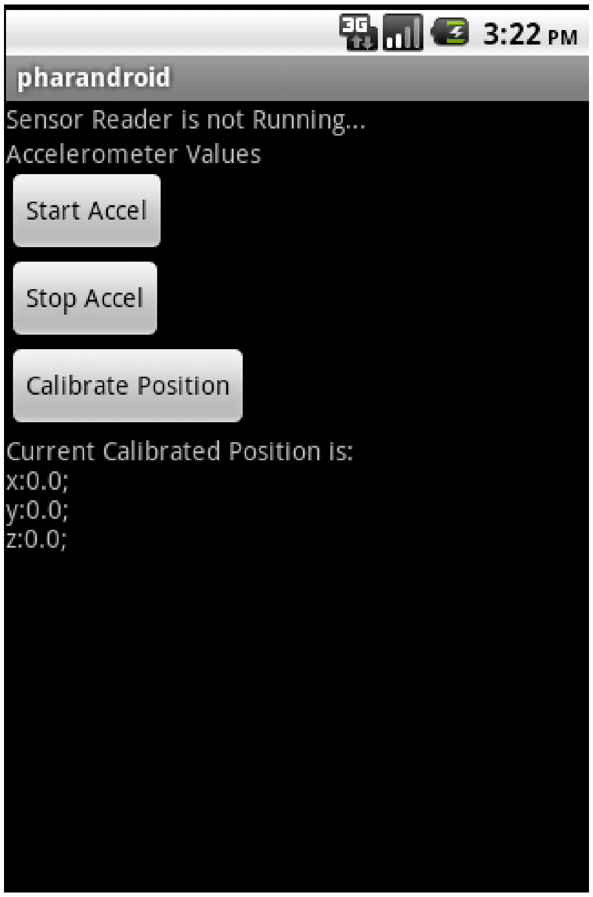

Sensor Reader is not Running...
Accelerometer Values

Current Calibrated Position is:
x:0.0;
y:0.0;
z:0.0;

Figure 50. Initial Phone Design

Because the phone communicates with the server, it too should also display pertinent system level information to provide remote users an insight into system operation. Remote users have access to phase shift information, the main beam's current location in terms of θ and φ, individual phase shifts for each of the elements and historical information of system operation state. While these features are no more necessary than a visually appearing phone application, they can provide useful information to improve future operation of the array. Power information is stored on the server which is analyzed to determine weak circuit components for replacements. Furthermore, visual graphics provide non-technical users insight to antenna operation and other characteristics of the system. With this in mind, the server display offers a chance for others to develop new innovative ideas that can be included in the research and progress the development of this project.

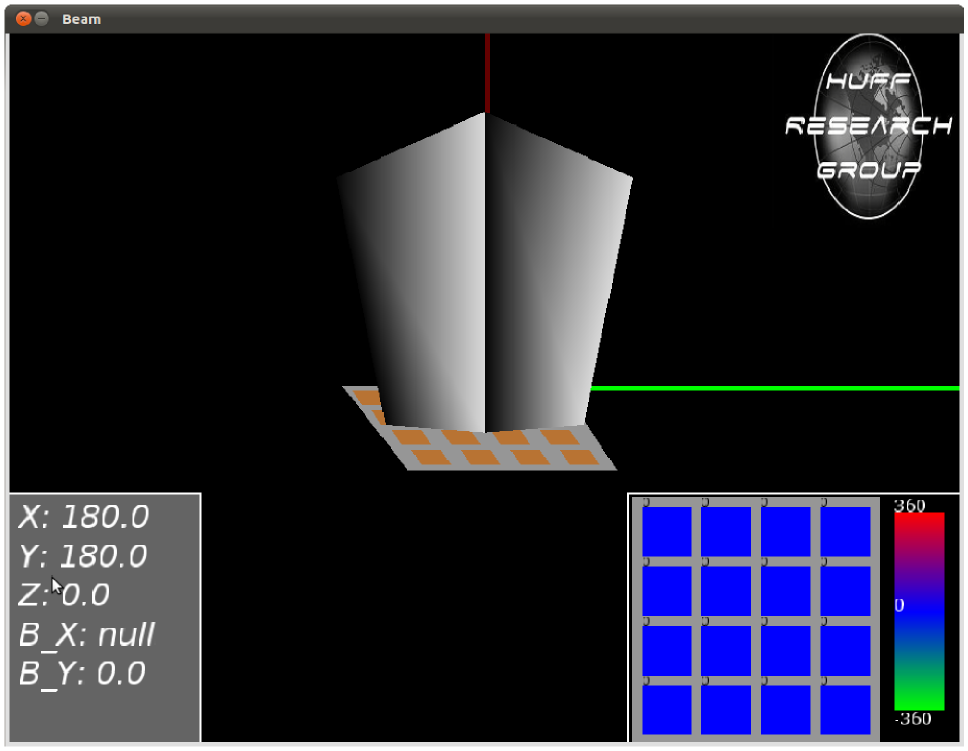

X: 180.0
Y: 180.0
Z: 0.0
B_X: null
B_Y: 0.0

Figure 51. Initial Server Display Design

CHAPTER V

COMPLETED DESIGN AND RESULTS

5.1 Completed design

This section presents the completed physical models of all designed sub-components including the phased antenna array, power divider, phase shifter, voltage control board, phone display and server display. Results are presented which correspond to simulated results in Chapter IV. Overall system experimental results are presented to show the functionality of the system as a whole and its success steering the beam of the array.

The finite array simulated in Chapter IV is etched on a 10 by 10 inch slab of Rogers 5880. From Figure 52, it is clear that the design resembles the image of the simulated array.

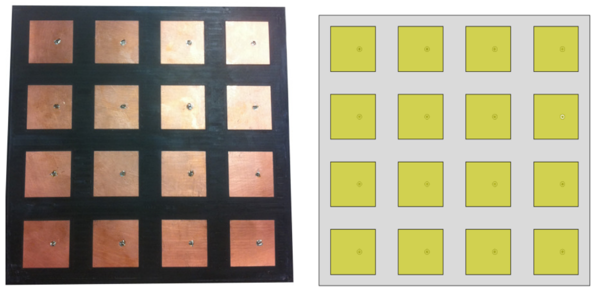

Figure 52. (*Left*) Fabricated Microstrip Patch Array (*Right*) Simulated Microstrip Patch Array

The array is tested with a network analyzer for several measurements. Individual antenna elements are tested for VSWR characteristics that are compared to simulated results. In addition, cross coupling noise is simulated among four patches to determine any losses associated with the fabricated array. Furthermore, input impedance is graphed on a smith chart to compare against simulated results. From Figure 53, it is clear that the VSWR of the fabricated array emulates that of the simulation.

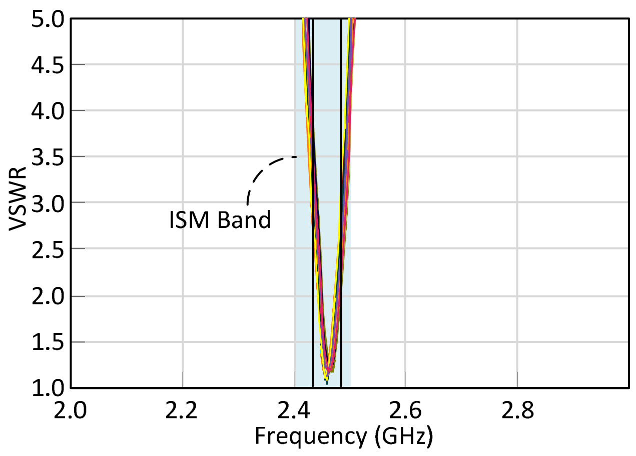

Figure 53. VSWR Fabricated Array

Each element has a VSWR less than 1.20 with a resonant frequency of f_r=*2.46* GHz, which is close to the expected model. It is also noted, that the VSWR for all elements falls in the ISM band, which satisfies another design criterion. Observing the smith chart in Figure 54, one can see that the input impedance of each element yields better results the simulated design.

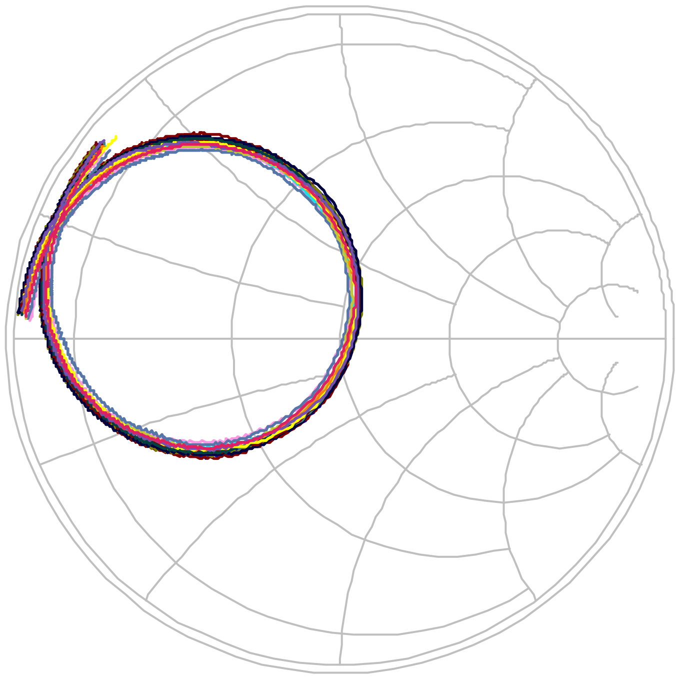

Figure 54. Input Impedance Fabricated Array

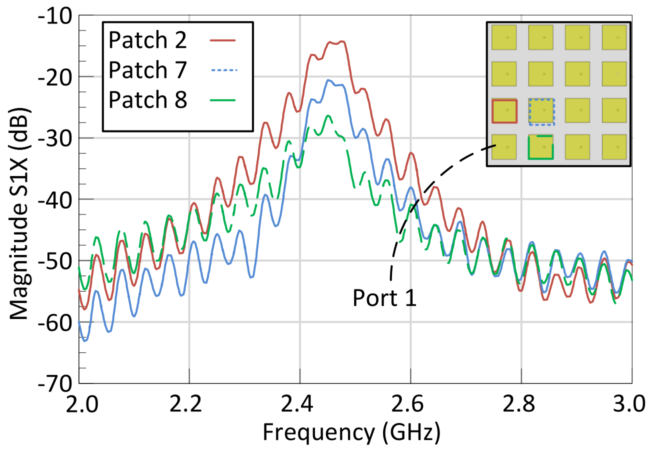

Figure 55. S21 Measurements 4x4 Array

The impedance for all 16 elements at resonance varies by 2%. In addition, it is important to observe the effects of neighboring patches, because many single elements are electrically close. Because some energy may leave one patch but reradiate into another, a test must be done to see how much energy dissipates from one patch to another. From Figure 55, it is clear that little energy is absorbed by the neighboring patches on the array. In addition, it is expected that Patch 2 will present the highest coupling to Port 1. For these experiments, it is important that most of the energy radiate from the patches to measure the radiation pattern accurately. Provided these test results, the fabricated array adequately meets the needs of this experiment.

Upon completion and testing of the phased array, other RF hardware components are now tested. The phase shifters are tested with the network analyzer using Labview to determine the accuracy of an applied voltage to a corresponding phase output. The Labview results of this experiment are shown in Figure 56.

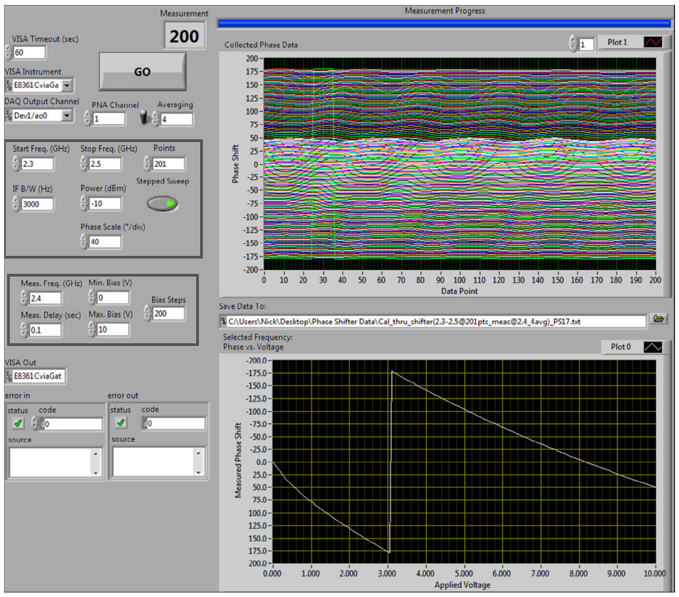

Measurement: 200

VISA Timeout (sec): 60

VISA Instrument: E8361CviaGa

DAQ Output Channel: Dev1/ao0

PNA Channel: 1

Averaging: 4

Start Freq. (GHz): 2.3

Stop Freq. (GHz): 2.5

Points: 201

IF B/W (Hz): 3000

Power (dBm): -10

Stepped Sweep

Phase Scale (°/div): 40

Meas. Freq. (GHz): 2.4

Min. Bias (V): 0

Bias Steps: 200

Meas. Delay (sec): 0.1

Max. Bias (V): 10

VISA Out: E8361CviaGat

error in: status ✓ code 0 source

error out: status ✓ code 0 source

Save Data To: C:\Users\Nick\Desktop\Phase Shifter Data\Cal_thru_shifter(2.3-2.5@201pts_meas@2.4_4avg)_PS17.txt

Figure 56. Graphical User Interface LabView for Hittite Phase Shifter Test

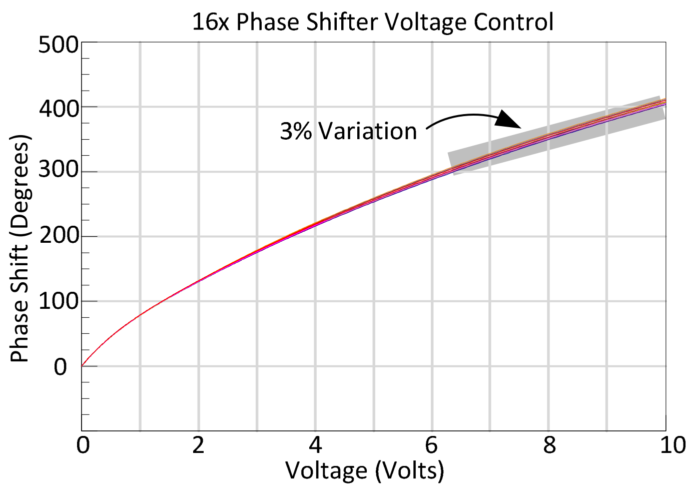

Figure 57. Test Results from 16 Hittite Phase Shifters

From the results in Figure 56, it is necessary to observe a similar graph as discussed in Chapter IV to determine an appropriate equation to use in the SPI algorithm. Figure 57 follows closely with the original graph provided in the datasheet and the Hittite graph; however, there exists some variation. Therefore, this variation must be accounted for in the algorithm on the microcontrollers.

$$Voltage = 2E-09*\deg^3+3E-05*\deg^2+0.0118*\deg-.0816 \qquad (0.26)$$

From Figure 57, there exists a noticeable change from the original voltage and degree relationship equation. From this variation, a new equation (0.26) is created through the same polynomial interpolation technique to map an input degree value *deg*, to a respective output voltage. Furthermore, (0.26) requires the op-amp stages to have a gain necessary to obtain all voltages. In reference to the op-amp feedback, the following resistors are selected

$$R_2 = 15k, R_1 = 7.3k\ (\Omega) \qquad (0.27)$$

These values provide a static gain of about 3. Thus, with the op-amps configured and a new equation, the change is accounted for in the code implementing the SPI algorithm on the slave microcontrollers explained in Chapter IV.

The control board was designed in Chapter IV using schematic and layout software. These files are sent to a PCB manufacturer and returned for testing. The final outcome of the board appears exactly as the simulated board. The board is shown in Figure 58 below.

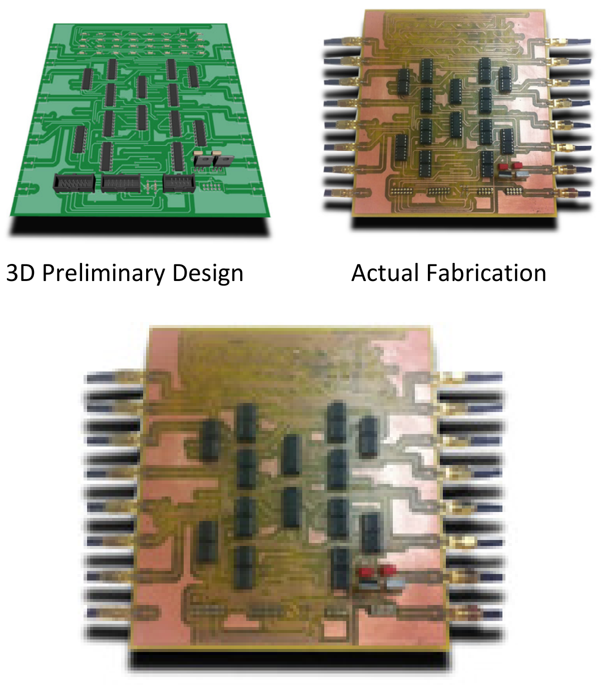

Figure 58. Simulated and Finished PCB

The microcontrollers are programmed with the necessary algorithms and are connected to the control board for testing. In this experiment, the phone is calibrated into a beginning position and then tilted to achieve some desired θ and φ. From this, we can measure the voltage using a voltmeter and correlate these values to distinct phase shifts measured by the lab view experiment. Two results are presented here.

Table 8. First Experimental Result Beam Steering

Voltage	Actual Phase Shift	Actual Phi	Actual Theta
1.094	84	42	46
2.79	170		
4.84	249		
7.33	333		
10.72	423		
7.66	344		
6.32	302		
2.91	172		
5.28	265		
7.88	350		
11.05	440		
2.9	172		
5.28	265		
3.12	184		
1.32	96		
8.24	360		

The voltages of all sixteen outputs are measured on the control board and are put into the respective column. Thereafter, the corresponding measured phase shift is calculated and inserted into the respective column. The phase shifts are entered into the simulation tool to provide a radiation pattern as shown in Figure 59.

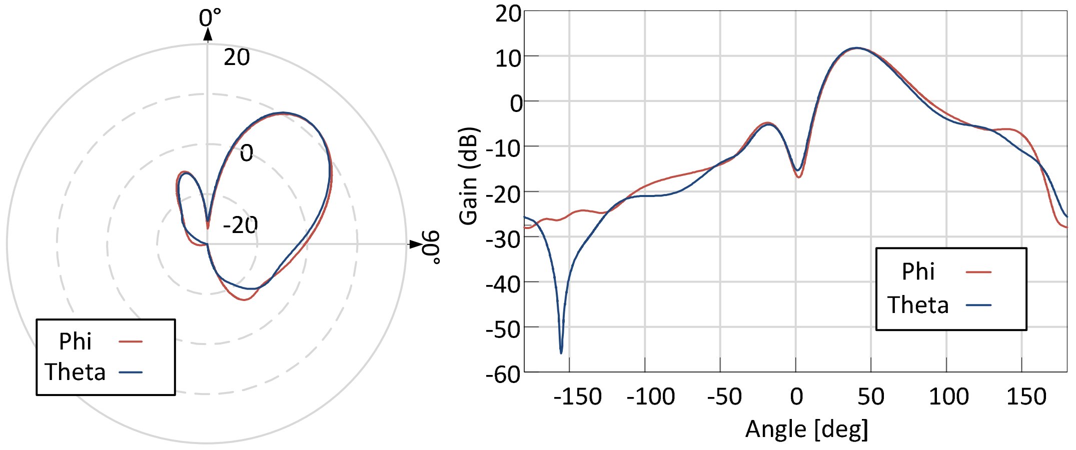

Figure 59.(Left) Polar Plot Experimental Results 45 Degree Cut Plane (Right) Rectangular Plot 45 Degree Cut Plane

The results shown indicate that the control board implements the voltage control algorithm correctly and provides correct voltages to the phase shifters as a ϕ=44 and θ=45 degrees is achieved. In addition, a second test is performed to ensure the algorithm can move a beam into different Cartesian quadrants, satisfying the original three dimensional beam steering requirement.

Table 9. Second Experimental Result Beam Steering

Voltage	Actual Phase Shift	Actual Phi	Actual Theta
8.1	356	307	42
5.29	265		
2.91	172		
1.09	84		
2.44	151		
4.71	245		
8.38	364		
10.81	427		
2.45	152		
10.02	407		
6.86	318		
4.26	227		
6.28	299		
9.33	389		
2.1	136		
4.27	228		

The results are displayed in Table 9 yield the following beam steering results shown in Figure 60.

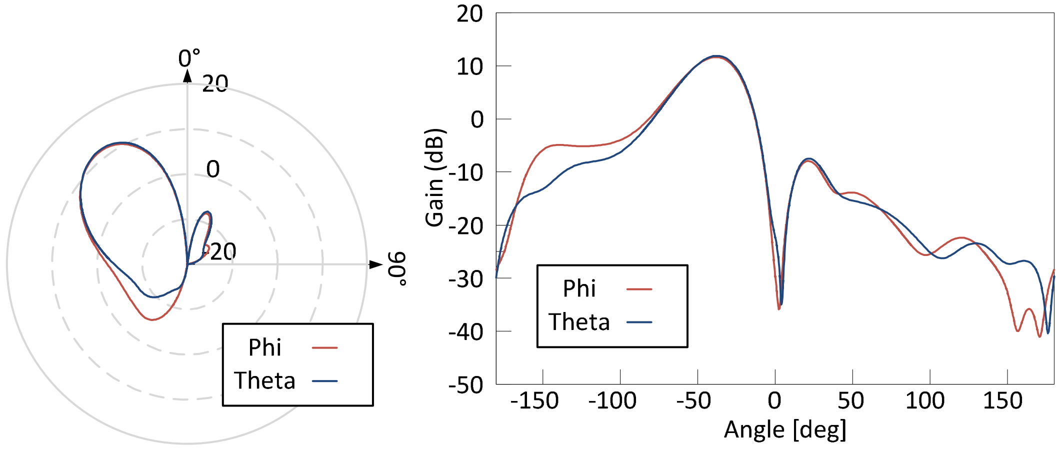

Figure 60. (Left) Polar Experimental Plot 135 Degree Cut Plane (Right) Rectangular Experimental Plot 135 Degree Cut Plane Electric Field

A ϕ=-45 and θ=-45 degrees is achieved. These results satisfy the desired values held in Table 9. It is clear from these results that beam steering in various Cartesian quadrants is accurately achieved as both *θ* and *φ* are pointed nearly -45 degrees on the 135 degree plane. These results yield promising outcomes for the system as a whole although the physical array is not yet connected to the system and tested at this point.

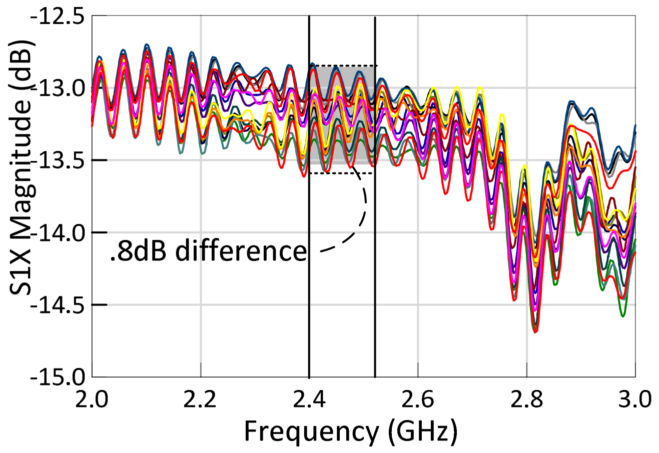

Figure 61. Power Divider Experimental S21 Gain Results

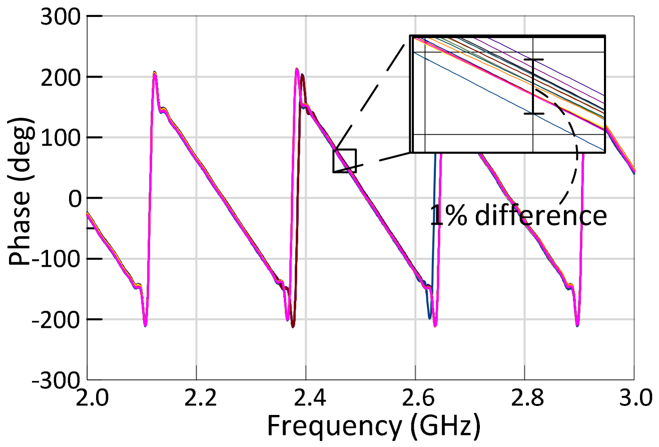

Figure 62. Power Divider Experimental S21 Phase Results

As addressed in Chapter III, the power divider was tested for reliability using the network analyzer. A measurement was taken to observe the S12 through S117 gain parameters to ensure a similar gain distribution among the ports. From Figure 61, it is clear that a .8 dB range exists among all the ports. These results signify little change from port to port which will allow the overall system experiments to be performed with greater accuracy. In addition, a measurement of phase difference for all ports is taken to ensure that any phase differences are accounted for in the algorithm.
From Figure 62, observations conclude that the range of phases from port to port is insignificant so as to not be an influence in the SPI phase shifting algorithm. In conclusion, the measurements from the power divider signify that it does not play a significant role in changing overall system state with respect to gain or phase.

The phone interface is designed to allow the user to have complete dynamic control of the system. The interface for the primary screen is shown in Figure 63.

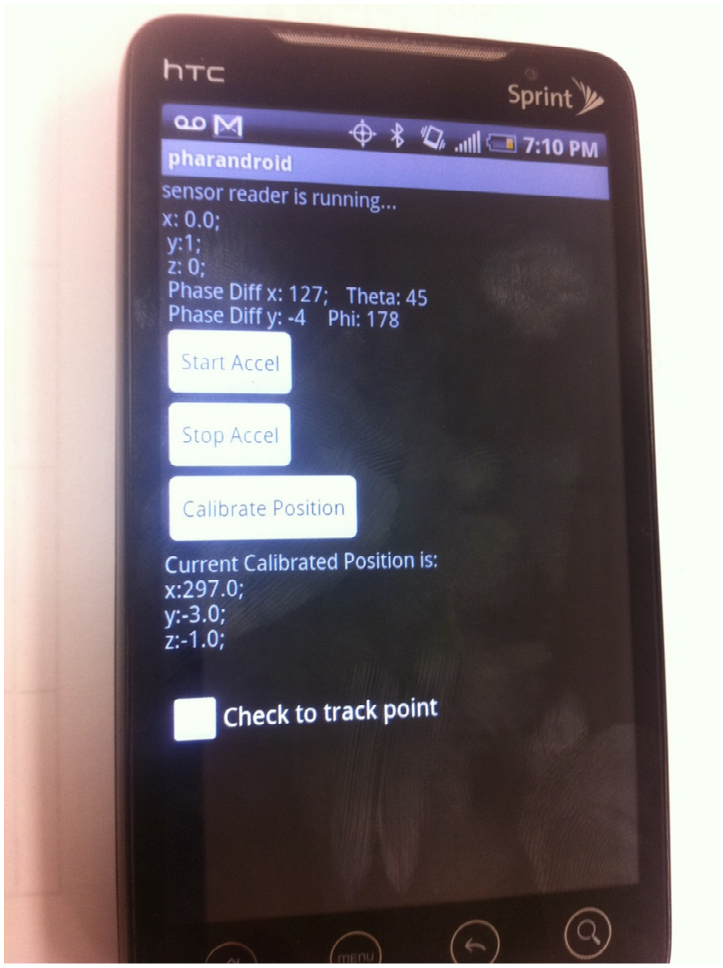

sensor reader is running...
x: 0.0;
y:1;
z: 0;
Phase Diff x: 127; Theta: 45
Phase Diff y: -4 Phi: 178

Current Calibrated Position is:
x:297.0;
y:-3.0;
z:-1.0;

Figure 63. Phone Executing Algorithm and Displaying Information

The screen has several parts. The calibration button is used to gain an initial condition for the array; the system will not function without pushing this button first. Above the calibrate button sits a start button, which begins reading data from the phone. Active displays of phase shifts along with θ and φ are presented to show the user current beam location information. Furthermore a switch is implemented as a checkbox which that allows a user to change from “Manual User Control” to “Manual Object Tracking”. In a similar association, there is also a checkbox to enter "Autonomous Object Tracking". A second page, accessed by pressing the "Menu" button, leads a user to a form that prompts entry of an IP address to connect to the server. Other important network information is also displayed.

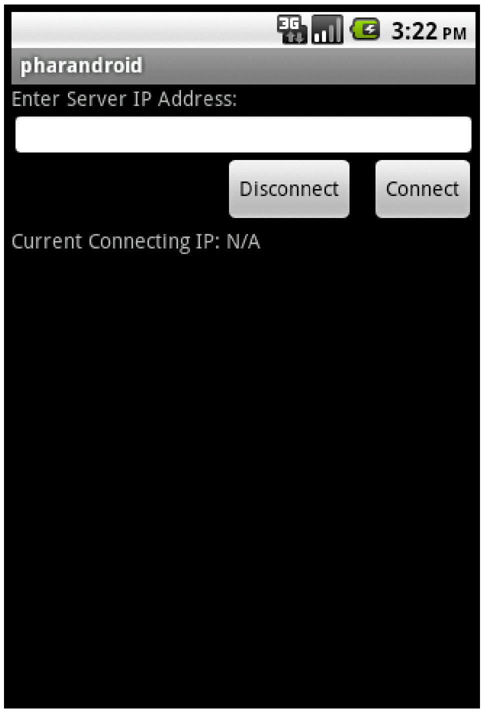

Figure 64. Server Communication Page

Other information can be displayed on the phone that is perhaps, important to the phone's or system's algorithm. This is covered in Chapter VI under future work.

Information displayed on the server is also valuable as discussed in Chapter IV. The design for the server displays system information such as 3-Dimensional beam location, phase shifts of elements and other characteristics. Network characteristics, such as power usage, are stored in a database and can be accessed via web. The Apache server is capable of responding to HTTP and HTTPS requests. The primary tool used to construct the graphical interpretation of the beam was through a tool called "Processing" and is written in Java.

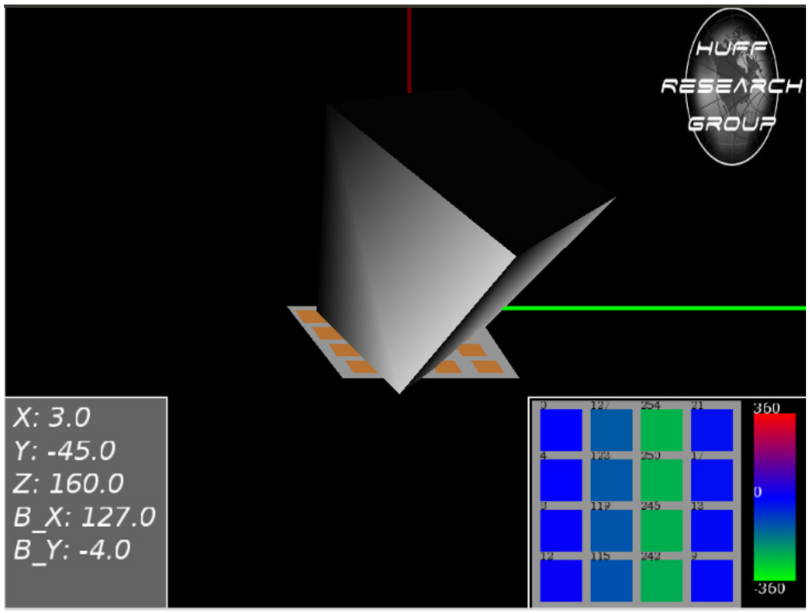

```
X: 3.0
Y: -45.0
Z: 160.0
B_X: 127.0
B_Y: -4.0
```

Figure 65. Real Time Server Display of System Information

The server display in Figure 65 displays the directional cosine angles from the calibrated axis shown as *X,Y,Z* and the progressive phase shifts are displayed as *B_X,B_Y* for the *x* and *y* axes respectively. In addition, a color coded map of each antenna element displays the progressive phase shift corresponding to the current data. The large object in the middle of the screen represents the beam of the array, and moves in real time corresponding to the movement of the actual beam of the array.

5.2 Experimental results

With each sub-component fabricated and tested, the final experiment compiles all modules into a single unit. Constructed from transparent acrylic glass, the final module resembles a portable phased array.

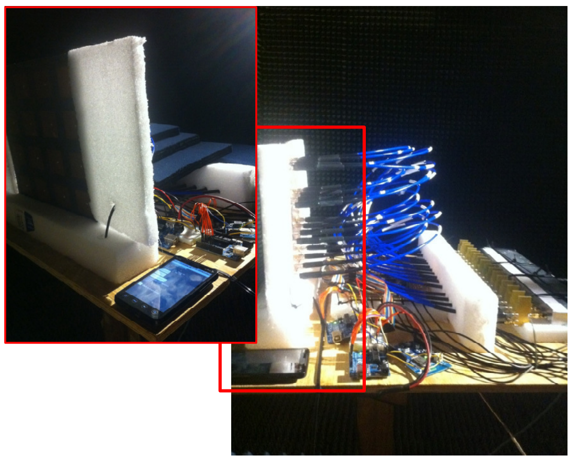

Figure 66. Completed System Design

The completed module, shown in Figure 66, is tested in an anechoic chamber to observe radiation pattern measurements in the presence of beam steering. The system sits on top of a piece of wood. The power divider and phase shifter are secured into a piece of Styrofoam and the cables to the phased array are secured with another piece of Styrofoam. The control board lies in front of these pieces directly behind the phased array. For the measurements, all metal pieces are covered with absorber material to decrease the reflections and measured noise. These measurements are compared to those achieved by generating voltages and observing the simulation as recorded earlier in this chapter.

The first measurement shown in Figure 67, is the radiation pattern of the array at broadside radiation. This outcome corresponds strongly with the single element pattern aforementioned in Chapter IV, however; it is strongly noted that the beam of the array is thinner than that of the single element radiation pattern; this is expected.

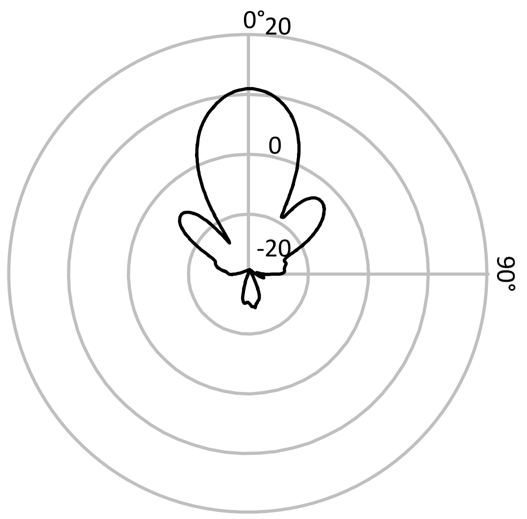

Figure 67. Antenna Broadside Radiation Pattern

Given the outcome of the radiation pattern, several measurements were taken to obtain the electric fields in both the θ and φ directions. Figure 69, shows the many scan angles taken in the measurement. The total scan ranges from -45 degrees to +45 degrees at 15 degree intervals. In these measurements, the anechoic chamber is capable of measuring in a plane, not in three dimensions. Because of this, it is necessary to configure the measurements such that the scan angles can be captured in the plane of radiation. With each measurement, we program the phone to generate a phase shift that is coplanar which generates a distinguishable measurable phase shift. In addition, we also program the phone to take a perpendicular measurement to the radiation plane. In this measurement, we see that the gain at broadside radiation drops because the beam is steered off broadside. This is demonstrated in Figure 68.

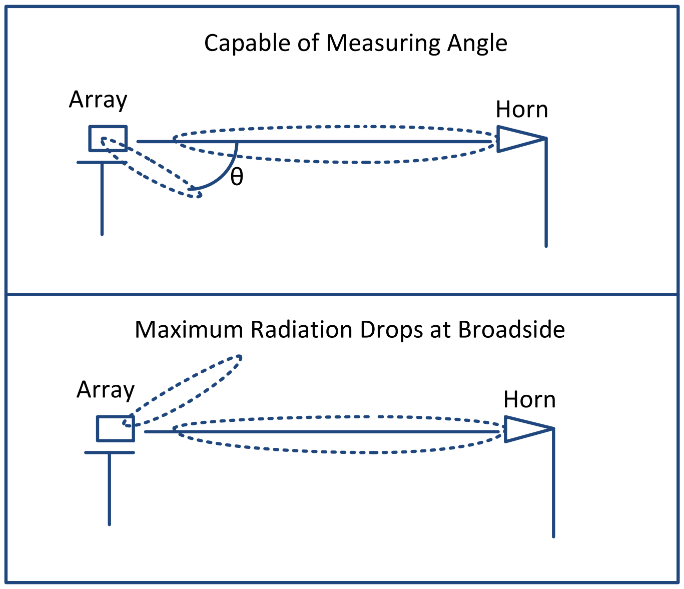
Capable of Measuring Angle
Array
Horn
θ
Maximum Radiation Drops at Broadside
Array
Horn

Figure 68. Measurement Process Inside the Anechoic Chamber

In the first series of measurements, we capture the electric fields with respective phase shifts plotted in Figure 69.

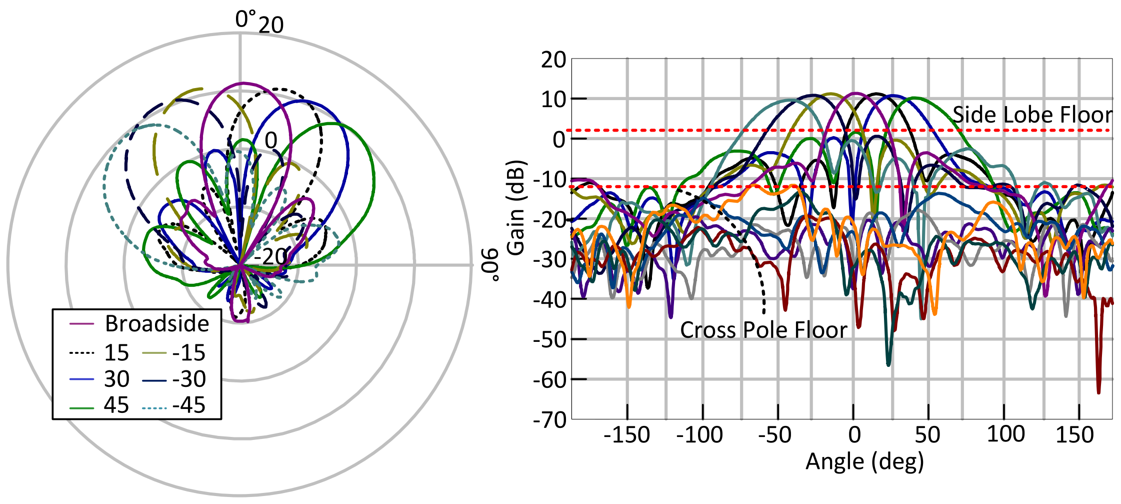

Figure 69. (Left) Co-Planar Measured Electric Field in Phi Direction (Right) Measurement Fields with Cross Pole

Clearly, the results achieved are closely related to those achieved in simulation. The system demonstrates a successful capability to scan at angles within this range as each measurement was taken according to the phase shifts generated from the phone. We note that the drop in gain is around .3 dB with each progressive 15 degree phase shift. It is also noted that the cross pole floor is low to the gain of the antenna which demonstrates successful antenna operation.

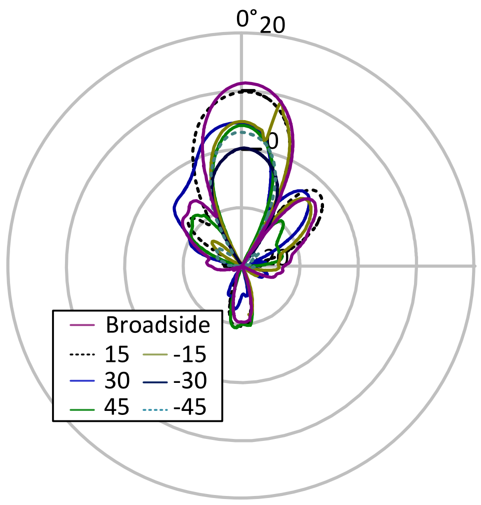

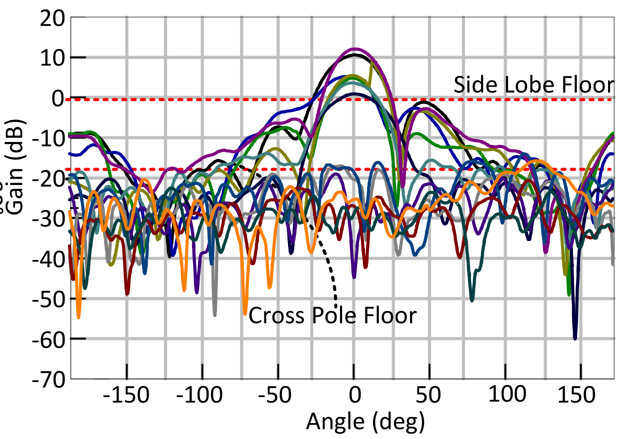

Figure 70. (Left) Normal Measured Electric Field in Phi Direction (Right) Measurement Fields with Cross Pole

Figure 70 shows the measurement that is perpendicular to the measurement plane. We see that the maximum radiation at broadside drops with each progressive 15 degree phase shift. This signifies that the beam is steered away from the measurement plane by the angle programmed from the phone. At a closer look, we view a discontinuity for the -15 degree measurement. After analysis of the raw data, we conclude that this error is due to a measurement error during the data gathering process. With proper review, we apply the estimated measurement error to the raw data set and achieve Figure 70.

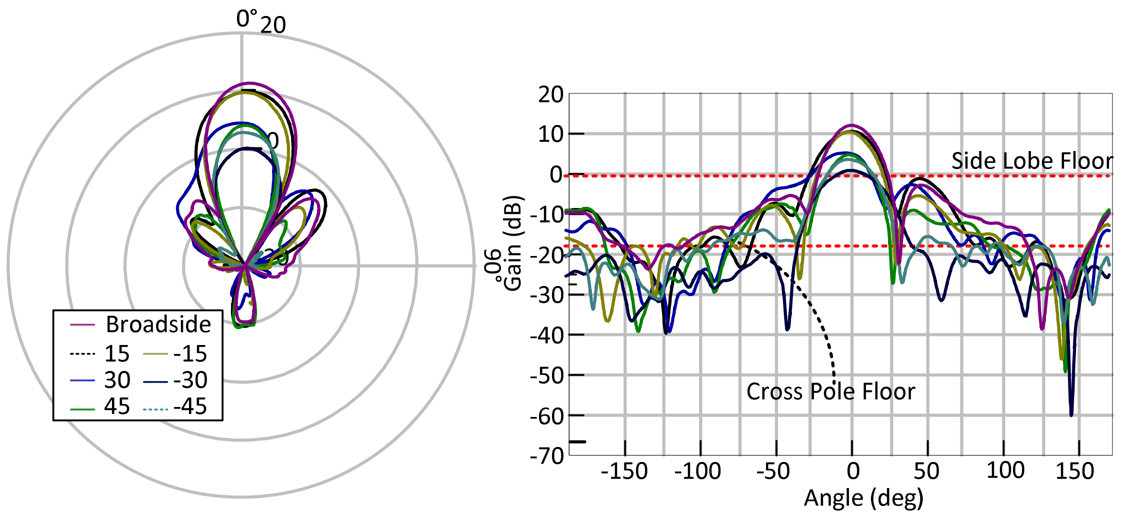

Figure 71. Adjusted Data Set Due to Measurement Error

From Figure 71, we can see that after the measurement error adjustment, the corresponding data provides an accurate result to proper array operation. As expected, the -15 degree broadside beam is slightly less (1.5 dB) than the broadside beam. It is also necessary to compare the measured results with the simulated results to determine the accuracy and validity of the previous results.

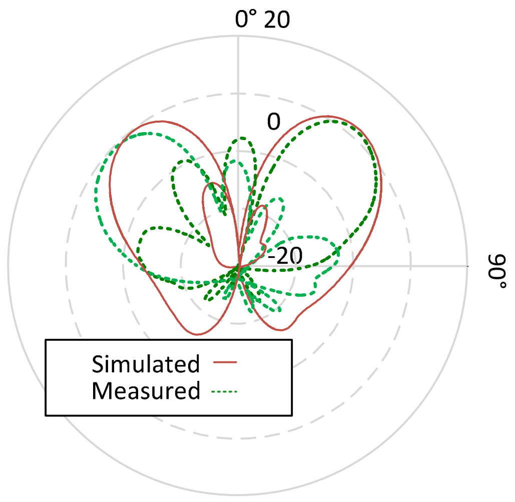

Figure 72. Simulated and Measured Comparison at +45 and -45 Degree Scan Angles

From Figure 72, we see that the measured results align closely with the simulated results. This verifies our initial assessment of the system and confirms the previous tests run on the modules in the system. Furthermore, the electric fields in the θ direction, similar to those in the φ direction, are also shown below with the same measurement process.

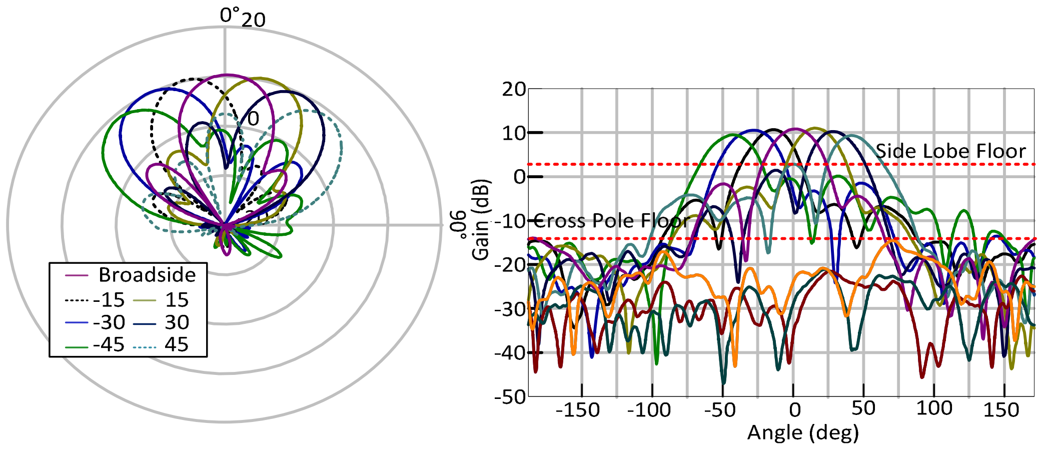

Figure 73. (Left) Co-Planar Measured Electric Fields Theta Direction (Right) Measured Fields with Cross Pole

These results are taken after the array has been physically turned to obtain the electric field in a perpendicular direction. From Figure 73, we can see the beam shift is present over the measurement range and the cross pole measurement also agrees with the previous results.

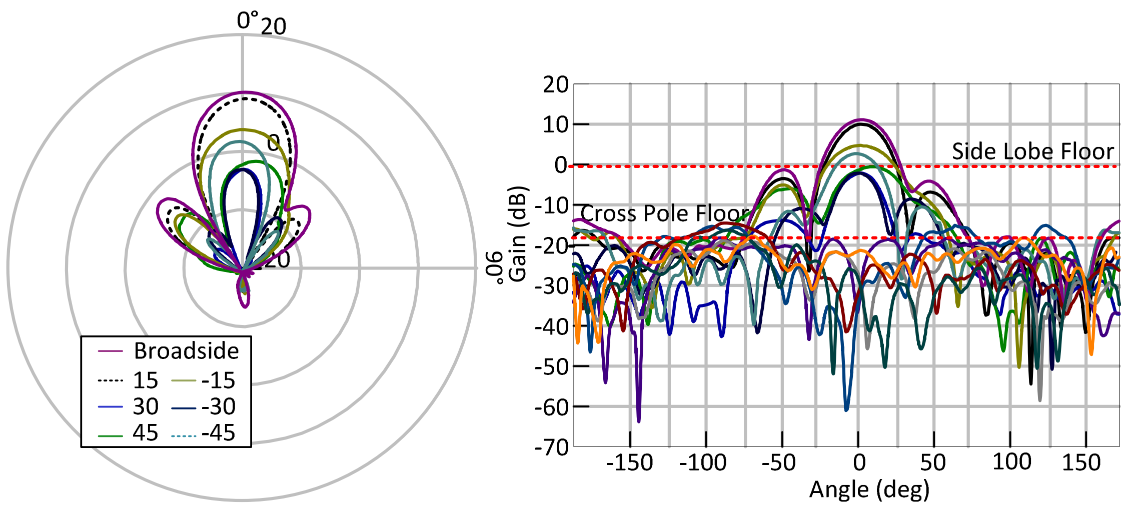

Figure 74. (Left) Normal Measured Electric Fields Theta Direction (Right) Measured Fields with Cross Pole

Again, the normal measurement indicates a drop in gain at broadside for the radiation pattern. This result agrees with the other results and indicates successful system operation.

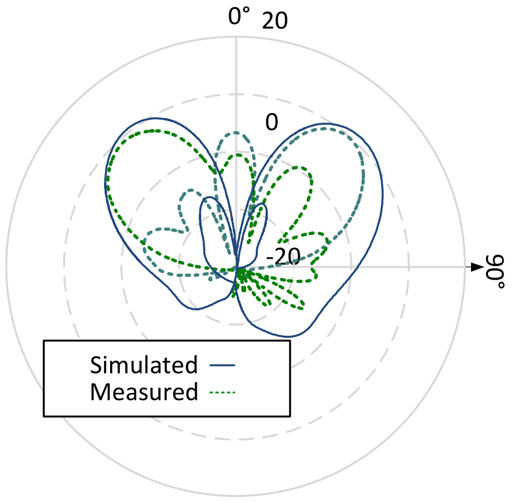

Figure 75. Simulated and Measured Comparison Electric Fields Theta Direction

The electric field correlates closely with the simulated results. From these results, it is clear that the smartphone is capable of controlling this complex system and achieving beam steering in 3-D space. Because of the setup of the anechoic chamber, we are incapable of measuring a 3-D scan, however; since both results successfully demonstrate beam steering, we conclude that the system is capable of beam steering in 3-D space. In addition, it is necessary to observe the response of the system and antenna at frequencies within the operating bandwidth. This will indicate how the antenna operates off of resonance.

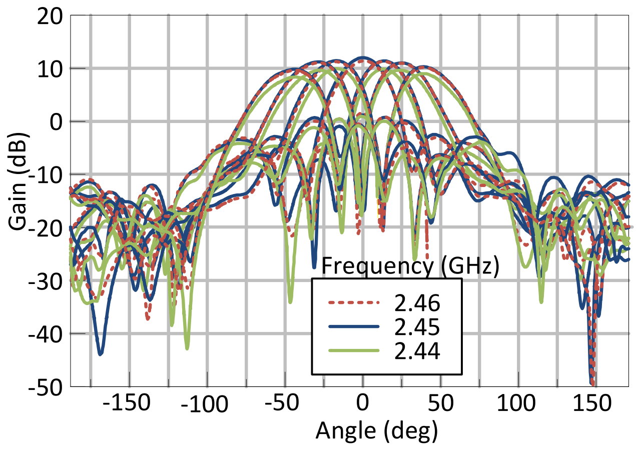

Figure 76. Frequency Comparison Implementing Beam Steering

From Figure 76, we can see that the system and antenna are similar at frequencies of 2.45 and 2.46 GHz. We note that the resonant frequency of the antenna itself is approximately 2.455 GHz. This correlation of measurement verifies the antenna operating frequency. Furthermore, the antenna implements the phase shift correctly at 2.4 GHz but with less total gain. From these results, we conclude that the antenna is responsive over a 20 MHz bandwidth and the system is capable of shifting control across this bandwidth.

In summary, Table 10 and Table 11 provide the desired beam steering direction and the actual measured angle. The percent error is given as a difference in degrees divided by the total scan angle which is 90 degrees in this case.

Table 10. Measured Results Phi Direction

Scan Angle	Measured	Error	Scan Angle (-)	Measured	Error
15	15	0%	15	13	2%
30	31	1%	30	30	0%
45	43	2%	45	43	2%

Table 11. Measured Results Theta Direction

Scan Angle	Measured	Error	Scan Angle (-)	Measured	Error
15	14	1%	15	14	2%
30	31	1%	30	32	2%
45	44	1%	45	43	2%

The results shown in Table 10 and Table 11, coupled with the previous figures, demonstrate the capability of the system to steer the beam in 3-D space. The source of control is implemented by a smartphone that implements dynamic algorithms using internal sensors and the system functions cohesively at many levels of operation. Beam steering accuracy within 2% is achieved. These results demonstrate the capability of the system to act as a whole and successfully steer the main beam of the phased array in the controlled environment. Through the dynamic programming ability of the phone, we also expect that the other system level algorithms to operate in accordance with these results.

CHAPTER VI

CONCLUSIONS AND FUTURE WORK

6.1 Summary

The culmination of research, fundamental theories and external insight brought forth a successful project. Each individual model, with intricate planning, yielded results that showed promised that are confirmed with the conclusion of the final experiment. A smart phone has been successfully integrated as an instrument for control and human integration into an otherwise difficult, complex system.

While the phased microstrip patch array is a fundamental structure, not requiring extensively complex mathematical calculations, it is a necessary component that requires previous knowledge of electromagnetics. Accordingly, the fabricated phased array followed the scientific process closely and provided good results from mathematical derivation. Indeed, the fabricated array performed better than the mathematical simulation. In addition, supplemental knowledge was gained about the interaction of microstrip patches placed in array, such as coupling, despite no impact of this result on the overall system. Additional knowledge was gained on power dividers, while although one was not designed and fabricated for this project, as its presence impacts the overall success of the system.

Using a divide and conquer methodology, additional modules such as the control board were developed with success. As the center connection for all sub-modules, the control board served to generate appropriate voltages for the phase shifters and in addition, provided a common meeting point for external controllers and sensors. The implementation of the circuitry on this PCB provided deeper understanding into control theory and process design. Upon the successful completion of the final experiment, it is clear that the control board worked properly and ultimately, provided a strong pillar of functionality to the entire project.

As an end result, the system successfully implements a smart phone cognitive phased array. The cognitive radio network has many modes of operation that are reconfigurable via the smart phone; all modes of operation successfully implement beam steering in addition to tracking an object. In reference to previous works, this work takes a successful novel approach to object tracking and phased array control that potentially prepares a new line of research. Other research may find an advantage to having a mobile computing resource that is dynamic and fundamentally resourceful for complex networks. Furthermore, the true extent and usability of the smart phone has yet to be used. Future work in this arena is promising and can easily stem from the results of this research.

6.2 Future work

The future work of this project can take on many forms because of the dynamic ability of the smart phone and phased array. There are a considerable amount of changes that can be used to further this project.

Because this research is a modular system, pieces may be removed or added as the research permits. One example of change is found in adding various array structures to the control module. This research highlights the use of a microstrip patch array, which is a fundamentally simple structure; however, other research using spiral antennas or other reconfigurable arrays using fluidics or mechanical mechanisms are easily integrated. In addition, the control board provides power and communications extensions to external controls or sensors that may be used to reconfigure the array.

A second approach of future work in this project is to implement closed loop control algorithms. Currently, the control algorithm assumes that the digital potentiometers are set to a correct voltage level and that the phase shifters assume a corresponding phase shift value; however, to more accurately steer the beam, feedback knowledge can accurately improve the voltage calculation and thereby the phase shift. Furthermore, larger digital potentiometers can be used to obtain more accurate voltage steps. Other styles of closed loop algorithms imply the usage of Kalman filters to track an object in space [10, 11, 13] or other tracking algorithms referenced in the literature. Other sensors may also be used from the server side, such as a camera that tracks motion of an object.

The motion and coordinate values can be relayed through the server to the phone implementing the algorithm. This information is enough to determine phase shifts and thereby control the array.

A third option for future work is found in exploring other sensors and capabilities of the array. Because the transmit and receive patterns of an antenna are the same, an array can be used to determine the incoming direction of RF energy. This style of beam scanning offers an opportunity to relay 3-Dimensional spatial RF energy information to the screen of the phone. An ideal scenario of this use could be a soldier searching for RF activated bombs or determining the direction of foreign communication. In addition, the phased array system could be activated by the phone to send jamming signals in the direction that the energy was found. This type of capability provides a unique advantage during a battle. This type of electromagnetics research can easily stem from this project.

REFERENCES

[1] L. Choon Sae and V. Thiagarajan, "Microstrip Array with Semiconductor Phase Shifter," *IEEE Military Communications Conference, 1996. MILCOM '96, Conference Proceedings,* 1996, pp. 364-368 vol.2.

[2] K. Nakada, T. Marumoto, and R. Iwata, "180&deg;/&alpha;&deg; Combined Phase Shifter," *IEEE Antennas and Propagation Society International Symposium, 1999.* 1999, pp. 218-221 vol.1.

[3] M. A. Johnson, "Phased-Array Beam Steering by Multiplex Sampling," *Proceedings of the IEEE,* vol. 56, pp. 1801-1811, 1968.

[4] J. Pike. (2000). *PAVEPAWS*. Available: http://www.fas.org/spp/military/program/track/pavepaws.htm

[5] K. Boone. (2012). *MESSENGER: Mission to Mercury*. Available: http://www.nasa.gov/mission_pages/messenger/main/index.html

[6] K. F. Braun, "Electrical Oscillations and Wireless Telegraphy," 1909. Available: http://www.nobelprize.org/nobel_prizes/physics/laureates/1909/braun-lecture.pdf

[7] G. W. Kant, P. D. Patel, S. J. Wijnholds, M. Ruiter, and E. van der Wal, "EMBRACE: A Multi-Beam 20,000-Element Radio Astronomical Phased Array Antenna Demonstrator," *IEEE Transactions on Antennas and Propagation,* vol. 59, pp. 1990-2003, 2011.

[8] Alarm.com. (2000). *Mobile Apps: Home Security Systems*. Availabe: http://www.alarm.com/customer/for_your_home.aspx

[9] F. J. Langley, "Commercial Micro Computer Chips for Integrated Phased Array Control," *Microwave Symposium Digest, 1974 S-MTT International*, 1974, pp. 50-53.

[10] G. Soysal and M. Efe, "Performance Comparison of Tracking Algorithms for a Ground Based Radar," *The IEEE Seminar on (Ref. No. 2006/11359) Target Tracking: Algorithms and Applications, 2006.* 2006, pp. 39-46.

[11] F. Daum and R. Fitzgerald, "Decoupled Kalman Filters for Phased Array Radar Tracking," *IEEE Transactions on Automatic Control,* vol. 28, pp. 269-283, 1983.

[12] M. Munu, I. Harrison, and M. S. Woolfson, "Comparison of the Kalman and &alpha;&beta; Filters for the Tracking of Targets Using Phased Array Radar," *Radar 92. International Conference*, 1992, pp. 196-199.

[13] J. Ferrante, "A Kalman Filter-Based Radar Track Data Fusion Algorithm Applied to a Select ICBM Case," *Proceedings of the IEEE Radar Conference, 2004.* 2004, pp. 457-462.

[14] W. Lan-yun, Z. Yong-jun, and W. Wei-xiang, "Study on Theory of Multi-target Tracking and Data Association Algorithms in Phased Array Radar," *ITS 2006 6th International Conference on Telecommunications Proceedings,* 2006, pp. 1232-1235.

[15] G. A. Watson and W. D. Blair, "Tracking performance of a Phased Array Radar with Revisit Time Controlled Using the IMM Algorithm," *Record of the 1994 IEEE National Radar Conference, 1994.,* 1994, pp. 160-165.

[16] C. A. Balanis, *Antenna theory: analysis and design*. New Jersey: John Wiley, 2005.

[17] K. Carver and J. Mink, "Microstrip antenna technology," *IEEE Transactions on Antennas and Propagation,* vol. 29, pp. 2-24, 1981.

[18] Y. Lo, D. Solomon, and W. Richards, "Theory and experiment on microstrip antennas," *IEEE Transactions on Antennas and Propagation,* vol. 27, pp. 137-145, 1979.

[19] E. J. Wilkinson, "An N-Way Hybrid Power Divider," *IRE Transactions on Microwave Theory and Techniques,*vol. 8, pp. 116-118, 1960.

[20] Hittite, "450 Degree Analog Phase Shifter," ed: Hittite, 2009. Available: http://www.hittite.com/content/documents/data_sheet/hmc928lp5.pdf

[21] C. E. K. Thomas H. Cormen, and Ronald L. Rivest. (2000). *Introduction to Algorithms.* The United States of America: MIT Press, 2000.

[22] G. F. Franklin, J. D. Powell, and A. Emami-Naeini, *Feedback Control of Dynamic Systems.* New Jersey: Pearson Prentice Hall, 2006.

[23] HTC. (2012). *HTC Evo*. Available: http://www.htc.com/us/products/evo-sprint

[24] Arduino. (2012). *Arduino*. Available: www.arduino.cc

[25] T. Instruments, "Dual 2-Line to 4-Line Decoders/Demultiplexers," in *Texas Instruments*, ed: Texas Instruments, 1995, p. 12. Available: http://www.ti.com/lit/ds/symlink/sn74ls156.pdf

[26] Microchip. (2012). *MCP4131 Digital Potentiometer*. Available: http://www.microchip.com/wwwproducts/Devices.aspx?dDocName=en531882

[27] I. O. f. Standardization. (2012). *Freely Available Standards*. Available: http://standards.iso.org/ittf/PubliclyAvailableStandards/index.html

[28] J. G. Jones and S. Barry, *CCNA*: Que, 2003.

[29] X. Zhang. (2012). *Lecturing Notes 1-12*. Available: http://ece.tamu.edu/~xizhang/ECEN621/start.php

[30] P. Semiconductors. (1999). *I2C-bus: the worldwide standard for IC communication*. Available: http://www.diakom.com.ru/el/communication/i2c/i2c_ov.pdf

[31] Motorola. (2000, November 11, 2011). *SPI Block Guide*. Available: http://www.ee.nmt.edu/~teare/ee308l/datasheets/S12SPIV3.pdf

[32] B. S. Inc. (2011). *Bluetooth Fast Facts*. Available: http://www.bluetooth.com/Pages/fast-facts.aspx

[33] B. S. Inc. (2011). *Bluetooth Basics*. Available: http://www.bluetooth.com/Pages/Basics.aspx

[34] W.-F. Alliance. (2012). *Wi-Fi*. Available: www.wi-fi.org

[35] R. Corporation. (2012). *Rogers 5880 Properties*. Available: http://psas.pdx.edu/AntennaConstructionLV2/RT-Duroid_5880_Properties.pdf

[36] I. W. Components. (2012). *INStock Wireless 16 Way Power Divider*. Available: http://www.instockwireless.com/16way-n-type-rf-power-splitter-combiner-divider-pd2016.htm

APPENDIX A SMARTPHONE CODE

```
package jensen.research.pharandroid;
import android.app.Activity;
import android.content.BroadcastReceiver;
import android.content.Context;
import android.content.Intent;
import android.content.IntentFilter;
import android.os.Bundle;
import android.util.Log;
import android.view.Menu;a
import android.view.MenuInflater;
import android.view.MenuItem;
import android.view.View;
import android.view.animation.Animation;
import android.view.animation.AnimationUtils;
import android.widget.Button;
import android.widget.EditText;
import android.widget.TextView;
import android.widget.CheckBox;
import at.abraxas.amarino.Amarino; //need to import amarino library.jar
import at.abraxas.amarino.AmarinoIntent;
import android.os.Handler;
import java.net.InetAddress;
import java.net.Socket;
import java.util.List;
import java.io.BufferedWriter;
import java.io.OutputStreamWriter;
import java.io.PrintWriter;
import java.io.IOException; //we never use this, except for error catching
import android.hardware.Sensor;
import android.hardware.SensorEvent;
import android.hardware.SensorEventListener;
import android.hardware.SensorManager;
import android.os.SystemClock;
public class pharandroid extends Activity {
/** Called when the activity is first created. */
@Override
public void onCreate(Bundle savedInstanceState) {
super.onCreate(savedInstanceState);
setContentView(R.layout.main);
if(savedInstanceState != null){
Bundle load = savedInstanceState.getBundle(ICICLE_KEY);
restorestate(load); //this code is to capture and reload a saved state
GoAccel();
}
GoAccel();
}
//started making everything public, bad coding but quick and dirty
public boolean connected = false; //global var used to determine connected state to server
public String serverIpAddress = ""; //global var to store server IP address
private EditText serverIp; //inbox to have user input for server ip address
private TextView displayconnected; //line of text to show current connected servers
public Socket socket; //standard java socket, need to have networking enabled!
public PrintWriter out; //output buffer for socket
private EditText Serverwords; //input for talking to server on test server page
private String Serverstring = ""; //storage for information to be sent to server
private TextView senttoserver;
private TextView homedisplaystatus;
private TextView pos;
//everything for the goACCEL function
private TextView accText;
private TextView pointdisp;
private SensorManager myManager;
private List<Sensor> sensors;
private Sensor accSensor;
private double disptheta,dispphi;
private Boolean showdispflag = false;
private float oldX, oldY, oldZ,cX,cY,cZ,dispx,dispy,dispz,checksum,sendandroidx,sendandroidy = 0f;
private Handler mHandler = new Handler();
public float thisX,thisY,thisZ;
public long mStartTime = 0L;
private Button accelstart; //start accel button on home screen, public
private Button accelstop; //stop button on home screen
private Button calibratebutton; //calibrate button on home screen
private CheckBox trackposition;
private boolean accelstarted = false;
private boolean calibrated = false;
public float[] sensorarray = new float[3];
public float[] calibratearray = new float[3];
public float[] phasediffarray = new float[2];
private float[] displayPhases = new float[2];
SystemClock thread;
private static String ICICLE_KEY = "pharandroid";
//This is using amarino to connect to an Arduino BT, put the MAC of the BT
private static final String DEVICE_ADDRESS =  "00:07:80:99:56:34";
//Arduino receiver, from amarino library, receives data back from BT
private ArduinoReceiver arduinoReceiver = new ArduinoReceiver();
//create options menu happens when user presses menu button, see /res/menu/mainmenu
@Override
public boolean onCreateOptionsMenu(Menu menu) {
//this is standard code from Android Developer website
MenuInflater inflater = getMenuInflater();
inflater.inflate(R.menu.mainmenu, menu);
return true;
}
```

```
//each menu item must have a corresponding xml layout
@Override
public boolean onOptionsItemSelected(MenuItem item) {
//TextView display = (TextView) findViewById(R.id.display);
// Handle item selection
switch (item.getItemId()) {
//firstcase is for the main homescreen with all information display
case R.id.start:
setContentView(R.layout.main);
//GoAccel() is a continuous running function of sub functions
GoAccel();
return true;
//server case is to configure a socket
case R.id.server:
setContentView(R.layout.serverconfigure);
ConnectToServer();
return true;
//just a test case, if protocol not used, this page is used to send random information
case R.id.talk:
setContentView(R.layout.communicator);
ServerTalk();
return true;
default:
return super.onOptionsItemSelected(item);
}
}
//function to load xml and to make a socket connection as client
public void ConnectToServer(){
//setting up the xml on the server configure page
serverIp = (EditText) findViewById(R.id.server_ip);
displayconnected = (TextView) findViewById(R.id.text1);
Button ServerConnect = (Button) findViewById(R.id.connect_phones);
Button Disconnect =  (Button) findViewById(R.id.cancel);
//if we are already connected, use global var serverIPaddress to display connection
//connected is a global variable
if(connected){
displayconnected.setText("Connected to: "+serverIpAddress);
}
//create the listener on the disconnect button
Disconnect.setOnClickListener(new View.OnClickListener() {
@Override
public void onClick(View v) {
//we need to be connected to disconnect
if(connected){
try{
socket.close();
displayconnected.setText("Disconnected from :"+serverIpAddress);
connected = false;
}catch (Exception e) {
Log.e("ClientActivity", "S: Error", e);
}
}else{
displayconnected.setText("Not Currently Connected, enter IP Address");
}
//       unregisterReceiver(arduinoReceiver);
}
});
//button to connect to server
ServerConnect.setOnClickListener(new View.OnClickListener() {
public void onClick(View v) {
//only can connect if we haven't already
if (!connected) {
//when the button is pressed, snag the ip from serverIp edittext
serverIpAddress = serverIp.getText().toString();
//just in case the network is congested, inform user we are connecting
displayconnected.setText("Connecting To " + serverIpAddress);
if (!serverIpAddress.equals("")) {
//Thread cThread = new Thread(new ClientThread());
//      cThread.start();
try{
InetAddress serverAddr = InetAddress.getByName(serverIpAddress);
Log.d("ClientActivity", "C: Connecting...");
//standard socket connection, random port 4444
socket =  new Socket(serverAddr, 4444);
//set global var connected to true
connected = true;
//confirm to the user that we have connected to serverIpAddress
displayconnected.setText("Connected To " + serverIpAddress);
out = new PrintWriter(new BufferedWriter(new OutputStreamWriter(socket
.getOutputStream())), true);
//assuming user running processing "BEAM", this starts the beam appropriately
out.println("180,180,0,-105");
}catch (Exception e) {
Log.e("ClientActivity", "S: Error", e);
}
}
}
}
});
}

//just a test page, probably won't work if protocol is running on server
public void ServerTalk(){
Button Serversend = (Button) findViewById(R.id.send);
Serverwords = (EditText) findViewById(R.id.textservertalk);
final TextView senttoserverstatus = (TextView) findViewById(R.id.senttoserverstatus);
Serversend.setOnClickListener(new View.OnClickListener() {
@Override
public void onClick(View v) {
if(connected){
```

```
try{
Serverstring = Serverwords.getText().toString();
out.println(Serverstring);
senttoserver.setText(Serverstring);
}catch (Exception e) {
Log.e("ClientActivity", "S: Error", e);
}
}else{
senttoserverstatus.setText("Not Connected");
senttoserver.setText("Nothing sent because we're not connected");
}
//       unregisterReceiver(arduinoReceiver);
}
});

}
//main thread, runs information gathering and calculations..
public void GoAccel(){
homedisplaystatus = (TextView) findViewById(R.id.display);
pos = (TextView) findViewById(R.id.calibratepos);
pos.setText("Current Calibrated Position is:\nx:"+cX+";\ny:"+cY+";\nz:"+cZ+";\n");
if(accelstarted){
//if we have calibrated and started accel button
homedisplaystatus.setText("Sensor Reader is Running...");

//mhandler is the "timer" of the program we can remove any requests before making a new one
mHandler.removeCallbacks(mUpdateTimeTask);
mHandler.postDelayed(mUpdateTimeTask,100);
}else{
homedisplaystatus.setText("Sensor Reader is not Running...");
}
myManager = (SensorManager)getSystemService(Context.SENSOR_SERVICE);

//in newer versions of android TYPE_ORIENTATION deprecated
sensors = myManager.getSensorList(Sensor.TYPE_ORIENTATION);

if(sensors.size() > 0)
{
accSensor = sensors.get(0);
}

//lets create our buttons
accelstart = (Button) findViewById(R.id.startaccel);
accelstop = (Button) findViewById(R.id.stopaccel);
calibratebutton =  (Button) findViewById(R.id.calibrate);
trackposition = (CheckBox) findViewById(R.id.CheckBox01);
pointdisp = (TextView) findViewById(R.id.point);

//check to see that we've calibrated our position
if(calibrated){
```

```
//listen for user to hit the start button to start reading accelerometer
accelstart.setOnClickListener(new View.OnClickListener() {

@Override
public void onClick(View v) {
accelstarted = true;
homedisplaystatus.setText("sensor reader is running...");
//mStartTime is for the mhandler, by default it should always be 0L
if (mStartTime == 0L) {
mStartTime = System.currentTimeMillis();
mHandler.removeCallbacks(mUpdateTimeTask);
mHandler.postDelayed(mUpdateTimeTask, 100);
}


}
});
}
else{
homedisplaystatus.setText("CALIBRATE POSITION FIRST!");
}

//create listener if user decides to hit stop button
accelstop.setOnClickListener(new View.OnClickListener() {

@Override
public void onClick(View v) {
//if we press stop, don't update task, stop the accelerometer, set default time,
//and start main app
mHandler.removeCallbacks(mUpdateTimeTask);
accelstarted = false;
homedisplaystatus.setText("Sensor Reader is not running...");
mStartTime = 0L;
GoAccel();
}
});

//button for calibration, it is constantly active in case of recalibration
calibratebutton.setOnClickListener(new View.OnClickListener() {

@Override
public void onClick(View v) {
//oldX,oldY,oldZ are in updateTV, they are current reading of Accelerometer
//old... are always updated on change of the accelerometer, see updateTV
cX = oldX;
cY = oldY;
cZ = oldZ;

//calibratearray is an array to store the calibrate position in case we leave the program
calibratearray[0]=cX;
calibratearray[1]=cY;
calibratearray[2]=cZ;

//let the user know that we've calibrated, and restart main page
calibrated = true;
pos.setText("Current Calibrated Position is:\nx:"+cX+";\ny:"+cY+";\nz:"+cZ+";\n");
GoAccel();
}
});

}

//this is the main thread, gets executed by mHandler
private Runnable mUpdateTimeTask = new Runnable() {
public void run() {
accText = (TextView) findViewById(R.id.accelvalues);
final long start = mStartTime;
long millis = SystemClock.uptimeMillis() - start;
int seconds = (int) (millis / 1000);
int minutes = seconds / 60;
seconds     = seconds % 60;
dispx = oldX - cX;
dispy = oldY - cY;
dispz = oldZ - cZ;
displayPhases = phasediff(dispx,dispy,dispz);
sensorarray[0] = dispx;
sensorarray[1] = dispy;
sensorarray[2] = dispz;
//checksum = 255 - (Math.round(dispx)+Math.round(dispy)+Math.round(dispz));
if(connected){
out.println(Math.round(dispx)+","+Math.round(dispy)+","+Math.round(dispz)+","+Math.round(Math.toD
egrees((double)displayPhases[0]))+","+Math.round(Math.toDegrees((double)displayPhases[1])));
}
send_arduino(200.0,displayPhases); //200.0 is frametype for phasedata
//sendandroidx = Math.round(Math.toDegrees((double)displayPhases[0]));
//sendandroidy = Math.round(Math.toDegrees((double)displayPhases[1]));
///Amarino.sendDataToArduino(pharandroid.this,"00:07:80:99:56:34", 'B',dispx);
//thread.sleep(100);
//Amarino.sendDataToArduino(pharandroid.this,"00:07:80:99:56:34", 'B',sendandroidx);
//thread.sleep(100);
//Amarino.sendDataToArduino(pharandroid.this,"00:07:80:99:56:34", 'B',sendandroidy);
accText.setText("x: " + dispx + ";\n y:" + Math.round(dispy) + ";\n z: " + Math.round(dispz) +";\n Phase
Diff x: "+ Math.round(Math.toDegrees((double)displayPhases[0]))+";\t Theta:
"+Math.round(Math.toDegrees(disptheta))+"\n Phase Diff y:
"+Math.round(Math.toDegrees((double)displayPhases[1]))+"\t Phi:
"+Math.round(Math.toDegrees(dispphi)));
mHandler.postDelayed(this,300); //this is to loop every 300 ms
}
};
```

```
public float[] phasediff(float x2, float y2, float z2){
float returnarray[] = new float[2];
double w_hat = 0;
double PhaseBx,PhaseBy = 0;
double a_hat = 0;
double phireal = 0;
double thetareal = 0;
double newpoint[]={0,0,0};
double psi = y2*Math.PI/180;
double theta = z2*Math.PI/180;
double phi = x2*Math.PI/180;
double rotmatrix[][] = {{Math.cos(theta)*Math.cos(phi),-
1.0*Math.cos(psi)*Math.sin(phi)+Math.sin(psi)*Math.sin(theta)*Math.cos(phi),Math.sin(phi)*Math.sin(p
si)+Math.cos(psi)*Math.sin(theta)*Math.cos(phi)},
{Math.cos(theta)*Math.sin(phi),Math.cos(psi)*Math.cos(phi)+Math.sin(psi)*Math.sin(theta)*Math.sin(p
hi),-1.0*Math.sin(psi)*Math.cos(phi)+Math.cos(psi)*Math.sin(theta)*Math.sin(phi)},
{-1.0*Math.sin(theta),Math.sin(psi)*Math.cos(theta),Math.cos(psi)*Math.cos(theta)}
};

double mypoint[] = {0.00001,0.00000001,1.0}; //these are the plane's xyz coordinates
int m1rows = rotmatrix.length;
if(trackposition.isChecked()){
mypoint[0] = 0.1;
mypoint[1] = 0.1;
mypoint[2] = 1.0;
}
//int m1cols = rotmatrix[0].length;
//int m2rows = mypoint.length;
double result = 0;
if(trackposition.isChecked()){
if(!showdispflag){
showpoint();
pointdisp.setText("Tracking point x: "+mypoint[0]+" y: "+mypoint[1]+" z: "+mypoint[2]);
showdispflag = true;
}
for(int i=0;i<m1rows;++i){
result = 0;
for(int j=0;j<m1rows;++j){
result = 1*rotmatrix[i][j]*mypoint[j]+result;
}
newpoint[i]=result;
}
}else{
if(showdispflag){
hidepoint();
showdispflag = false;
showpoint();
pointdisp.setText("You currently have control of beam direction");
}
for(int i=0;i<m1rows;++i){
result = 0;
for(int j=0;j<m1rows;++j){
result = -1*rotmatrix[i][j]*mypoint[j]+result;
}
newpoint[i]=result;
}
}
if(newpoint[1]<0){
w_hat = -1*(Math.sqrt(Math.pow(newpoint[0],2)+Math.pow(newpoint[1],2)));
phireal = Math.PI + Math.acos(newpoint[0]/w_hat);
}
if(newpoint[1]>=0){
w_hat = Math.sqrt(Math.pow(newpoint[0],2)+Math.pow(newpoint[1],2));
phireal = Math.acos(newpoint[0]/w_hat);
}
a_hat = Math.sqrt(Math.pow(w_hat, 2)+Math.pow(newpoint[2], 2));
w_hat = Math.sqrt(Math.pow(newpoint[0],2)+Math.pow(newpoint[1],2));
thetareal =  .5*Math.PI - Math.acos(w_hat/a_hat); //pi/2 - angle to get theta
disptheta = thetareal;
dispphi = phireal;
PhaseBx = -1*Math.PI*Math.sin(thetareal)*Math.cos(phireal);
PhaseBy = -1*Math.PI*Math.sin(thetareal)*Math.sin(phireal);
returnarray[0]= (float) PhaseBx;
returnarray[1]= (float)PhaseBy;
return returnarray;
}

public void showpoint(){
Animation animation = AnimationUtils.loadAnimation(this,
android.R.anim.slide_in_left);
pointdisp.setVisibility(View.VISIBLE);
pointdisp.startAnimation(animation);
}

public void hidepoint(){
Animation animation = AnimationUtils.loadAnimation(pharandroid.this,
android.R.anim.slide_out_right);
pointdisp.startAnimation(animation);
pointdisp.setVisibility(View.GONE);
}
public void updateTV(float x, float y, float z)
{
//thisX = x - oldX * 10;
//thisY = y - oldY * 10;
//thisZ = z - oldZ * 10;

// accText.setText("x: " + Math.round(thisX) + ";\n y:" + Math.round(thisY) + ";\n z: " +
Math.round(thisZ));
oldX = x;
```

```
oldY = y;
oldZ = z;
}

public void send_arduino(double frametype,float[] values){
final double startbyte = 255.0;
final int intlength = (int)values.length;
final double length = (double)values.length;
final int sleeptime = 20;
final double frameid = 1.0;
final char funcflag = 'B';
double checksum = startbyte+length+frametype+frameid;
Amarino.sendDataToArduino(pharandroid.this,DEVICE_ADDRESS, funcflag,startbyte);
thread.sleep(sleeptime);
Amarino.sendDataToArduino(pharandroid.this,DEVICE_ADDRESS, funcflag,length);
thread.sleep(sleeptime);
Amarino.sendDataToArduino(pharandroid.this,DEVICE_ADDRESS, funcflag,frametype);
thread.sleep(sleeptime);
Amarino.sendDataToArduino(pharandroid.this,DEVICE_ADDRESS, funcflag,frameid);
thread.sleep(sleeptime);
for(int i=0;i<intlength;++i){
sendandroidx = Math.round(Math.toDegrees((double)values[i]));
if(sendandroidx < 0){
checksum=checksum+256+sendandroidx;
}else{
checksum+=sendandroidx;
}
Amarino.sendDataToArduino(pharandroid.this,DEVICE_ADDRESS, funcflag,sendandroidx);
thread.sleep(sleeptime);
}
checksum = Math.round((double)checksum % 6);
Amarino.sendDataToArduino(pharandroid.this,DEVICE_ADDRESS, funcflag,checksum);
}
private final SensorEventListener mySensorListener = new SensorEventListener()
{
public void onSensorChanged(SensorEvent event)
{
updateTV(event.values[0],
event.values[1],
event.values[2]);
}

public void onAccuracyChanged(Sensor sensor, int accuracy) {}
};
@Override
protected void onStart()
{
super.onStart();
myManager.registerListener(mySensorListener, accSensor, SensorManager.SENSOR_DELAY_GAME);
registerReceiver(arduinoReceiver, new IntentFilter(AmarinoIntent.ACTION_RECEIVED));
```

```
// this is how you tell Amarino to connect to a specific BT device from within your own code
//Amarino.connect(this, DEVICE_ADDRESS);
}
@Override
protected void onStop()
{
super.onStop();
//Amarino.disconnect(this, DEVICE_ADDRESS);
// do never forget to unregister a registered receiver
mHandler.removeCallbacks(mUpdateTimeTask);
unregisterReceiver(arduinoReceiver);
myManager.unregisterListener(mySensorListener);
}
public Bundle savestate(){
Bundle map = new Bundle();
map.putBoolean("accel", accelstarted);
map.putBoolean("calibrated",calibrated);
map.putFloatArray("calibratedvalues",calibratearray);
map.putBoolean("server", connected);
map.putString("oldip", serverIpAddress);
return map;
}
public void restorestate(Bundle icicle){
accelstarted = icicle.getBoolean("accel");
calibrated = icicle.getBoolean("calibrated");
sensorarray = icicle.getFloatArray("sensorvalues");
serverIpAddress = icicle.getString("oldip");
dispx = sensorarray[0];
dispy= sensorarray[1];
dispz = sensorarray[2];
connected = icicle.getBoolean("server");
calibratearray = icicle.getFloatArray("calibratedvalues");
cX = calibratearray[0];
cY = calibratearray[1];
cZ = calibratearray[2];
servereconnect(serverIpAddress);
}
public void servereconnect(String oldip){
try{
InetAddress serverAddr = InetAddress.getByName(oldip);
Log.d("ClientActivity", "C: Connecting...");

socket =  new Socket(serverAddr, 4444);
out = new PrintWriter(new BufferedWriter(new OutputStreamWriter(socket
.getOutputStream())), true);
}catch (Exception e) {
Log.e("ClientActivity", "S: Error", e);
}
```

```
}
@Override
public void onSaveInstanceState(Bundle outState) {
//Store the game state
outState.putBundle(ICICLE_KEY, savestate());
}
public class ArduinoReceiver extends BroadcastReceiver {
@Override
public void onReceive(Context context, Intent intent) {
String data = null;
final String address = intent.getStringExtra(AmarinoIntent.EXTRA_DEVICE_ADDRESS);

// the type of data
final int dataType = intent.getIntExtra(AmarinoIntent.EXTRA_DATA_TYPE, -1);

if (dataType == AmarinoIntent.STRING_EXTRA){
data = intent.getStringExtra(AmarinoIntent.EXTRA_DATA);
pos.setText(data);

if (data != null){
//mValueTV.setText(data);
try {
// since we know that our string value is an int number we can parse it to an integer
final int sensorReading = Integer.parseInt(data);
}
catch (NumberFormatException e) { /* oh data was not an integer */ }
}
}
}
}


}
```

APPENDIX B ARDUINO BT CODE

```
#include <MeetAndroid.h>
#include <Wire.h>

int pin12 = 12;
MeetAndroid meetAndroid;


void setup()
{
// use the baud rate your bluetooth module is configured to
// not all baud rates are working well, i.e. ATMEGA168 works best with 57600
Serial.begin(115200);  //using arduino BT, works best with 115200
Wire.begin();

// register callback functions, which will be called when an associated event occurs.
// - the first parameter is the name of your function (see below)
// - match the second parameter ('A', 'B', 'a', etc...) with the flag on your Android application
//   small letters are custom events, capital letters inbuilt Amarino events
meetAndroid.registerFunction(floatValues, 'B'); // float array
}
void loop()
{
meetAndroid.receive(); // you need to keep this in your loop() to receive events
}
void floatValues(byte flag, byte numOfValues)
{
// create an array where all event values should be stored
// the number of values attached to this event is given by
// a parameter(numOfValues)
float data[numOfValues];
// call the library function to fill the array with values
meetAndroid.getFloatValues(data);
digitalWrite(pin12,HIGH);
sendslave(4,data,numOfValues);
digitalWrite(pin12,LOW);
}
void sendslave(int whoto,float *values,byte count){
Wire.beginTransmission(whoto);
for (int i=0; i<count;i++)
{
Wire.send((int)values[i]);
}
Wire.endTransmission();
}
```

APPENDIX C ARDUINO SLAVE 1 CODE

```
//This is the framework for the API to receive frames from the android phone
//Dynamic allocation of memory is important as the size of the payload may vary but is set to 2 for now...

//Need wire and SPI libraries
#include <Wire.h>
#include <SPI.h>

//This is for the API to capture the correct data
int startbyte,length,frameid,frametype;
int *payload = (int *)calloc(2,sizeof(int));
int *frame = (int *)calloc(6,sizeof(int));
int y,bright1,bright2,bright3,bright4,bright5,bright6,bright7,bright8;
int count = 0;
int checksum = 0;
int payloadcount = 0;
//////////////////////////////////

//variables to control the circuitry, demux and opamps and digipots
const int _sck = 3;
const int _sdi = 4;
const int pinB = 10;
const int pinA = 9;
const int ctl = 8;
const int pinB2 = 7;
const int pinA2 = 6;
const int ctl2 = 5;
//////////////////////////////
void setup()
{

//Initialize control circuitry pins
pinMode (_sck, OUTPUT);
pinMode (_sdi, OUTPUT);
pinMode(pinB, OUTPUT);
pinMode(pinA, OUTPUT);
pinMode(ctl, OUTPUT);
pinMode(pinB2, OUTPUT);
pinMode(pinA2, OUTPUT);
pinMode(ctl2, OUTPUT);

digitalWrite(ctl,HIGH);
digitalWrite(pinA, LOW);
digitalWrite(pinB, LOW);
digitalWrite(ctl2,HIGH);
digitalWrite(pinA2, LOW);
digitalWrite(pinB2, LOW);
```

```
//////////////////////////

//Initialize frame
init_values();
Wire.begin(4); // join i2c bus with address #4
Wire.onReceive(receiveEvent); // register event

//need 115200 for communication with arduino BT
Serial.begin(115200); // start serial for output

// initialize SPI:
SPI.begin();
}
void loop()
{
delay(50);
}
// function that executes whenever data is received from master
// this function is registered as an event, see setup()
void receiveEvent(int howMany)
{
/*while(1 < Wire.available()) // loop through all but the last
{
//int x = Wire.receive();
//int y = Wire.receive(); // receive byte as an integer
// Serial.println(x);
//int c = Wire.receive(); // receive byte as a character
//Serial.print(c); // print the character
}*/
int x = Wire.receive();
//Serial.println(x);
if(x == 255){ // Look for startbyte
init_values();
startbyte = x;
checksum+=startbyte;
count++;
}else if(count == 1){ //only add to frame if you have received a startbyte
length = x;
checksum+=length;
payload = (int *)realloc(payload,length);
count++;
}else if(count == 2){
frametype = x;
checksum+=frametype;
count++;
}else if(count == 3){
frameid = x;
checksum+=frameid;
count++;
}else if(count > 3){
```

```
if(payloadcount < length){
payload[payloadcount] = x; //store payload as array
checksum+=x;
payloadcount++;
count++;
}else{
checksum = checksum % 6;
if(x == checksum){
x=payload[0]; //reuse memory variables
y=payload[1];
//Serial.println("Packets Match");
if(y >=128){
y = y-256;
}
if(x>=128){
x = x-256;
}
x=x*-1; //we are going to have no negative phase shifts in time...
y=y*-1;
int total;
if(x<0 && y>0){
total = -1*3*x; //if x is less than 0 and y not, we want to calculate the max value of a phase delay using
max X
bright1 = 0 + total;
bright2 = y + total;
bright3 = (2*y)+total;
bright4 = (3*y)+total;
bright5 = (3*y)+x+total;
bright6 = (2*y)+x+total;
bright7 = y+x+total;
bright8 = x+total;
}else if(x>0 && y<0){
total = -1*3*y;
bright1 = 0 + total;
bright2 = y + total;
bright3 = (2*y)+total;
bright4 = (3*y)+total;
bright5 = (3*y)+x+total;
bright6 = (2*y)+x+total;
bright7 = y+x+total;
bright8 = x+total;
}else if(x<0 && y<0){
total = -1*(3*x+3*y);
bright1 = 0 + total;
bright2 = y + total;
bright3 = (2*y)+total;
bright4 = (3*y)+total;
bright5 = (3*y)+x+total;
bright6 = (2*y)+x+total;
bright7 = y+x+total;
```

```
bright8 = x+total;
}else
{
//total = -1*2*x;
bright1 = 0 + total;
bright2 = y + total;
bright3 = (2*y)+total;
bright4 = (3*y)+total;
bright5 = (3*y)+x+total;
bright6 = (2*y)+x+total;
bright7 = y+x+total;
bright8 = x+total;
}

//Not a true time phase delay.. thus if we have values that are greater than n*2*pi we want to subtract
n*2*pi
if(bright1 > 720){
bright1=bright1-720;
}else if(bright1 > 360){
bright1 = bright1 - 360;
}

if(bright2 > 720){
bright2=bright2-720;
}else if(bright2 > 360){
bright2 = bright2 - 360;
}

if(bright3 > 720){
bright3=bright3-720;
}else if(bright1 > 360){
bright3 = bright3 - 360;
}

if(bright4 > 720){
bright4=bright4-720;
}else if(bright4 > 360){
bright4 = bright4 - 360;
}

if(bright5 > 720){
bright5=bright5-720;
}else if(bright5 > 360){
bright5 = bright5 - 360;
}

if(bright6 > 720){
bright6=bright6-720;
}else if(bright6 > 360){
bright6 = bright6 - 360;
```

```
}

if(bright7 > 720){
bright7=bright7-720;
}else if(bright7 > 360){
bright7 = bright7 - 360;
}

if(bright8 > 720){
bright8=bright8-720;
}else if(bright8 > 360){
bright8 = bright8 - 360;
}

/*bright1 = map(bright1,0,360,0,255);
bright2 = map(bright2,0,360,0,255);
bright3 = map(bright3,0,360,0,255);
bright4 = map(bright4,0,360,0,255);
//bright5 = map(bright5,0,360,0,255);*/
Serial.print(" Bright1: ");Serial.print(bright1);Serial.print(" Bright2: ");Serial.print(bright2);Serial.print("
Bright3: ");Serial.print(bright3);
Serial.print(" Bright4: ");Serial.print(bright4);
Serial.print(" Bright5: ");Serial.print(bright5);
Serial.print(" Bright6: ");Serial.print(bright6);
Serial.print(" Bright7: ");Serial.print(bright7);
Serial.print(" Bright8: ");Serial.print(bright8);
Serial.print("\n");
setpotvalue(0,bright1);
setpotvalue(1,bright2);
setpotvalue(2,bright3);
setpotvalue(3,bright4);
setpotvalue(4,bright5);
setpotvalue(5,bright6);
setpotvalue(6,bright7);
setpotvalue(7,bright8);

}else{
Serial.print(x);Serial.print(",");Serial.print(checksum);Serial.print("\n");
}
}
}else{
//int y = Wire.receive(); // receive byte as an integer
Serial.println(x); // print the integer
}
}

void init_values(){
startbyte = 0;
length = 0;
frameid = 0;
```

```
frametype = 0;
count = 0;
payloadcount = 0;
checksum = 0;
}

int activatepot(int selectpot){
if(selectpot == 0){
digitalWrite(ctl,LOW);
digitalWrite(pinA,LOW);
digitalWrite(pinB,LOW);
}else if(selectpot == 1){
digitalWrite(ctl,LOW);
digitalWrite(pinA,HIGH);
digitalWrite(pinB,LOW);
}else if(selectpot == 2){
digitalWrite(ctl,LOW);
digitalWrite(pinA,LOW);
digitalWrite(pinB,HIGH);
}else if(selectpot == 3){
digitalWrite(ctl,LOW);
digitalWrite(pinA,HIGH);
digitalWrite(pinB,HIGH);
}else if(selectpot == 4){
digitalWrite(ctl2,LOW);
digitalWrite(pinA2,LOW);
digitalWrite(pinB2,LOW);
}else if(selectpot == 5){
digitalWrite(ctl2,LOW);
digitalWrite(pinA2,HIGH);
digitalWrite(pinB2,LOW);
}else if(selectpot == 6){
digitalWrite(ctl2,LOW);
digitalWrite(pinA2,LOW);
digitalWrite(pinB2,HIGH);
}else if(selectpot == 7){
digitalWrite(ctl2,LOW);
digitalWrite(pinA2,HIGH);
digitalWrite(pinB2,HIGH);
}else{
digitalWrite(ctl,HIGH);
digitalWrite(ctl2,HIGH);
}
//delay(50);
}

int deactivatepot(){
//delay(50);
digitalWrite(ctl,HIGH);
digitalWrite(ctl2,HIGH);
```

```
}

int getvoltage(int phasediff){
int returnval;
float temp =
(.000000002*phasediff*phasediff*phasediff)+(.00003*phasediff*phasediff)+(.0118*phasediff)-.0816;
temp = temp/.12;
//Serial.println(temp);
int lowval = (int) temp;
float checklow = temp-.5;
int check = (int) checklow;
if(checklow < lowval){
returnval = lowval;
}else{
//Serial.print("Made It");
float rounding = temp+.5;
returnval = (int) rounding;
}
returnval=129-returnval;
Serial.println(returnval);
//Serial.print("Return Value: ");Serial.print(returnval);Serial.print("\n");
return returnval;



}

int setpotvalue(int digipot, int potvalue){
activatepot(digipot);
potvalue+=90;//this makes the error smaller but still not great
int newvolt = getvoltage(potvalue);
shiftOut(_sdi, _sck, MSBFIRST, (newvolt>>8));
shiftOut(_sdi, _sck, MSBFIRST, newvolt);
//shiftOut(_sdi, _sck, MSBFIRST, lowvalue);
deactivatepot();
}
```

APPENDIX D ARDUINO SLAVE 2 CODE

```
//This is the framework for the API to receive frames from the android phone
//Dynamic allocation of memory is important as the size of the payload may vary but is set to 2 for now...

//Need wire and SPI libraries
#include <Wire.h>
#include <SPI.h>

//This is for the API to capture the correct data
int startbyte,length,frameid,frametype;
int *payload = (int *)calloc(2,sizeof(int));
int *frame = (int *)calloc(6,sizeof(int));
int y,bright1,bright2,bright3,bright4,bright5,bright6,bright7,bright8;
int count = 0;
int checksum = 0;
int payloadcount = 0;
//////////////////////////////////

//variables to control the circuitry, demux and opamps and digipots
const int _sck = 3;
const int _sdi = 4;
const int pinB = 10;
const int pinA = 9;
const int ctl = 8;
const int pinB2 = 7;
const int pinA2 = 6;
const int ctl2 = 5;
////////////////////////////
void setup()
{

//Initialize control circuitry pins
pinMode (_sck, OUTPUT);
pinMode (_sdi, OUTPUT);
pinMode(pinB, OUTPUT);
pinMode(pinA, OUTPUT);
pinMode(ctl, OUTPUT);
pinMode(pinB2, OUTPUT);
pinMode(pinA2, OUTPUT);
pinMode(ctl2, OUTPUT);

digitalWrite(ctl,HIGH);
digitalWrite(pinA, LOW);
digitalWrite(pinB, LOW);
digitalWrite(ctl2,HIGH);
digitalWrite(pinA2, LOW);
digitalWrite(pinB2, LOW);
```

```
//////////////////////////

//Initialize frame
init_values();
Wire.begin(4); // join i2c bus with address #4
Wire.onReceive(receiveEvent); // register event

//need 115200 for communication with arduino BT
Serial.begin(115200); // start serial for output

// initialize SPI:
SPI.begin();
}
void loop()
{
delay(50);
}
// function that executes whenever data is received from master
// this function is registered as an event, see setup()
void receiveEvent(int howMany)
{
/*while(1 < Wire.available()) // loop through all but the last
{
//int x = Wire.receive();
//int y = Wire.receive(); // receive byte as an integer
// Serial.println(x);
//int c = Wire.receive(); // receive byte as a character
//Serial.print(c); // print the character
}*/
int x = Wire.receive();
//Serial.println(x);
if(x == 255){ // Look for startbyte
init_values();
startbyte = x;
checksum+=startbyte;
count++;
}else if(count == 1){ //only add to frame if you have received a startbyte
length = x;
checksum+=length;
payload = (int *)realloc(payload,length);
count++;
}else if(count == 2){
frametype = x;
checksum+=frametype;
count++;
}else if(count == 3){
frameid = x;
checksum+=frameid;
count++;
}else if(count > 3){
```

```
if(payloadcount < length){
payload[payloadcount] = x; //store payload as array
checksum+=x;
payloadcount++;
count++;
}else{
checksum = checksum % 6;
if(x == checksum){
x=payload[0]; //reuse memory variables
y=payload[1];
//Serial.println("Packets Match");
if(y >=128){
y = y-256;
}
if(x>=128){
x = x-256;
}
x=x*-1; //we are going to have no negative phase shifts in time...
y=y*-1;
int total;
if(x<0 && y>0){
total = -1*3*x; //if x is less than 0 and y not, we want to calculate the max value of a phase delay using
max X
bright1 = 2*x + total;
bright2 = 2*x + y + total;
bright3 = 2*x + (2*y)+total;
bright4 = (3*y)+2*x+total;
bright5 = (3*y)+3*x+total;
bright6 = (2*y)+3*x+total;
bright7 = y+3*x+total;
bright8 = 3*x+total;
}else if(x>0 && y<0){
total = -1*3*y;
bright1 = 2*x + total;
bright2 = 2*x + y + total;
bright3 = 2*x + (2*y)+total;
bright4 = (3*y)+2*x+total;
bright5 = (3*y)+3*x+total;
bright6 = (2*y)+3*x+total;
bright7 = y+3*x+total;
bright8 = 3*x+total;
}else if(x<0 && y<0){
total = -1*(3*x+3*y);
bright1 = 2*x + total;
bright2 = 2*x + y + total;
bright3 = 2*x + (2*y)+total;
bright4 = (3*y)+2*x+total;
bright5 = (3*y)+3*x+total;
bright6 = (2*y)+3*x+total;
bright7 = y+3*x+total;
```

```
bright8 = 3*x+total;
}else
{
//total = -1*2*x;
bright1 = 2*x + total;
bright2 = 2*x + y + total;
bright3 = 2*x + (2*y)+total;
bright4 = (3*y)+2*x+total;
bright5 = (3*y)+3*x+total;
bright6 = (2*y)+3*x+total;
bright7 = y+3*x+total;
bright8 = 3*x+total;
}

//Not a true time phase delay.. thus if we have values that are greater than n*2*pi we want to subtract
n*2*pi
if(bright1 > 720){
bright1=bright1-720;
}else if(bright1 > 360){
bright1 = bright1 - 360;
}

if(bright2 > 720){
bright2=bright2-720;
}else if(bright2 > 360){
bright2 = bright2 - 360;
}

if(bright3 > 720){
bright3=bright3-720;
}else if(bright1 > 360){
bright3 = bright3 - 360;
}

if(bright4 > 720){
bright4=bright4-720;
}else if(bright4 > 360){
bright4 = bright4 - 360;
}

if(bright5 > 720){
bright5=bright5-720;
}else if(bright5 > 360){
bright5 = bright5 - 360;
}

if(bright6 > 720){
bright6=bright6-720;
}else if(bright6 > 360){
bright6 = bright6 - 360;
```

```
}

if(bright7 > 720){
bright7=bright7-720;
}else if(bright7 > 360){
bright7 = bright7 - 360;
}

if(bright8 > 720){
bright8=bright8-720;
}else if(bright8 > 360){
bright8 = bright8 - 360;
}

/*bright1 = map(bright1,0,360,0,255);
bright2 = map(bright2,0,360,0,255);
bright3 = map(bright3,0,360,0,255);
bright4 = map(bright4,0,360,0,255);
//bright5 = map(bright5,0,360,0,255);*/
Serial.print(" Bright1: ");Serial.print(bright1);Serial.print(" Bright2: ");Serial.print(bright2);Serial.print("
Bright3: ");Serial.print(bright3);
Serial.print(" Bright4: ");Serial.print(bright4);
Serial.print(" Bright5: ");Serial.print(bright5);
Serial.print(" Bright6: ");Serial.print(bright6);
Serial.print(" Bright7: ");Serial.print(bright7);
Serial.print(" Bright8: ");Serial.print(bright8);
Serial.print("\n");
setpotvalue(0,bright1);
setpotvalue(1,bright2);
setpotvalue(2,bright3);
setpotvalue(3,bright4);
setpotvalue(4,bright5);
setpotvalue(5,bright6);
setpotvalue(6,bright7);
setpotvalue(7,bright8);

}else{
Serial.print(x);Serial.print(",");Serial.print(checksum);Serial.print("\n");
}
}
}else{
//int y = Wire.receive(); // receive byte as an integer
Serial.println(x); // print the integer
}
}

void init_values(){
startbyte = 0;
length = 0;
frameid = 0;
```

```
frametype = 0;
count = 0;
payloadcount = 0;
checksum = 0;
}

int activatepot(int selectpot){
if(selectpot == 0){
digitalWrite(ctl,LOW);
digitalWrite(pinA,LOW);
digitalWrite(pinB,LOW);
}else if(selectpot == 1){
digitalWrite(ctl,LOW);
digitalWrite(pinA,HIGH);
digitalWrite(pinB,LOW);
}else if(selectpot == 2){
digitalWrite(ctl,LOW);
digitalWrite(pinA,LOW);
digitalWrite(pinB,HIGH);
}else if(selectpot == 3){
digitalWrite(ctl,LOW);
digitalWrite(pinA,HIGH);
digitalWrite(pinB,HIGH);
}else if(selectpot == 4){
digitalWrite(ctl2,LOW);
digitalWrite(pinA2,LOW);
digitalWrite(pinB2,LOW);
}else if(selectpot == 5){
digitalWrite(ctl2,LOW);
digitalWrite(pinA2,HIGH);
digitalWrite(pinB2,LOW);
}else if(selectpot == 6){
digitalWrite(ctl2,LOW);
digitalWrite(pinA2,LOW);
digitalWrite(pinB2,HIGH);
}else if(selectpot == 7){
digitalWrite(ctl2,LOW);
digitalWrite(pinA2,HIGH);
digitalWrite(pinB2,HIGH);
}else{
digitalWrite(ctl,HIGH);
digitalWrite(ctl2,HIGH);
}
//delay(50);
}

int deactivatepot(){
//delay(50);
digitalWrite(ctl,HIGH);
digitalWrite(ctl2,HIGH);
```

```
}

int getvoltage(int phasediff){
int returnval;
float temp =
(.000000002*phasediff*phasediff*phasediff)+(.00003*phasediff*phasediff)+(.0118*phasediff)-.0816;
temp = temp/.12;
//Serial.println(temp);
int lowval = (int) temp;
float checklow = temp-.5;
int check = (int) checklow;
if(checklow < lowval){
returnval = lowval;
}else{
//Serial.print("Made It");
float rounding = temp+.5;
returnval = (int) rounding;
}
returnval=129-returnval;
Serial.println(returnval);
//Serial.print("Return Value: ");Serial.print(returnval);Serial.print("\n");
return returnval;



}

int setpotvalue(int digipot, int potvalue){
activatepot(digipot);
potvalue+=90;//this makes the error smaller but still not great
int newvolt = getvoltage(potvalue);
shiftOut(_sdi, _sck, MSBFIRST, (newvolt>>8));
shiftOut(_sdi, _sck, MSBFIRST, newvolt);
//shiftOut(_sdi, _sck, MSBFIRST, lowvalue);
deactivatepot();
}
```

APPENDIX E SERVER DISPLAY CODE

```
import processing.net.*;

int port = 4444;
Server myServer;
String indata;
int count = 0;
Float x,y,z,checksum,comparechksm,phaseBx,phaseBy = 0.0;
String [] numbers = null;
String startbyte = "ab";
PFont font,font2,font3;
PImage research;


String bad = "Are you there?";

void setup() {

size(960, 720, P3D);
myServer = new Server(this,port);

}

void draw() {
background(0,0,0);
research = loadImage("huffresearch.JPG");
image(research,width*.8,0,200.0,200.0);
Client thisClient = myServer.available();
if (thisClient != null){
indata = thisClient.readString();
}
if(indata != null){
++count;
if(indata.compareTo(bad) != 0){//cheap way to bypass handshake
numbers = split(indata,',');
try{
//checksum = Float.valueOf(numbers[3]).floatValue();
x = Float.valueOf(numbers[0]).floatValue();
y = Float.valueOf(numbers[1]).floatValue();
z = 180.0 + Float.valueOf(numbers[2]).floatValue();
phaseBx = Float.valueOf(numbers[3]).floatValue();
phaseBy = Float.valueOf(numbers[4]).floatValue();
//comparechksm = 255.0 - (x+y+z);
//print(checksum);print(",");print(comparechksm);
/*if(comparechksm != checksum){
x=180.0;y=180.0;z=180.0;
}*/
}catch(Exception e){
print("Didn't receive all information");
}
}
}

if(x == null){
x=180.0;
}
if(y == null){
y=180.0;
}
if(z == null){
z=0.0;
}
//quad(.2*width,.6*height,.6*width,.6*height,.7*width,.7*height,.3*width,.7*height);
drawAxis();
drawQuad(.35,.58,.42,.64,.5,.62);

lights();

// The font must be located in the sketch's
// "data" directory to load successfully
drawdatacase();
drawnamecase();
drawarraycase();
updatearray(phaseBx,phaseBy);
fill(255,255,255);
font = loadFont("SansSerif.italic-32.vlw");
textFont(font);
text("X: "+x+"\nY: "+y+"\nZ: "+z+"\nBeta_X: "+phaseBx+"\nBeta_Y: "+phaseBy,10.0,height*.7);

// ambientLight(255,0,0);
// directionalLight(255, 102, 102, 0, -1, 0);
translate(width / 2, height / 2);
// rotateX(map(y, 0, width, 0, 2*PI));
//rotateY(map(z, 0, width, 0, 2*PI));
//rotateZ(map(x, 0, height, 0, -PI));
rotateX(radians(y));
rotateY(radians(x));
rotateZ(radians(-1.0*z));
noStroke();
fill(255, 255, 255);
translate(0, -40, 0);
drawCylinder(100, 150, 250, 4);
// Draw a mix between a cylinder and a cone
//drawCylinder(70, 70, 120, 64); // Draw a cylinder
//drawCylinder(0, 180, 200, 4); // Draw a pyramid
}
```

```
void drawQuad(float shiftx1, float lengthx1,float shiftx2, float lengthx2, float shifty, float lengthy){
Float xspacing = 50.0;
Float x2spacing = 20.0;
Float yspacing = 20.0;
fill(150,150,150);

quad(shiftx1*width,shifty*height,lengthx1*width,shifty*height,lengthx2*width,lengthy*height,shiftx2*w
idth,lengthy*height);
fill(184,115,51);
noStroke();
for(Float k=0.0;k<4;k=k+1.0){
for(Float j=0.0;j<4;j=j+1.0){

quad((j*xspacing+k*x2spacing)+(shiftx1*width+10.0),k*yspacing+(shifty*height+5.0),(k*x2spacing+j*xsp
acing)+(shiftx1*width+40.0),k*yspacing+(shifty*height+5.0),(k*x2spacing+j*xspacing)+(shiftx1*width+50
.0),k*yspacing+(shifty*height+20.0),(k*x2spacing+j*xspacing)+(shiftx1*width+20.0),k*yspacing+(shifty*h
eight+20.0));
}
}
}
void drawdatacase(){
Float startpoint = .65;
fill(100,100,100);
rect(0,startpoint*height,.2*width,height);
fill(255,255,255);
rect(0,startpoint*height,.2*width,2.0);
rect(.2*width,startpoint*height,2.0,height);
}

void drawarraycase(){
Float xstartpoint = .65;
Float ystartpoint = .65;
fill(255,255,255);
rect(xstartpoint*width,ystartpoint*height,2.0,height);
rect(xstartpoint*width,ystartpoint*height,width,2.0);

}

void updatearray(Float Bx, Float By){
Float xstartpoint = .65;
Float ystartpoint = .65; //must be same for the drawarraycase(); would've made public... future work :)
Float patchwidth = 50.0;
Float patchheight = 50.0;
Float xshift = 5.0;
Float yshift = 5.0;
Float xshift2 = 15.0;
Float yshift2 = 15.0;
Float dispx = 60.0;
Float dispy = 60.0;
Float ystop = 5.0;
Float xwidth = 250.0;
Float yheight = 250.0;
Float totalphase = 0.0;
Float percentage = 0.0;
Boolean gogreen = true;
color startcolor = color(0,0,255);
color endcolorpos = color(255,0,0); //a PhaseBx of -100 is actually positive
color endcolorneg = color(0,255,0);
color finalcolor = color(0,0,0);

noStroke();
fill(150,150,150);
if(Bx == null){
    Bx = 0.0;
}
if(By == null){
    By = 0.0;
}

for(Float x = 0.0;x<100.0;x=x+1.0){
percentage = x/100.0;
finalcolor = lerpColor(endcolorpos,startcolor,percentage);
fill(finalcolor);
rect(xstartpoint*width + xshift+xwidth+xshift2,ystartpoint*height+20.0+x,50.0,1.0);
}
for(Float x = 0.0;x<100.0;x=x+1.0){
percentage = x/100.0;
finalcolor = lerpColor(startcolor,endcolorneg,percentage);
fill(finalcolor);
rect(xstartpoint*width + xshift+xwidth+xshift2,ystartpoint*height+120.0+x,50.0,1.0);
}
font3 = loadFont("CharterBT-Roman-14.vlw");
textFont(font3);
fill(150,150,150);
rect(xstartpoint*width + xshift,ystartpoint*height + yshift,xwidth,yheight);
for(float k = 0.0;k<4.0;k=k+1.0){
 for(float j = 0.0; j<4.0; j=j+1.0){
  gogreen = true;
  totalphase = (j*Bx)+(k*By);
  if(totalphase < 0.0){
  totalphase = totalphase*-1.0;
  gogreen = false;
  }
  if(totalphase>= 360.0 && totalphase <720){
  totalphase = totalphase - 360.0;
  }
  if(totalphase>=720.0){
  totalphase = totalphase - 720.0;
  }
  percentage = totalphase/360;
if(gogreen){
finalcolor = lerpColor(startcolor,endcolorneg,percentage);
}
else{
finalcolor = lerpColor(startcolor,endcolorpos,percentage);
}
fill(finalcolor);
rect(xstartpoint*width + xshift2 +j*dispx,ystartpoint*height + yshift2
+k*dispy,patchwidth,patchheight);
fill(0,0,0);
text(round(totalphase),xstartpoint*width+xshift2+j*dispx,ystartpoint*height+yshift2+k*dispy);
}
}
font3 = loadFont("CharterBT-Roman-18.vlw");
textFont(font3);
fill(255,255,255);
text("360",xstartpoint*width + xshift+xwidth+xshift2,ystartpoint*height+20.0);
text("0",xstartpoint*width + xshift+xwidth+xshift2,ystartpoint*height+120.0);
text("-360",xstartpoint*width + xshift+xwidth+xshift2,ystartpoint*height+235.0);


}


void drawnamecase(){
int p;
Float casewidth = 250.0;
noStroke();
for(p=0;p<100;p=p+5){
fill(255-p,255-p,255-p);
rect(0,p*1,casewidth,5.0);
}
fill(255,255,255);
rect(0,p*1,casewidth,2.0);
rect(casewidth,0,2.0,p*1+2.0);
fill(0,0,0);
font2 = loadFont("SansSerif.italic-32.vlw");
textFont(font2);
text("Phased Array\nBy: Jeff Jensen",5.0,35.0);

}

void drawAxis(){

fill(100,0,0);
rect(width/2,0,5,.3*height);
fill(0,0,255);
quad(width/2,height/2,4.0+width/2,height/2,.4*width,.5*height,.4*width-4.0,.5*height);
fill(0,255,0);
rect(width/2,height/2,width/2,5);
```

```
}

void drawCylinder(float topRadius, float bottomRadius, float tall, int sides) {
float angle = 0;
float angleIncrement = TWO_PI / sides;
beginShape(QUAD_STRIP);
for (int i = 0; i < sides + 1; ++i) {
//stroke(0);
for (int p=0;p<250;++p){
fill(255-p,255-p,255-p);
vertex(topRadius*cos(angle), 0, topRadius*sin(angle));
vertex(bottomRadius*cos(angle), tall, bottomRadius*sin(angle));
}
angle += angleIncrement;
}
endShape();

// If it is not a cone, draw the circular top cap
if (topRadius != 0) {
angle = 0;
beginShape(TRIANGLE_FAN);

// Center point
vertex(0, 0, 0);
for (int i = 0; i < sides + 1; i++) {
vertex(topRadius * cos(angle), 0, topRadius * sin(angle));
angle += angleIncrement;
}
endShape();
}

// If it is not a cone, draw the circular bottom cap
if (bottomRadius != 0) {
angle = 0;
beginShape(TRIANGLE_FAN);

// Center point
vertex(0, tall, 0);
for (int i = 0; i < sides + 1; i++) {
vertex(bottomRadius * cos(angle), tall, bottomRadius * sin(angle));
angle += angleIncrement;
}
endShape();
}
}
```

VITA

Name:	Jeffrey Scott Jensen
Address:	Zachary Enginering Center, EML Lab College Station, TX, 77843-3128
Email Address:	jensen.jeffrey.s@gmail.com
Education:	B.S., Electrical Engineering, Texas A&M University, 2010 M.S., Electrical Engineering, Texas A&M University, 2012